

Division of Pharmaceutical Chemistry
Faculty of Pharmacy
University of Helsinki

Activity and Enzyme Kinetics of Human UDP-Glucuronosyltransferases:

***Studies of Psilocin Glucuronidation and the Effects of Albumin on the
Enzyme Kinetic Mechanism***

Nenad Manevski

ACADEMIC DISSERTATION

*To be presented, with the permission of the Faculty of Pharmacy of the University of Helsinki,
for public examination in Auditorium 1041 (Viikinkaari 5, Biocenter 2) on 7 March 2013 at 12
noon.*

Helsinki 2013

Supervised by:

Docent Moshe Finel
Centre for Drug Research
Faculty of Pharmacy
University of Helsinki
Finland

Professor Jari Yli-Kauhaluoma
Division of Pharmaceutical Chemistry
Faculty of Pharmacy
University of Helsinki
Finland

Reviewed by:

Docent Mikko Koskinen
Head of DMPK
Orion Corporation
Espoo, Finland

Professor Rory Rempel
Department of Medicinal Chemistry
College of Pharmacy
University of Minnesota
Minneapolis, MN, USA

Opponent:

Professor Brian Houston
Centre for Applied Pharmacokinetic Research
Drug Metabolism and Pharmacokinetic Research Group
School of Pharmacy and Pharmaceutical Sciences
University of Manchester
Manchester, UK

© Nenad Manevski 2013

ISBN 978-952-10-8624-3 (Paperback)

ISBN 978-952-10-8625-0 (PDF)

ISSN 1799-7372

<http://ethesis.helsinki.fi>

Helsinki University Print
Helsinki 2013

Contents

PREFACE	5
ABSTRACT	6
LIST OF ORIGINAL PUBLICATIONS	8
ABBREVIATIONS	9
LIST OF FIGURES	10
LIST OF TABLES	11
1 INTRODUCTION	12
2 REVIEW OF THE LITERATURE	14
2.1 UGT ENZYMES	14
2.1.1 <i>Family of human UDP-glycosyltransferases</i>	14
2.1.2 <i>The genes of human UGTs</i>	15
2.1.3 <i>Molecular structure and membrane topology of UGTs</i>	18
2.1.4 <i>Catalytic mechanism of glucuronidation</i>	20
2.1.5 <i>UGT expression in human tissues</i>	22
2.2 UGT SUBSTRATE SPECIFICITY	25
2.2.1 <i>Glucuronidation of drugs of abuse</i>	27
2.2.2 <i>Glucuronidation of psilocin</i>	28
2.2.3 <i>Glucuronidation of endo- and xenobiotics with the indole scaffold</i>	29
2.3 MEASUREMENT AND PREDICTION OF UGT ACTIVITY BASED ON IN VITRO ASSAYS	32
2.3.1 <i>Experimental conditions of the in vitro UGT assay</i>	33
2.3.2 <i>Albumin effect in human UGTs and CYPs</i>	34
2.3.3 <i>Significance of the albumin effect for in vitro–in vivo extrapolation</i>	37
2.3.4 <i>Mechanism of the albumin effect</i>	38
2.3.5 <i>Drug binding to albumin and enzyme sources</i>	40
2.3.6 <i>Principles of in vitro–in vivo extrapolation</i>	40
2.3.7 <i>Prediction of inhibitory drug-drug interactions</i>	41
2.4 ENZYME KINETICS OF UGT-CATALYZED REACTIONS	41
2.4.1 <i>Enzyme kinetic mechanism of UGT-catalyzed reactions</i>	43
2.4.2 <i>Substrate inhibition in UGT-catalyzed reactions</i>	46
2.4.3 <i>Inhibition of UGT-catalyzed reactions</i>	48
2.4.4 <i>Atypical enzyme kinetics of UGT-catalyzed reactions</i>	49
2.4.5 <i>Substrate depletion assays</i>	51
2.4.6 <i>Key statistical concepts used in enzyme kinetics</i>	52
3 AIMS OF THE STUDY	55
4 MATERIALS AND METHODS	56
4.1 CHEMICALS	56
4.2 IN VITRO GLUCURONIDATION ASSAYS	57
4.3 ENZYME KINETIC ASSAYS	58
4.4 ANALYTICAL METHODS	58
4.5 DATA ANALYSIS	59
5 RESULTS AND DISCUSSION	60
5.1 GLUCURONIDATION OF PSILOCIN AND 4-HI BY HUMAN UGTs (I)	60
5.1.1 <i>Prevention of psilocin degradation in vitro</i>	60
5.1.2 <i>Screening assays with HLM, HIM, and recombinant UGTs</i>	61

5.1.3	<i>Enzyme kinetics of psilocin and 4-HI glucuronidation</i>	63
5.1.4	<i>Expression of UGT enzymes that glucuronidate psilocin</i>	65
5.2	ALBUMIN EFFECTS IN HUMAN UGTs (II, III, AND IV)	66
5.2.1	<i>Drug binding to albumin and enzyme sources</i>	67
5.2.2	<i>Optimization of in vitro assay conditions</i>	69
5.2.3	<i>Differences between enzyme sources</i>	72
5.2.4	<i>Scope of albumin effects in human UGTs</i>	74
5.3	ENZYME KINETIC MECHANISM OF UGT1A9 (IV)	79
5.3.1	<i>Bisubstrate enzyme kinetics of UGT1A9-catalyzed reactions</i>	79
5.3.2	<i>Product and dead-end inhibition of UGT1A9-catalyzed reactions</i>	84
5.3.3	<i>Conclusions about the enzyme kinetic mechanism</i>	85
6	SUMMARY AND CONCLUSIONS	86
	REFERENCES	87

Preface

The work on this Ph.D. thesis was performed at the Faculty of Pharmacy, University of Helsinki in the period of 2008–2012. I express sincere gratitude to my supervisors, Docent Moshe Finel and Professor Jari Yli-Kauhaluoma, for their full support and encouragement during this period. You were always there for me; helping with research plans and experiments, giving invaluable guidance, correcting manuscripts to the highest scientific standards, supporting the funding applications and, equally important, offering a warm and friendly support in the times of hardship. I have learned a lot and had a privilege to have you as supervisors. Thank you for all the help.

The special gratitude goes to my dear colleagues and coauthors of publications: Mika Kurkela, Johanna Troberg, Camilla Höglund, Paolo Svaluto Moreolo, Timo Mauriala, and Klaudyna Dziedzic. All of you gave your best efforts at the time, stayed long hours in the laboratory, and helped produce some of the finest results for this thesis. Thank you for the enthusiasm, as well as for the energetic and cheerful discussions we had. I deeply thank Antti Siiskonen and Liisa Laakkonen for invaluable advices and passionate discussions about science. I have learned a lot from you. I would like to thank Mikko Vahermo, Gustav Boije af Gennäs, Alexandros Kiriazis, Leena Keurulainen, Päivi Uutela, Taina Sten, Nina Sneitz, Hongbo Zhang as well as all the other colleagues from the Division of Pharmaceutical Chemistry and Centre for Drug Research. The morning coffee would have never been that cheerful without you. I also express my sincere gratitude to the pre-examiners Docent Mikko Koskinen and Professor Rory Remmel for their large efforts in reviewing and improving this thesis.

The unique appreciation goes for the pharmacy owners Markku and Leena Suominen. You helped me many times and supported my Ph.D. studies to great extent. My gratitude also goes to Professor Sote Vladimirov from the Faculty of Pharmacy, University of Belgrade for genuine support and interest in my work. I would like to thank my dear friends from Helsinki: Aleksandar, Ivan and Danijela, Zlatko and Marija, Tea, Nebojša and Emilija and all others for priceless friendship over the years. I am also in debt to many of my friends from Belgrade: Vlada, Nikola, Tamara, Sanja, and Adam, who always encouraged and supported me.

Finally, I express deepest gratitude to my mother Ljiljana Petrović, who wholeheartedly supported and encouraged my studies over the years. I thank my father Marjan Manevski who always helped and gave valuable advices. My brothers, Marko and Verdan, thank you for your continuously cheerful and optimistic attitude; you always helped me stay positive and focused.

In Helsinki, January 2013

Nenad Manevski

Nenad Manevski

Abstract

Human UDP-glucuronosyltransferases (UGTs) are important in the metabolic elimination of xenobiotics and endogenous compounds from the body. These enzymes transfer glucuronic acid moiety from the cosubstrate, UDP-glucuronic acid (UDPGA), to nucleophilic groups of small organic molecules, such as hydroxyl, carboxylic, or amino group. The conjugation of these molecules with polar glucuronic acid usually diminishes their pharmacodynamic activity, promotes aqueous solubility and enhances recognition by efflux transporters in the cells, all of which contributes to the efficient metabolic elimination and excretion of the conjugate from the body. Due to these unique properties, UGT enzymes play major roles in drug metabolism and pharmacokinetics.

The main goal of this thesis was to investigate the activity and enzyme kinetics of UGTs, as well as the *in vitro* assay conditions needed to accurately determine the enzyme kinetic parameters. Particular attention focused on the glucuronidation of psilocin, the enhancement of UGT activity by the inclusion of purified bovine serum albumin (BSA), and the enzyme kinetic mechanism of UGT1A9. These goals are especially important in the early phases of preclinical drug development, where *in vitro* assays serve to explain and predict the glucuronidation of the drug *in vivo*, both qualitatively and quantitatively.

As a starting point, we studied the glucuronidation of psilocin, the hallucinogenic indole alkaloid from mushrooms of the genus *Psilocybe*, by all the human UGTs of subfamilies 1A, 2A, and 2B. To understand the substrate selectivity of human UGTs, we also studied the glucuronidation of 4-hydroxyindole, a chemically simpler analog of psilocin which lacks the *N,N*-dimethylaminoethyl side chain. We successfully prevented the oxidative degradation of psilocin, a problem we encountered early in the study, by including an antioxidant (1 mM dithiothreitol) in the assays. Our results showed that psilocin is glucuronidated mainly by UGTs 1A10 and 1A9, whereas the activities of UGTs 1A8, 1A7, and 1A6 were lower. On the other hand, 4-hydroxyindole was glucuronidated mainly by UGT1A6, whereas the activities of UGTs 1A7–1A10 closely correlated with their respective rates of psilocin glucuronidation. To understand in which human tissues psilocin glucuronidation takes place, we studied the expression levels of mRNA for UGTs 1A7–1A10; this work was performed in collaboration with Dr. Michael H. Court of the Tufts University School of Medicine, Boston, Massachusetts. The combined results of the activity and expression studies indicate that although the intestinal enzyme UGT1A10 shows the highest glucuronidation clearance, UGT1A9, an enzyme abundantly expressed in both the liver and kidneys, may be the main contributor to psilocin glucuronidation *in vivo*.

The inclusion of purified albumin is known to significantly enhance glucuronidation rates *in vitro*. In subsequent studies, we focused our attention on the scope and mechanism of this activity enhancement and investigated “albumin effects” in a total of 11 human UGTs. Before proceeding with enzyme kinetic assays, we carefully measured the binding of substrates to BSA by either ultrafiltration or rapid equilibrium dialysis. Our results showed that the inclusion of BSA significantly enhances the *in vitro* glucuronidation activity of almost all the UGTs we tested, either by increasing the apparent substrate affinity (lower K_m) or the reaction-limiting velocity (higher V_{max}), or both. The nature of albumin effects, however, varied greatly and depended both on the UGT enzyme and the substrate employed. The highest activity increases in

the presence of BSA were observed in UGTs 1A7, 1A9, 1A10, 2A1, and 2B7, whereas BSA stimulation was comparatively less pronounced in UGTs 1A1, 1A6, 1A8, 2B4, and 2B15. On the other hand, depending on the substrate used, the addition of BSA to UGTs 1A1, 1A6, and 2B17 sometimes resulted in a lack of any stimulatory effects. Moreover, the activity enhancement by BSA appears independently of the enzyme source used, since both native enzymes in human liver microsomes and recombinant enzymes expressed in *Sf9* insect cells yielded similar results.

To investigate the mechanism of albumin effects, as well as to elucidate the enzyme kinetic mechanism of human UGTs, we studied bisubstrate enzyme kinetics, the product inhibition, and dead-end inhibition kinetics of UGT1A9. For this purpose, we employed 4-methylumbelliferone as the aglycone substrate and investigated both forward- and reverse-direction UGT-catalyzed reactions. The combined results of our experiments strongly suggest that UGT1A9 follows the compulsory-order ternary-complex mechanism with UDPGA binding first. The addition of BSA quantitatively changes the enzyme kinetic parameters, presumably by removing “internal” inhibitors that bind to binary (enzyme • UDPGA) or ternary (enzyme • UDPGA • aglycone) complexes, but the underlying compulsory-order ternary-complex mechanism remains unaffected. In addition, based on enzyme kinetic parameters measured in the forward and reverse reaction, we elucidated the thermodynamic equilibrium constant of the overall reaction ($K_{eq} = 574$), as well as the relative magnitude of the individual rate constants.

In summary, the results obtained deepen our current knowledge of UGT enzyme kinetics and set new guidelines for performing *in vitro* UGT assays. The study of psilocin and 4-hydroxyindole glucuronidation revealed that relatively small structural modifications, such as the loss of the side chain, lead to major changes in UGT substrate selectivity. And provided the substrate binding to BSA is accounted for, the addition of BSA significantly enhances the activities of almost all the UGTs tested and improves the accuracy of the measured enzyme kinetic parameters. These features are especially important for the prediction of UGT activity *in vivo*. Finally, our results deepen our current understanding of the UGT enzyme kinetic mechanism and conclusively show that UDPGA is the first, and the aglycone substrate is the second binding substrate to form a ternary complex in UGT1A9-catalyzed reactions.

List of original publications

This thesis is based on the following publications:

- I** Manevski N, Kurkela M, Höglund C, Mauriala T, Court MH, Yli-Kauhaluoma J, and Finel M. (2010) Glucuronidation of psilocin and 4-hydroxyindole by the human UDP-glucuronosyltransferases. *Drug Metab Dispos* **38**:386-395.
- II** Manevski N, Moreolo PS, Yli-Kauhaluoma J, and Finel M. (2011) Bovine serum albumin decreases K_m values of human UDP-glucuronosyltransferases 1A9 and 2B7 and increases V_{max} values of UGT1A9. *Drug Metab Dispos* **39**:2117-2129.
- III** Manevski N, Troberg J, Svaluto-Moreolo P, Dziedzic K, Yli-Kauhaluoma J, and Finel M. (2013) Albumin stimulates the activity of the human UDP-glucuronosyltransferases 1A7, 1A8, 1A10, 2A1 and 2B15, but the effects are enzyme and substrate dependent. *PLoS ONE* **8**: e54767.
- IV** Manevski NM, Yli-Kauhaluoma J, and Finel M. (2012) UDP-Glucuronic acid binds first and the aglycone substrate binds second to form a ternary complex in UGT1A9-catalyzed reactions, in both the presence and absence of BSA. *Drug Metab Dispos* **40**:2192-2203.

The publications are designated in the text by their Roman numerals.

Abbreviations

ABC	ATP-binding cassette transporters
AIC_c	Corrected Akaike's information criterion
AUC	Area under the plasma drug concentration vs. time curve
BSA	Bovine serum albumin
CL_{int}	Intrinsic clearance, corresponds to V_{\max}/K_m ratio
CL_{max}	Maximal clearance that results from autoactivation (see Eq. 17)
CL_H	Hepatic clearance
CYP	Cytochrome P450
E_H	Hepatic extraction ratio
EMA	European medicines agency
FDA	U.S. Food and drug administration
FMO	Flavin-containing monooxygenases
GT	Glycosyltransferases
HEK293	Human embryonic kidney 293 cells
4-HI	4-Hydroxyindole
6-HI	6-Hydroxyindole
5-HT	5-Hydroxytryptamine
HIM	Human intestinal microsomes
HKM	Human kidney microsomes
HLM	Human liver microsomes
HPLC	High-performance liquid chromatography
HSA	Human serum albumin
IC₅₀	Concentration of inhibitor that inhibits 50% of enzyme activity
IFABP	Human intestinal fatty acid-binding protein
k_{cat}	Catalytic constant (turnover number)
K_{eq}	Thermodynamic equilibrium constant
K_m	Michaelis-Menten constant
K_s	Equilibrium dissociation constant
LC-MS	Liquid chromatography-mass spectrometry
MDMA	3,4-Methylenedioxy-N-methylamphetamine (ecstasy)
NSAID	Non-steroidal anti-inflammatory drugs
4-MU	4-Methylumbelliferone
4-MUG	4-Methylumbelliferone-β-D-glucuronide
OATP	Organic anion transporting polypeptide
RED	Rapid equilibrium dialysis
RT-PCR	Reverse transcriptase-polymerase chain reaction
qRT-PCR	Quantitative reverse transcriptase-polymerase chain reaction (real time)
Sf9	Cell line from the pupal ovarian tissue of the Fall armyworm (<i>Spodoptera frugiperda</i> , J.E. Smith, 1797)
SULTs	Sulfotransferases
UDP	Uridine diphosphate
UDPGA	UDP-α-D-glucuronic acid
UGT	UDP-Glucuronosyltransferase
UPLC	Ultra-performance liquid chromatography
V_{max}	The limiting velocity of the enzyme reaction (maximum velocity)

List of Figures

Figure 1. Reaction catalyzed by UDP-glycosyltransferases.....	14
Figure 2. Family of glycosyltransferases.....	15
Figure 3. The phylogenic tree of human UGTs.....	16
Figure 4. Structure of human UGT1A genes.....	16
Figure 5. Structure of human UGT2A and UGT2B genes.....	18
Figure 6. Schematic representation of the primary structure of UGT.....	18
Figure 7. Putative UGT structure in the membrane of the endoplasmic reticulum.....	20
Figure 8. Catalytic mechanism of O-glucuronidation.....	21
Figure 9. Catalytic mechanism of N-glucuronidation.....	22
Figure 10. The relative expression of UGT mRNA in the liver, small intestine, and kidneys.....	25
Figure 11. Metabolic pathways of psilocybin and psilocin in humans.....	29
Figure 12. Metabolism of endogenous indoles in the human body.....	30
Figure 13. Chemical structures of therapeutic and abused drugs with indole scaffold.....	31
Figure 14. Chemical structures of fatty acids identified as inhibitors of UGTs and CYPs.....	39
Figure 15. Enzyme reaction scheme used to derive the Michaelis-Menten equation.....	42
Figure 16. Saturation profile for the Michaelis-Menten equation.....	43
Figure 17. Compulsory-order ternary-complex and substituted-enzyme kinetic mechanisms.....	44
Figure 18. Saturation profiles of the substrate inhibition and the Michaelis-Menten equation.....	47
Figure 19. Enzyme kinetic models used to describe the substrate inhibition.....	47
Figure 20. Modalities of reversible enzyme inhibition.....	49
Figure 21. Saturation profiles for the sigmoidal and the biphasic enzyme kinetics.....	50
Figure 22. Substrate depletion assay.....	52
Figure 23. Representation of data with Gaussian distribution.....	52
Figure 24. Presentation of SS_{reg} and SS_{tot} in the analysis of the enzyme kinetic data.....	54
Figure 25. Influence of DTT on the glucuronidation of psilocin and 17 β -estradiol by UGT1A10.....	60
Figure 26. Glucuronidation of psilocin and 4-HI by HLM and HIM.....	61
Figure 27. Glucuronidation of psilocin and 4-HI by 19 human recombinant UGTs.....	62
Figure 28. Enzyme kinetics of psilocin glucuronidation by UGT1A10 and UGT1A9.....	63
Figure 29. Enzyme kinetics of 4-HI glucuronidation by UGT1A6, UGT1A10, and UGT2A1.....	64
Figure 30. Binding of entacapone to 0.1% BSA in the absence and presence of an enzyme source.....	69
Figure 31. Influence of different BSA concentrations on 4-MU glucuronidation by UGT2A1.....	70
Figure 32. Effects of BSA concentration on the K_m values for 4-MU glucuronidation.....	71
Figure 33. Entacapone glucuronidation by UGT1A8 in the absence and presence of 0.1% BSA.....	72
Figure 34. Zidovudine glucuronidation by HLM and UGT2B7 with and without 1% BSA.....	73
Figure 35. Entacapone glucuronidation by HLM: in-house-produced and commercial UGT1A9.....	74
Figure 36. Effects of BSA on the K_m (or S_{50}) and V_{max} values in recombinant human UGTs.....	76
Figure 37. Effects of BSA on the CL_{int} in recombinant human UGTs, HLM, and HIM.....	78
Figure 38. Effects of BSA on the bisubstrate kinetics of UGT1A9-catalyzed 4-MU glucuronidation.....	80
Figure 39. Bisubstrate kinetics of UGT1A9-catalyzed 4-MU glucuronidation with substrate inhibition.....	81
Figure 40. Bisubstrate kinetics of the reverse reaction.....	83
Figure 41. Proposed mechanism of the UGT1A9-catalyzed 4-MU glucuronidation reaction.....	85

List of Tables

Table 1. <i>Expression of UGT enzymes in human tissues.</i>	23
Table 2. <i>Overview of typical and selective substrates for human UGTs</i>	26
Table 3. <i>List of abused drugs eliminated by glucuronidation</i>	27
Table 4. <i>Albumin effects on glucuronidation enzyme kinetics in human microsomal fractions.</i>	35
Table 5. <i>Albumin effects on the glucuronidation enzyme kinetics in recombinant human UGTs.</i>	35
Table 6. <i>Albumin effects on the inhibition of glucuronidation in HLM and recombinant UGTs.</i>	36
Table 7. <i>Albumin effects on the enzyme kinetics of CYP-catalyzed reactions in HLM and CYPs.</i>	37
Table 8. <i>Previous studies that described the enzyme kinetic mechanism of UGT enzymes.</i>	46
Table 9. <i>UGT substrates and inhibitors used in this study</i>	56
Table 10. <i>Psilocin and 4-HI glucuronidation kinetics</i>	65
Table 11. <i>Expression of UGTs 1A6, 1A7, 1A8, 1A9, and 1A10 mRNA in human tissues.</i>	66
Table 12. <i>Binding of drugs to BSA and enzyme sources</i>	67
Table 13. <i>Bisubstrate enzyme kinetic parameters of 4-MU glucuronidation by UGT1A9</i>	83
Table 14. <i>Relative individual rate constants for the UGT1A9-catalyzed 4-MU glucuronidation.</i>	84

1 Introduction

The metabolism of xenobiotics and endogenous compounds is the body's own detoxifying system, which is crucial for its survival. Small and lipophilic organic molecules of various origins, such as therapeutic drugs, secondary plant metabolites, alimentary ingredients, environmental pollutants, and endogenous metabolites, may accumulate to toxic levels in the body. To prevent this undesirable scenario, the body employs a multitude of metabolic enzymes in an effort to modify the chemical structure of lipophilic molecules (biotransformation), render them more polar and hydrophilic, and ultimately eliminate them from the body. Such metabolic elimination takes place in many human tissues, most notably the liver, intestine, and kidneys.

The metabolism of endo- and xenobiotics is, in many cases, a two-phase process. In the first phase, lipophilic molecules usually undergo reactions of oxidation, reduction, or hydrolysis. These reactions are catalyzed by enzymes of the cytochrome P450 family (CYPs; Guengerich, 2008, Nebert and Russell, 2002), flavin-containing monooxygenases (FMOs; Phillips and Shephard, 2008), alcohol and aldehyde dehydrogenases (Hoog *et al.*, 2001, Vasiliou *et al.*, 2004), aldehyde oxidase (Pryde *et al.*, 2010), monoamine oxidases (Strolin Benedetti *et al.*, 2007), and a variety of esterases (Hosokawa, 2008). Oxidoreductive or "phase I" metabolic reactions often lead to the introduction or exposure of new functional groups, mainly hydroxyl, carboxylic, amino, or thiol functionalities. Although these structural changes somewhat increase the polarity and hydrophilicity of the parent compound, initial "phase I" metabolites are often pharmacologically active, chemically reactive, or even toxic.

To diminish pharmacological activity and toxicity, as well as to facilitate excretion from the body, "phase I" metabolites are coupled with a variety of endogenous molecules, such as glucuronic acid, glutathione, and amino acids, or functional groups such as sulfonyl, methyl and acetyl. This process is generally referred to as conjugative, or "phase II", metabolic reactions. These conjugative reactions occur at nucleophilic groups of the parent compound, such as hydroxyl, carboxyl, or amino groups. Nucleophilic groups may already be present in the structure of the molecule, as in the case of zidovudine or entacapone, which enables conjugative reactions without any preceding oxidoreductive (phase I) reactions. Alternatively, oxidoreductive metabolic reactions may introduce nucleophilic groups. A variety of metabolic enzymes, most notably UDP-glucuronosyltransferases (UGTs; Guillemette *et al.*, 2010, Miners *et al.*, 2010), sulfotransferases (SULTs; Lindsay *et al.*, 2008), glutathione *S*-transferases (Higgins and Hayes, 2011), and *N*-acetyltransferases (Sim *et al.*, 2012) catalyze conjugative reactions. The resultant conjugates are usually, but not always, more hydrophilic and pharmacologically inactive, and are substrates for efflux transporters in the plasma membrane of the cells; all of these properties contribute to their efficient metabolic elimination and excretion from the body.

Efflux transporters are also considered an important part of the metabolic elimination process (Eckford and Sharom, 2009, Benet, 2009, International Transporter Consortium, 2010). ATP-binding cassette (ABC) transporters are a large family of efflux transporters that use ATP-hydrolysis to excrete xenobiotics and endogenous metabolites across the plasma membrane of the cell (Eckford and Sharom, 2009). Important members of the ABC transporter family are P-glycoprotein (P-gp; ABCB1 family), breast cancer resistance protein (BCRP; ABCG2 family), and multidrug resistance-associated proteins (MRPs; ABCC family) (Eckford and Sharom, 2009, Benet, 2009). Influx (or uptake) transporters, although not directly involved in metabolite

excretion, may also play roles in metabolic elimination and pharmacokinetics (International Transporter Consortium, 2010). The family of organic anion transporting polypeptides (OATPs, SLC family; Niemi *et al.*, 2011), for example, accelerates xenobiotic uptake from the blood into the hepatocytes, the principal cells involved in xenobiotic metabolism.

Since xenobiotic metabolism affects both the pharmacokinetic and pharmacodynamic properties of therapeutic drugs, a detailed understanding of drug metabolizing enzymes is important for successful pharmacotherapy. From the perspective of drug discovery and development, it is important to fully explain and understand the fate of the drug in the human body. This knowledge significantly reduces the possibility of adverse drug reactions caused by unidentified drug metabolites, as well as identifies crucial metabolic enzymes that may mediate drug-drug interactions. The importance to understand the metabolic pathways is also highlighted in recent regulatory guidelines on drug interactions from the European Medicines Agency (EMA) and U.S. Food and Drug Administration (FDA) (documents can be accessed from <http://www.ema.europa.eu/ema/> and <http://www.fda.gov/>). In the future, a crucial breakthrough would be the ability to accurately predict drug metabolism *in vivo* based on simple *in vitro*, or even computational *in silico*, experiments. The ability to understand and predict drug metabolism would especially benefit the early, preclinical, phases of drug development if only molecules with suitable metabolic profile could be selected. This early-on selection may prevent costly failures in the clinical stages due to undesirable drug metabolism, or help avoid drug-drug interactions through drug-metabolizing enzymes. Sufficiently understanding drug-metabolizing enzymes and accurately predicting the phenomena *in vivo*, however, pose considerable challenges. The enzyme source used, the assay conditions of *in vitro* experiments, the analytical methods available, the enzyme kinetic models used for data analysis, and subsequent scaling factors all contribute to the accuracy of a prediction.

This thesis focuses on the most important enzymes of conjugative (phase II) metabolism: the human UGTs. These enzymes mostly exhibit broad substrate selectivity and eliminate many therapeutic drugs (Miners *et al.*, 2010, Williams *et al.*, 2004), numerous endogenous compounds such as bilirubin (Schmid, 1956), 17 β -estradiol (Sandberg and Slaunwhite, 1957) and thyroxine (Kato *et al.*, 2008), secondary plant metabolites like flavonoids and polyphenolic compounds (Wu *et al.*, 2011), drugs of abuse such as 3,4-methylenedioxy-*N*-methylamphetamine metabolites (ecstasy; Schwaninger *et al.*, 2009), and environmental pollutants such as benzo[*a*]pyrene (Dellinger *et al.*, 2006). We studied the *in vitro* activity and enzyme kinetics of UGT enzymes in order to deepen our knowledge of the human endo- and xenobiotic metabolism. We trust that the new results presented in this thesis will contribute to a more complete understanding of UGT enzymes and, ultimately, to safer pharmacotherapy.

2 Review of the Literature

Human UGTs transfer the glucuronic acid moiety from UDP- α -D-glucuronic acid (UDPGA) to nucleophilic groups on small organic molecules. This conjugation with glucuronic acid is also referred to as glucuronidation. This literature review focuses on the function and structure of human UGTs, with particular emphasis on the three topics studied in this Ph.D. thesis: (1) the glucuronidation of drugs of abuse, (2) the effects of including purified bovine serum albumin (BSA) in the reaction mixture, and (3) the enzyme kinetics of UGT enzymes.

2.1 UGT enzymes

2.1.1 Family of human UDP-glycosyltransferases

Human UGT enzymes belong to the family of UDP-glycosyltransferases (Meech *et al.*, 2012, Mackenzie *et al.*, 2005). In general, UDP-glycosyltransferases catalyze the transfer of the hexose moiety from the cosubstrate, UDP- α -D-activated hexose, to the nucleophilic groups of organic molecules (Figure 1). The product of this reaction is β -D-glycoside, the conjugate of the aglycone substrate with hexose.

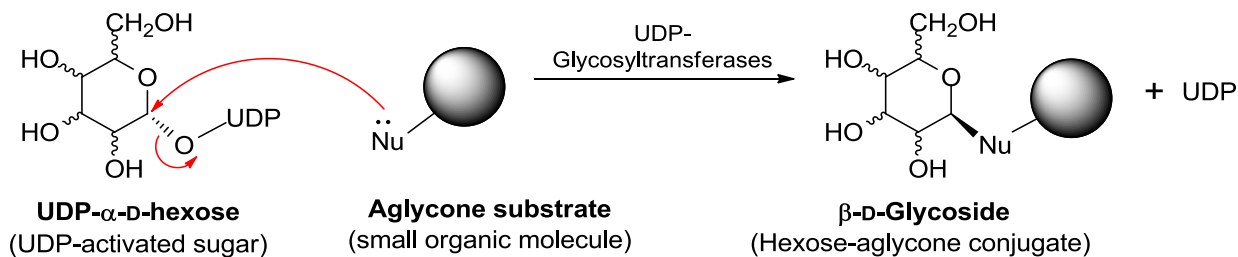


Figure 1. UDP-Glycosyltransferases catalyze the transfer of the hexose moiety from UDP-activated hexose to the nucleophilic groups of organic molecules. Symbol Nu designates the nucleophilic group on the small organic molecule.

Sugar moieties usually consist of glucuronic acid, glucose, galactose, xylose, or *N*-acetylglucosamine. Conjugation with the hexose moiety, usually referred to as glycosidation, prevents the accumulation of lipophilic molecules to toxic levels in the body and facilitates their excretion into the urine and bile. In humans, the family of UDP-glycosyltransferases comprises four subfamilies: UDP-glycosyltransferases 1, 2, 3, and 8. Enzymes from subfamilies 1 and 2 use UDP- α -D-glucuronic acid as the sugar donor. These enzymes are called UDP-glucuronosyltransferases (UGTs) and are the main focus of this thesis. The sugar specificity of UGTs, however, appears not absolute since UGT1A1 and UGT2B7 are also reported to use UDP- α -D-xylose (Senafi *et al.*, 1994) and UDP- α -D-glucose (Mackenzie *et al.*, 2003), respectively. On the other hand, UDP- α -D-*N*-acetylglucosamine (Mackenzie *et al.*, 2008), as well as UDP- α -D-glucose and UDP- α -D-xylose (MacKenzie *et al.*, 2011) are the sugar donors for the enzymes of subfamily 3. Lastly, UDP-glycosyltransferase 8 uses UDP- α -D-galactose (Sprong *et al.*, 1998). These subfamilies also play distinct physiological roles. While enzymes from subfamilies 1, 2, and 3 are involved in the metabolic elimination of endo- and xenobiotics (Meech *et al.*, 2012), UDP-glycosyltransferase 8 is responsible for the glycosidation of ceramides, the principal constituents of the myelin layer around neurons (Sprong *et al.*, 1998).

Human UDP-glycosyltransferases belong to glycosyltransferases, a superfamily of enzymes present in all kingdoms of life which play various physiological roles (Lairson *et al.*, 2008) (Figure 2). Regardless of the broad variability in sequence and function, most glycosyltransferases adopt only two distinct structural folds, either GT-A or GT-B (Lairson *et al.*, 2008, Chang *et al.*, 2011). Moreover, according to the stereochemical course of the reaction, all glycosyltransferases are classified as either inverting or retaining, depending whether or not the anomeric carbon on the sugar moiety changes its configuration upon reaction. Based on these criteria, all mammalian UDP-glycosyltransferases are classified as inverting glycosyltransferases with a GT-B fold, and further subclassified into the GT1 family, together with related enzymes such as UGT71B1, from the *Arabidopsis thaliana* plant (Carl Linnaeus) (Brazier-Hicks *et al.*, 2007), or bacterial GtfB (Mulichak *et al.*, 2001) and OleD (Bolam *et al.*, 2007).

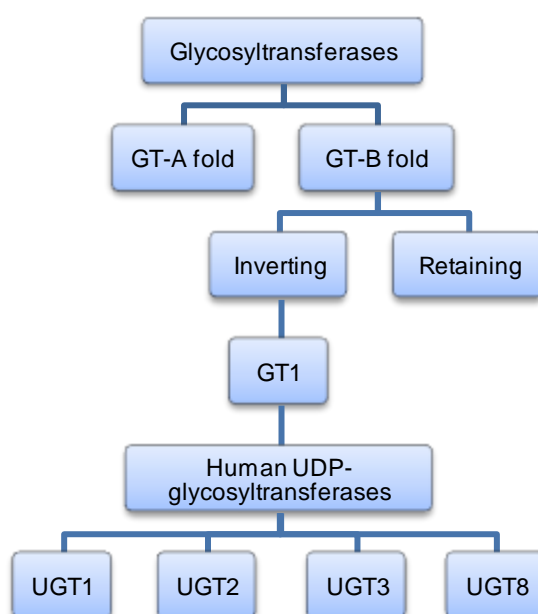


Figure 2. Human UDP-glycosyltransferases belong to the GT1 family of inverting GT-B fold glycosyltransferases. Only UDP-glycosyltransferase families 1 and 2 use UDP- α -D-glucuronic acid as the sugar donor.

2.1.2 The genes of human UGTs

Based on their sequence similarity, chromosomal location and historical reasons, human UGTs are classified into three subfamilies: UGT1A, UGT2A, and UGT2B (Guillemette *et al.*, 2010, Meech *et al.*, 2012, Mackenzie *et al.*, 2005). Individual enzymes are marked with an Arabic numeral following the subfamily name. The phylogenetic tree of human UGTs is presented in Figure 3. Their corresponding human UGT genes are named in a similar manner to proteins, but denoted in *Italic* typeface (e.g. *UGT1A9* is the human gene for the human protein UGT1A9).

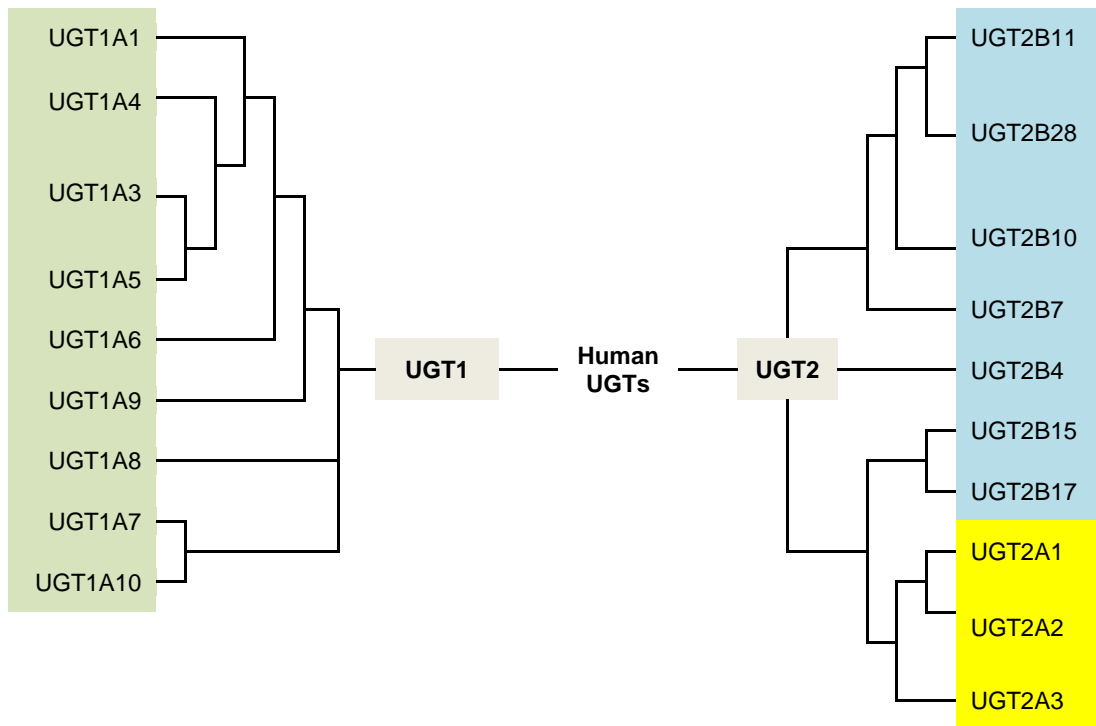


Figure 3. The phylogenetic tree of human UGTs (adapted from Guillemette *et al.*, 2010).

A single-gene locus on human chromosome 2q37 encodes the entire subfamily of UGT1A enzymes. The human *UGT1A* gene locus encodes nine functional proteins, namely UGT1A1 and UGTs 1A3–1A10. Functional diversity is achieved by the set of unique first promoters and exons that are spliced with shared exons 2–5 (Figure 4). The first exons encode the N-terminal domain, which is responsible mainly for substrate binding, while the shared exons 2–5 encode the C-terminal domain that contains the UDPGA binding site and the transmembrane helix. While there are 13 different first exons, only 9 of them encode functional proteins (UGTs 1A1, 1A3, 1A4, 1A5, 1A6, 1A7, 1A8, 1A9, and 1A10); the remaining 4 contain internal stop codons in humans and are therefore pseudogenes (UGT1A2p, UGT1A11p, UGT1A12p, and UGT1A13p). Based on their sequence similarity, *UGT1A* genes can be grouped into *A1*, *A2P–A5*, *A6*, and *A7–A12P* clusters (Guillemette *et al.*, 2010, Meech *et al.*, 2012, Mackenzie *et al.*, 2005). Exons *A1* and *A6* encode proteins that are approximately 50% identical. Within the *A2P–A5* and *A7–A13P* exon clusters, however, encoded polypeptides are 75–92% identical (Mackenzie *et al.*, 2005).

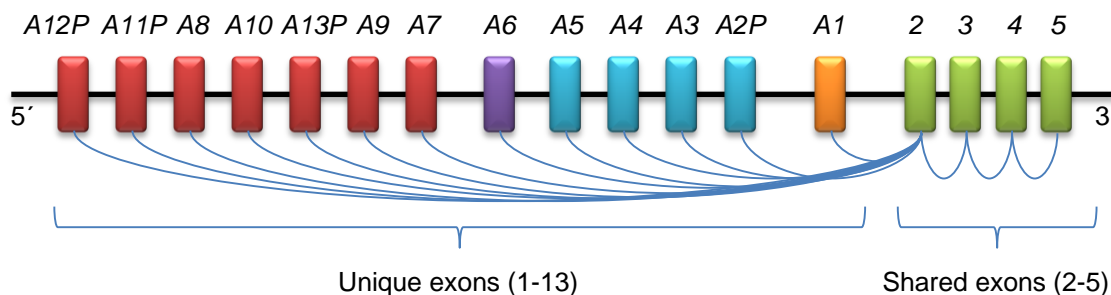


Figure 4. Structure of the human *UGT1A* gene locus. The first 13 exons and corresponding promoters are unique; exons 2–5 are shared.

Recently, several alternative splicing events were discovered within the *UGT1A* gene locus (Guillemette *et al.*, 2010). Most notably, the new exon 5b was located within the common region of the gene, between exons 4 and 5, whereas the previously called exon 5 has now been renamed exon 5a (Girard *et al.* 2007; Levesque *et al.* 2007). The mRNA transcribed with exon 5b leads to a slightly shorter protein without the transmembrane helix, but with binding sites for both the aglycone substrate and UDPGA. This led to the discovery of nine new UGT1A proteins known as isoforms 2 (i2), specifically UGT1A1_i2 and UGT1A3_i2–UGT1A10_i2. In most human tissues, UGT1A_i2 proteins are expressed together with their active UGT1A_i1 analogs (Levesque *et al.* 2007). The i2 variants, however, are catalytically inactive (Girard *et al.* 2007; Levesque *et al.* 2007). Nevertheless, if coexpressed with active UGT1A_i1 enzymes, the i2 proteins suppressed glucuronidation activity (Girard *et al.* 2007). Although the physiological role of UGT1A_i2 proteins remains poorly understood, some researchers have suggested that they are involved in the regulation of UGT1A activity (Girard *et al.* 2007; Levesque *et al.* 2007; Bellemare *et al.*, 2010), possibly through the formation of i1–i2 heterodimers. The existence of UGT1A_i2 proteins may complicate determination of the expression levels of active UGTs in human tissues. New studies of UGT mRNA expression levels must take this alternative splicing into account by, for example, designing suitable polymerase chain reaction (PCR) primers that can distinguish between exons 5a and 5b.

Human *UGT2A* and *UGT2B* genes are located on chromosome 4q13 (Guillemette *et al.*, 2010, Meech *et al.*, 2012, Mackenzie *et al.*, 2005). In contrast to the *UGT1A* gene locus, the enzymes of UGT2A and 2B subfamilies are encoded mainly by separate genes comprised of six unique exons (Figure 5). The exceptions are UGTs 2A1 and 2A2, which, like the *UGT1A* gene locus, are encoded by a separate exon 1 and share remaining exons 2–6, thus resulting in identical C-terminal domains (Sneitz *et al.*, 2009). The genes within subfamilies *UGT2A* and *UGT2B* generally share more than 70% of their gene sequences (Meech *et al.*, 2012). This high level of sequence similarity, resulting in a complicated orthologous relationship between species, led to the adoption of the sequential numbering system for *UGT2A* and *UGT2B* genes based on the chronological order of their discovery (Mackenzie *et al.*, 1997). Similarly to the *UGT1A* genes, alternative splicing was also found in *UGT2A* and *UGT2B* genes (Guillemette *et al.*, 2010). At the moment, however, the extent and functional significance of these phenomena remain poorly understood and should be addressed in future studies.

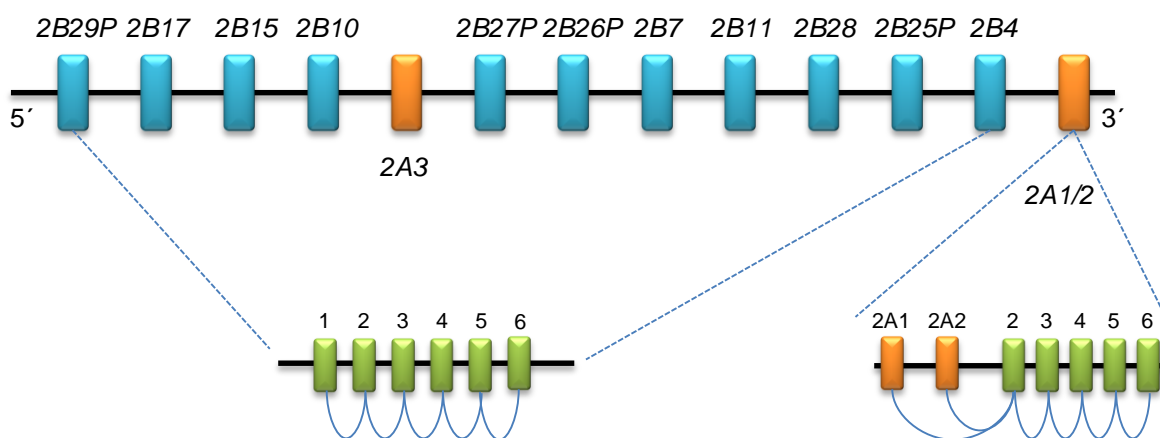


Figure 5. Structure of human *UGT2A* and *UGT2B* family genes on chromosome 4q13. Most of the proteins are encoded by separate genes consisting of six unique exons. For UGTs 2A1 and 2A2, however, similar to the *UGT1A* gene locus, only the first exon is unique; exons 2–6 are common.

2.1.3 Molecular structure and membrane topology of UGTs

Human UGTs are membrane proteins located in the endoplasmic reticulum of the cell. In addition, some studies have also located UGTs in the Golgi and nucleus membranes (Radomska-Pandya *et al.*, 2002, Hauser *et al.*, 1984). UGT polypeptides are synthesized as the precursors of approximately 530 amino acids, containing an N-terminal signal sequence peptide that directs the integration of the protein into the endoplasmic reticulum (Ouzzine *et al.*, 1999b, Ouzzine *et al.*, 1999a, Mackenzie and Owens, 1984). After membrane integration, although the order of events remains only partially understood, the signal sequence is cleaved and the protein is probably *N*-glycosylated (Nakajima *et al.*, 2010, Barbier *et al.*, 2000, Mackenzie, 1990). The mature UGT protein is approximately 505 residues long. A schematic representation of the UGT primary structure appears in Figure 6.

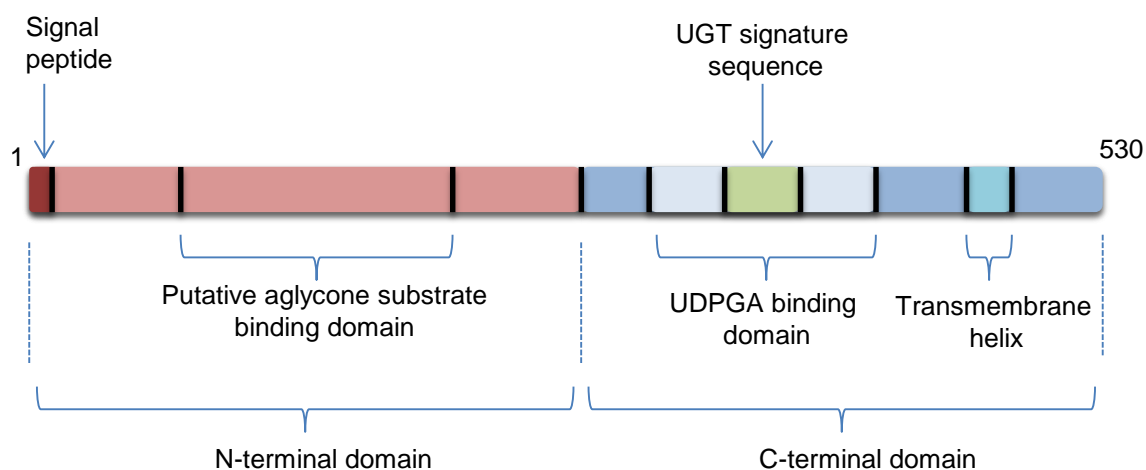


Figure 6. Schematic representation of the UGT primary structure.

The UGT polypeptide consists of two similarly sized parts: N- and C-terminal domains. Of these two domains, the C-terminal domain is generally more conserved across different UGTs and contains the UDPGA binding domain (Miley *et al.*, 2007, Patana *et al.*, 2007), as well as the

transmembrane helix, which anchors the protein into the membrane (Meech *et al.*, 1996, Meech and Mackenzie, 1998). Apart from its primary anchoring function, the transmembrane domain and C-terminal tail may also function as a membrane-targeting sequence (Meech and Mackenzie, 1998, Ouzzine *et al.*, 2006). In addition, the C-terminal domain also contains a “UGT signature sequence”, a 44-residue-long sequence within the UDPGA binding site found in all glycosyltransferases (sequence PDOC00359; <http://prosite.expasy.org/>; last accessed on 24 October 2012). On the other hand, the N-terminal domain is more variable within the UGT family and contains a putative domain responsible for the binding of the aglycone substrate (Lewis *et al.*, 2007, Itäaho *et al.*, 2010, Fujiwara *et al.*, 2009a).

In contrast to their primary structure, the secondary and tertiary structures of UGTs, as well as the corresponding membrane topology, remain largely unknown. Despite significant research efforts thus far, the full-length X-ray crystal structure of mammalian UGT is unavailable, presumably due to considerable difficulties in isolating and purifying fully active UGTs, as well as in crystallizing membrane proteins. Until now, only a partial crystal structure of UGT2B7 C-terminal domain, without the “envelope helices” (see below), the trans-membrane helix, and the cytoplasmic tail, was elucidated (Miley *et al.*, 2007). That study revealed that the C-terminus of UGT2B7 is a globular domain with a Rossmann-type fold. The core of the protein is a single parallel β -sheet consisting of six individual strands surrounded by seven α -helices (Miley *et al.*, 2007). Due to the lack of sufficient crystallographic data from the N-terminal domain, numerous studies addressed the complete structure of UGTs by means of homology modeling using plant and bacterial glycosyltransferases from the GT1 family as templates (Lewis *et al.*, 2011, Laakkonen and Finel, 2010, Fujiwara *et al.*, 2009b, Li and Wu, 2007, Locuson and Tracy, 2007).

The consensus results of crystallography and modeling indicate that UGTs are GT-B fold glycosyltransferases with type I membrane topology (Figure 7). In the GT-B fold structure, both the N- and C-terminal domains are $\beta/\alpha/\beta$ Rossmann-type domains connected by a flexible linker (Lairson *et al.*, 2008). UGT domains are flexibly linked and face each other; the active site lies positioned within the resulting cleft (Miley *et al.*, 2007, Laakkonen and Finel, 2010, Fujiwara *et al.*, 2009b). In addition to the two large domains, a recent modeling study of UGT1A1 identified two C-terminal “envelope” helices that extend over both domains (Laakkonen and Finel, 2010) (Figure 7). The N-terminal domain is associated with the binding of the aglycone substrate, whereas the C-terminal domain binds UDPGA. The main mass of the protein, including the active site, is located on the luminal side of the endoplasmic reticulum membrane (for reviews, see Bock, 2010, Magdalou *et al.*, 2010, Radomska-Pandya *et al.*, 2005b). The C-terminal domain also contains a transmembrane helix as well as the 20- to 25-residue-long cytoplasmic “tail” (Figure 7). Apart from the C-terminal transmembrane helix, possible additional membrane-binding regions were suggested within the N-terminal domain (Meech and Mackenzie, 1998, Ciotti *et al.*, 1998).

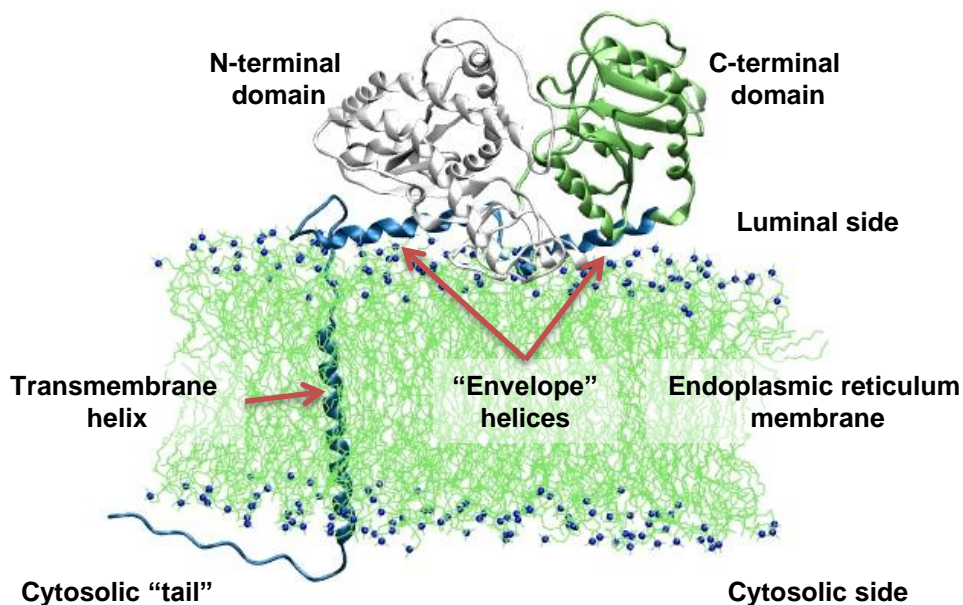


Figure 7. Graphical representation of the putative UGT structure in the membrane of the endoplasmic reticulum (picture prepared by Docent Liisa Laakkonen).

The intraluminal orientation of human UGTs necessitates a number of active transporters for the successful catalytic function, in specific the uptake of UDPGA and efflux of formed glucuronides. For example, the nucleotide sugar transporters transfer the UDPGA from the cytosol into the lumen of the endoplasmic reticulum (reviewed by, Csala *et al.*, 2007), whereas other transporters are involved in the glucuronide excretion from the lumen of the endoplasmic reticulum into cytosol (Battaglia and Gollan, 2001, Csala *et al.*, 2004, Revesz *et al.*, 2012). However, if activity assays are performed *in vitro*, for example in human liver microsomes (HLM), the transporters are not functional and the UGT enzymes exhibit diminished activity, commonly referred to as “UGT latency” (for details, see Section 2.3.1). The *in vitro* “UGT latency” is commonly removed by the addition of either detergent or pore-forming antibiotic alamethicin (Banhegyi *et al.*, 1993, Little *et al.*, 1997, Fisher *et al.*, 2000, Soars *et al.*, 2003). In addition, a number of studies reported that UGT enzymes form oligomers, most probably homo- and heterodimers (for examples, see Lewis *et al.*, 2011, Finel and Kurkela, 2008). The oligomerization of human UGTs may have significant consequences with respect to substrate selectivity and enzyme kinetic properties (Uchaipichat *et al.*, 2008, Zhou *et al.*, 2010, Zhou *et al.*, 2011).

2.1.4 Catalytic mechanism of glucuronidation

Human UGTs transfer the glucuronic acid moiety from the cosubstrate, UDP- α -D-glucuronic acid (UDPGA), to nucleophilic groups of small lipophilic molecules to yield exclusively β -D-glucuronides (Figure 8). The nucleophilic groups on the aglycone substrates are usually hydroxyl, amino, or carboxyl functionalities. Less often, glucuronidation may also occur on thiol and enolate functionalities or even on carbons with a weak C–H bond (“acidic carbons”) (Argikar, 2012). The catalytic mechanism resembles S_N2 -like nucleophilic substitution where the nucleophilic group of the aglycone substrate attacks the anomeric carbon of the UDP- α -D-glucuronic acid. The S_N2 -like direct displacement mechanism is supported by the inversion of

the anomeric carbon configuration from α in the UDP- α -D-glucuronic acid to β in the resultant β -D-glucuronide (Axelrod *et al.*, 1958, Johnson and Fenselau, 1978), as well as the influence of substituents on the reaction rate (Yin *et al.*, 1994).

Studies of the glucuronidation reaction suggest that UGT enzymes follow a serine protease-like mechanism, with a catalytic dyad — aspartate and histidine — activating the hydroxy group of the aglycone for the nucleophilic attack (Miley *et al.*, 2007, Patana *et al.*, 2008, Ouzzine *et al.*, 2003, Li *et al.*, 2007). According to this mechanism, histidine acts as a general base and accepts a proton from the aglycone hydroxy group. A conserved acidic residue in the proximity of catalytic histidine, such as the aspartate, would stabilize the protonated histidine through a “charge-relay” mechanism (Figure 8). The negative charge on the β -phosphate moiety of the departing UDP group would be stabilized by another histidine residue (Miley *et al.*, 2007, Li *et al.*, 2007).

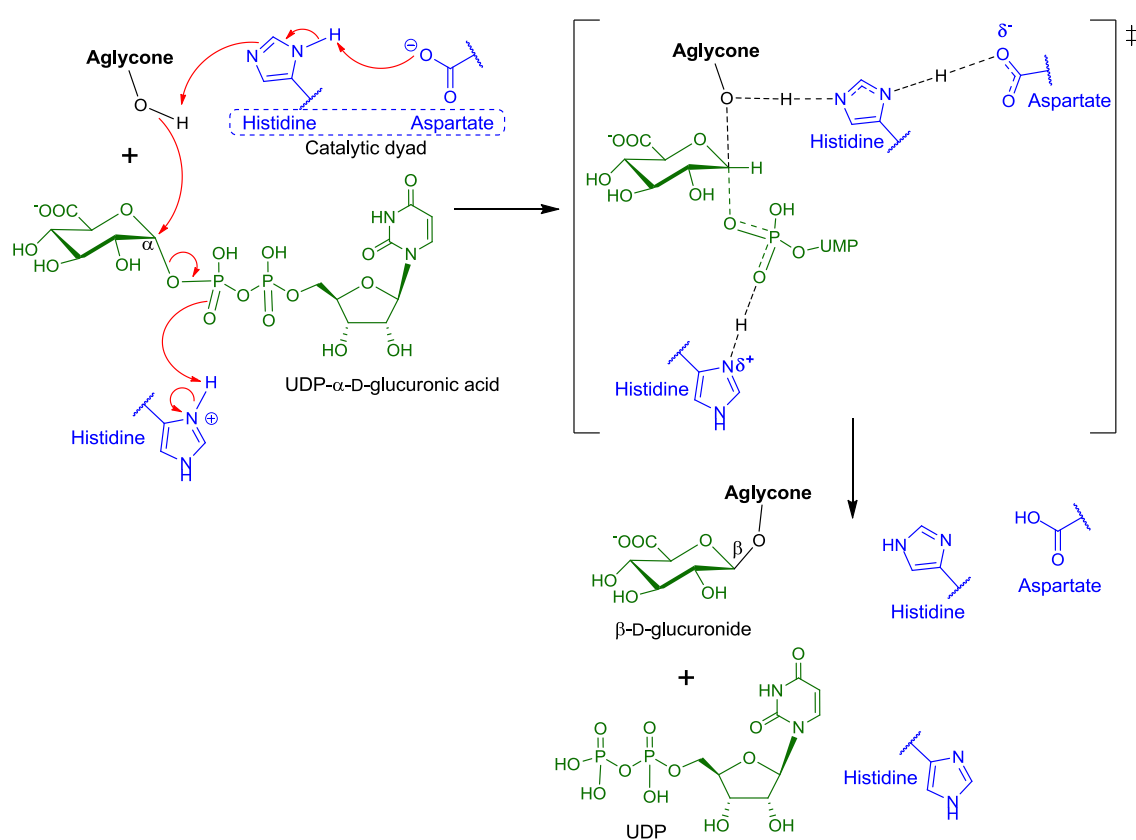


Figure 8. The transfer of the glucuronic acid moiety to the hydroxy group of aglycone substrate resembles S_N2 -like nucleophilic substitution. Histidine and aspartate form a catalytic dyad.

A study of UGT1A9 identified histidine 37 and aspartate 143 as the catalytic dyad (Patana *et al.*, 2008). Similarly to the UGT1A9 results, histidine 35 and aspartate 151 in UGT2B7 (Miley *et al.*, 2007), and histidine 38 and aspartate 150 in UGT1A6 (Li *et al.*, 2007) were identified as the key catalytic residues. Moreover, as expected for the amino acids responsible for the catalytic activity, the histidine-aspartate catalytic dyad is highly conserved among human UGTs. An important exception occurs in UGT enzymes specialized in *N*-glucuronidation, namely UGTs 1A4 and 2B10, where a proline or leucine residue respectively replace the catalytic histidine (Kubota *et al.*, 2007, Kerdpin *et al.*, 2009).

In addition, the mutation of catalytic histidine to alanine in position 37 fully abolished the activity of UGT1A9 with phenolic substrates but, interestingly, only moderately decreased the activity toward substrates with amino group (Patana *et al.*, 2008). On the other hand, the same study showed that the mutations of aspartate 143 led to an inactive UGT1A9 enzyme, regardless of the aglycone substrate used. Taken together with the lack of catalytic histidine in UGTs 1A4 and 2B10, these results indicate that the catalytic mechanisms of *O*- and *N*-glucuronidation may differ. In contrast to *O*-glucuronidation, histidine is not essential to deprotonate the *N*-nucleophile; instead, only the aspartate is required to stabilize the developing positive charge during the *N*-nucleophile attack on the anomeric atom of glucuronic acid (Figure 9) (Patana *et al.*, 2008).

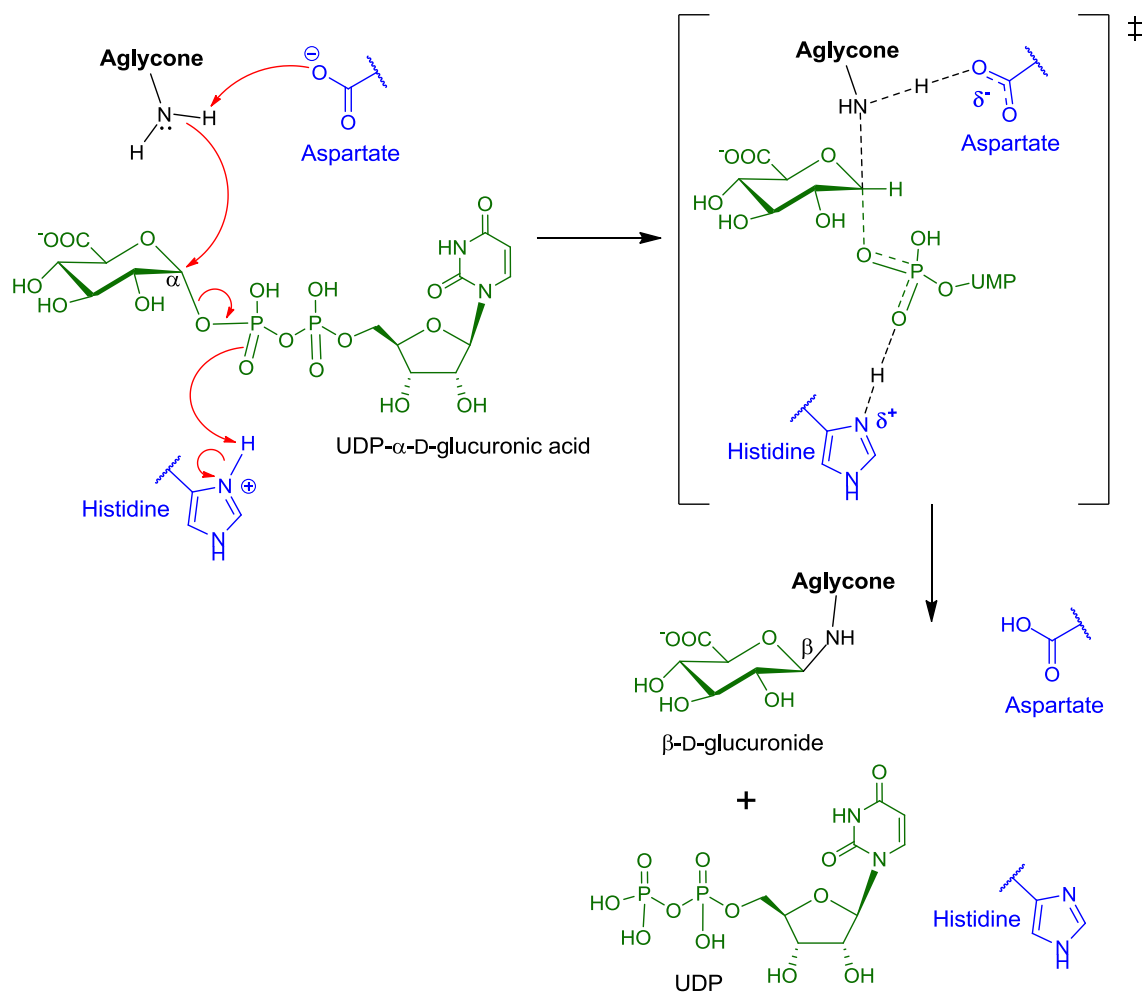


Figure 9. The catalytic mechanism of *N*-glucuronidation. In contrast to *O*-glucuronidation, the histidine residue is unnecessary for catalysis. As an alternative, the aspartate residue stabilizes the developing positive charge during the *N*-nucleophilic attack on the anomeric atom of glucuronic acid.

2.1.5 UGT expression in human tissues

UGT enzymes are expressed in a variety of human tissues and organs, most notably those tissues that are in imminent contact with xenobiotics, such as the liver, intestine, and kidneys (Table 1). Unfortunately, due to the lack of UGT-specific antibodies, direct immunochemical detection and

quantification of UGT proteins in tissues is rarely possible. Such antibodies are difficult to prepare mainly due to the high sequence similarity of UGT enzymes (Girard *et al.*, 2004). Until now, the literature has reported only a few UGT-specific antibodies, most notably a recent monoclonal antibody for UGT1A9 (Oda *et al.*, 2012). Polyclonal antibodies for UGTs 1A1, 1A3, 1A4, 1A6, and 1A9 were also reported (Ikushiro *et al.*, 2006), but examination of some of them in our laboratory, or in the Japanese laboratory with our recombinant UGTs 1A4 and 1A9, failed to yield a detectable response (Finel M., unpublished observations). In addition, several UGT-specific antibodies are commercially available for UGTs 1A1, 1A4, 1A6, 1A9, and 2B4, although these products may partially cross-react with similar UGT enzymes (Oda *et al.*, 2012, Izukawa *et al.*, 2009).

In the absence of reliable UGT-specific antibodies, most studies estimate UGT expression indirectly by measuring the expression of specific mRNA within the target tissue. Whereas older studies employed the (so-called) semiquantitative reverse transcriptase–polymerase chain reaction (RT-PCR) methodology (Strassburg *et al.*, 2000, Strassburg *et al.*, 1997, Turgeon *et al.*, 2001, Nakamura *et al.*, 2008), newer studies use quantitative, real-time qRT-PCR to determine the exact copy-number of specific mRNAs (Izukawa *et al.*, 2009, Court *et al.*, 2012, Ohno and Nakajin, 2009, Nishimura and Naito, 2006). Although useful for approximating UGT-protein expression levels, particularly the lack of expression if mRNA proved undetectable, studies of mRNA expression may be limited by poor correlation between measured mRNA levels and actual protein levels (Oda *et al.*, 2012, Izukawa *et al.*, 2009). Recent advances in liquid chromatography–mass spectrometry (LC–MS) could solve this problem through direct quantification of UGT proteins (Harbourt *et al.*, 2012, Fallon *et al.*, 2008), but not even they can distinguish between active, inactive, or incorrectly folded UGTs (Oda *et al.*, 2012, Zhang *et al.*, 2012a). The combined results of recent qRT-PCR studies of UGT mRNA expression and LC–MS analyses are presented in Table 1.

Table 1. Expression of UGT enzymes in human tissues.

Enzyme	Tissues	Method	References
UGT1A1	Liver > intestine >> kidney, trachea, prostate	qRT-PCR	(Court <i>et al.</i> , 2012)
	Liver > intestine, kidney	LC–MS	(Harbourt <i>et al.</i> , 2012)
	Liver	qRT-PCR	(Izukawa <i>et al.</i> , 2009)
	Liver > intestine	qRT-PCR	(Ohno and Nakajin, 2009)
	Liver > intestine >> kidney, trachea, prostate	qRT-PCR	(Nishimura and Naito, 2006)
UGT1A3	Liver > intestine, trachea, kidney, adipose, thymus, testis, prostate, uterus, nasal	qRT-PCR	(Court <i>et al.</i> , 2012)
	Liver	LC–MS	(Harbourt <i>et al.</i> , 2012)
	Liver	qRT-PCR	(Izukawa <i>et al.</i> , 2009)
	Liver > intestine	qRT-PCR	(Ohno and Nakajin, 2009)
UGT1A4	Liver > trachea > intestine, kidney, nasal, adipose, thymus, testis, prostate, uterus	qRT-PCR	(Court <i>et al.</i> , 2012)
	Kidney, liver	LC–MS	(Harbourt <i>et al.</i> , 2012)
	Liver	qRT-PCR	(Izukawa <i>et al.</i> , 2009)
UGT1A5	Liver	qRT-PCR	(Ohno and Nakajin, 2009)
	Intestine, liver, kidney, nasal	qRT-PCR	(Court <i>et al.</i> , 2012)
	Intestine, trachea, kidney, esophagus, trachea, prostate, placenta, liver	qRT-PCR	(Ohno and Nakajin, 2009)

UGT1A6	Nasal, liver, trachea > kidney, intestine, prostate, uterus, thymus, adipose	qRT-PCT	(Court <i>et al.</i> , 2012)
	Liver > kidney, intestine	LC-MS	(Harbourt <i>et al.</i> , 2012)
	Liver	qRT-PCR	(Izukawa <i>et al.</i> , 2009)
	Kidney, liver > intestine, adrenal, bladder, trachea	qRT-PCR	(Ohno and Nakajin, 2009)
UGT1A7	Liver, kidney > intestine, trachea	qRT-PCR	(Nishimura and Naito, 2006)
	Kidney, intestine, liver, nasal, trachea, adrenal	qRT-PCR	(Court <i>et al.</i> , 2012)
	Kidney, intestine	LC-MS	(Harbourt <i>et al.</i> , 2012)
UGT1A8	Esophagus, cervix, kidney, trachea, intestine	qRT-PCR	(Ohno and Nakajin, 2009)
	Nasal, intestine > adipose	qRT-PCR	(Court <i>et al.</i> , 2012)
UGT1A9	Intestine, kidney	LC-MS	(Harbourt <i>et al.</i> , 2012)
	Intestine, adrenal > bladder, trachea, breast	qRT-PCR	(Ohno and Nakajin, 2009)
	Liver, kidney > intestine, adipose	qRT-PCR	(Court <i>et al.</i> , 2012)
	Kidney > liver > intestine	LC-MS	(Harbourt <i>et al.</i> , 2012)
	Kidney > liver >> intestine	Immunochem.	(Oda <i>et al.</i> , 2012)
UGT1A10	Liver	qRT-PCR	(Izukawa <i>et al.</i> , 2009)
	Kidney > liver > intestine, adrenal, Kidney >> liver	qRT-PCR	(Ohno and Nakajin, 2009)
	Intestine > nasal, adipose	qRT-PCR	(Nishimura and Naito, 2006)
UGT2A1	Intestine > intestine	qRT-PCR	(Court <i>et al.</i> , 2012)
	Kidney > intestine	LC-MS	(Harbourt <i>et al.</i> , 2012)
UGT2A2	Intestine > esophagus, trachea, adrenal	qRT-PCR	(Ohno and Nakajin, 2009)
	Nasal	qRT-PCR	(Court <i>et al.</i> , 2012)
UGT2A3	Nasal	qRT-PCR	(Sneitz <i>et al.</i> , 2009)
	Nasal	qRT-PCR	(Nishimura and Naito, 2006)
UGT2B4	Trachea > lung	qRT-PCR	(Court <i>et al.</i> , 2012)
	Intestine, liver, adipose > pancreas, kidney	qRT-PCR	(Sneitz <i>et al.</i> , 2009)
	Liver >> intestine	qRT-PCR	(Court <i>et al.</i> , 2012, Court <i>et al.</i> , 2008)
UGT2B7	Liver >> intestine	qRT-PCR	(Court <i>et al.</i> , 2012)
	Liver	qRT-PCR	(Izukawa <i>et al.</i> , 2009)
	Liver >> heart > kidney, prostate, esophagus, trachea	qRT-PCR	(Ohno and Nakajin, 2009)
	Liver, kidney > intestine, pancreas, uterus, testis	qRT-PCR	(Nishimura and Naito, 2006)
UGT2B10	Liver >> intestine > pancreas	qRT-PCR	(Court <i>et al.</i> , 2012)
	Liver >> testis	qRT-PCR	(Izukawa <i>et al.</i> , 2009, Ohno and Nakajin, 2009, Nishimura and Naito, 2006)
UGT2B15	Liver	qRT-PCR	(Court <i>et al.</i> , 2012)
	Liver, kidney, breast > pancreas, nasal	qRT-PCR	(Court <i>et al.</i> , 2012)
	Liver > intestine >> nasal, pancreas, prostate	qRT-PCR	(Court <i>et al.</i> , 2012)
UGT2B17	Liver	qRT-PCR	(Izukawa <i>et al.</i> , 2009)
	Liver >> intestine, breast, prostate > trachea, testis	qRT-PCR	(Ohno and Nakajin, 2009)
	Liver >> intestine	qRT-PCR	(Nishimura and Naito, 2006)
	Adipose > nasal, liver, intestine, pancreas >> testis, trachea, bone marrow, thymus	qRT-PCR	(Court <i>et al.</i> , 2012)
UGT2B28	Liver	qRT-PCR	(Izukawa <i>et al.</i> , 2009)
	Intestine >> liver, adrenal, lung, thymus, spleen, trachea, kidney	qRT-PCR	(Ohno and Nakajin, 2009)
	Liver >> intestine > trachea, testis, pancreas	qRT-PCR	(Nishimura and Naito, 2006)
UGT2B28	Liver	qRT-PCR	(Court <i>et al.</i> , 2012)

As mentioned previously, out of all studied human tissues, the overall UGT expression appears most abundant in liver, small intestine, and kidneys. From the perspective of drug discovery and development, it is very important to know the absolute and relative abundance of UGT enzymes in these tissues. Harbourt *et al.* (2012) recently employed LC-MS to measure the absolute abundance of UGT1A enzymes in microsomal protein digest. Authors found that absolute

enzyme expression varied from 3 to 96 pmol per mg of protein in liver, intestinal, and kidney microsomes (Harbourt *et al.*, 2012). The relative expression of UGTs mRNA in liver, small intestine, and kidneys appears in Figure 10.

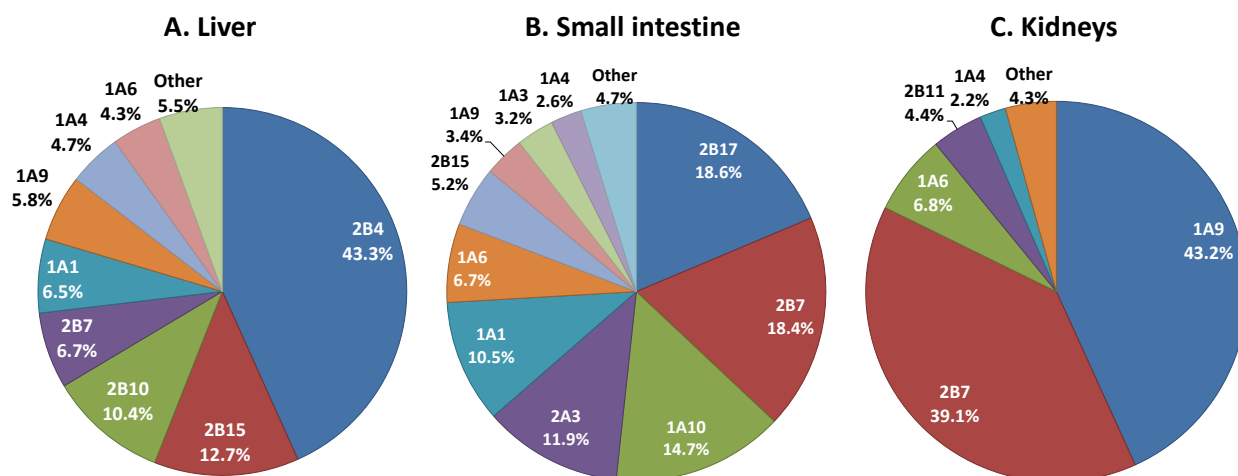


Figure 10. The relative expression of UGT mRNA (% of total) in (A) liver, (B) small intestine, and (C) kidneys. For the liver expression pie chart we have combined and averaged data from Court *et al.*, 2012, Ohno and Nakajin, 2009, and Izukawa *et al.*, 2009. For small intestine and kidney pie charts we combined and averaged the data from Court *et al.*, 2012 and Ohno and Nakajin, 2009. To our best knowledge, these are the only studies that both use modern methodology (*qRT-PCR* or *LC-MS*) and cover a wide selection of UGT enzymes.

The expression of individual UGT enzymes also exhibits interindividual variability with respect to age, sex, enzyme inducers, and genetic polymorphisms (Izukawa *et al.*, 2009, Court, 2010). Important factors responsible for interindividual variation may include: (1) UGT polymorphisms, alternate splicing, and epigenetic variation; (2) liver-enriched transcription factors such as hepatic nuclear factors $\alpha 1$ and $\alpha 4$; and (3) ligand-activated transcription factors such as AhR, Nrf2, PXR, CAR, and PPAR α (recently reviewed in Bock, 2010).

A detailed list of UGT polymorphisms can be found on the following webpage www.pharmacogenomics.pha.ulaval.ca/cms/ugt_alleles/ (last accessed on 24 October 2012).

2.2 UGT substrate specificity

UGT enzymes exhibit broad and partially overlapping substrate specificity. In many cases, a single substrate is glucuronidated by multiple UGT enzymes, although at different affinities and turnover rates. The recognition of substrates by individual UGT enzymes generally depends on molecular size and geometry, lipophilicity ($\log P$), acid-base properties (pK_a), hydrogen bond acceptors and donors, and the spatial orientation of the nucleophilic group on the acceptor molecule (reviewed by Smith *et al.*, 2004, Miners *et al.*, 2004, Dong *et al.*, 2012). Despite broad substrate specificity, UGTs may still exhibit a high degree of regioselectivity and stereoselectivity (Bichlmaier *et al.*, 2006, Sten *et al.*, 2006, Sten *et al.*, 2009, Itäaho *et al.*, 2008, Kaivosari *et al.*, 2008). One should note, however, that even if a molecule is not a substrate for the specific UGT enzyme, it might still bind to its active site and act as an inhibitor. Selective

substrates and inhibitors are rarely known for UGT enzymes, especially those exhibiting high affinity and exclusive selectivity (for reviews, see Miners *et al.*, 2010, Court, 2005). The list of both typical and selective substrates for human UGTs appears in Table 2. The list of UGT substrates presented is not a comprehensive review of this complex subject, but rather a general overview of the most common substrates. Moreover, the selectivity of the presented UGT-selective substrates is rarely absolute and may depend on assay conditions, the observation of specific products formed, or tissues studied (see original references for further details).

Table 2. *The overview of typical and selective substrates for human UGTs. If the substrate is UGT-selective only within the specific tissue, but not for all UGT enzymes expressed in the human body, the tissue is indicated within parenthesis. The list of literature references appears below the table.*

UGT enzyme	Typical substrates	Proposed selective substrates
UGT1A1	Bilirubin ^{1,5} , estrogens ^{2,4} , various phenols ^{2,3} , anthraquinones ^{2,3} , flavones ² , coumarins ³	Bilirubin ⁵ , etoposide ⁶
UGT1A3	Various phenols ^{2,3} , anthraquinones ^{2,3} , flavones ² , amines ^{7,8} , bile acids ² , coumarins ³ , carboxylic acids ^{2,3} , estrogens ^{2,4}	Zolarsartan ⁸
UGT1A4	Various amines and <i>N</i> -heterocycles ⁷ , estradiols ⁴ , sapogenins ³ , phenols ^{2,3} , aliphatic alcohols ^{2,3}	1'-Hydroxymidazolam ⁹ , midazolam <i>N</i> -glucuronide ³² , trifluoperazine ¹⁰
UGT1A5	<i>Orphan enzyme, substrates are currently unknown</i> ³¹	
UGT1A6	Small and planar phenols ^{2,3}	Serotonin ¹¹ , deferiprone ¹²
UGT1A7	Various phenols ^{2,3} , estradiols ⁴	
UGT1A8	Various phenols ^{2,3} , flavonoids ^{2,3} , anthraquinones ^{2,3} , some steroids ⁴	
UGT1A9	Various phenols ^{2,3} , anthraquinones ^{2,3} , flavones ^{2,3} , coumarins ^{2,3} , amines and <i>N</i> -heterocycles ^{3,7} , carboxylic acids ³	Entacapone (liver) ¹³ , mycophenolic acid (liver) ¹⁴ , phenylbutazone ¹⁵ , propofol ¹⁶
UGT1A10	Various phenols ^{2,3} , estrogens ⁴	Dopamine ¹⁷
UGT2A1	Phenolic compounds ^{18,21} , aliphatic and monoterpene alcohols ²¹ , estrogens ⁴ , androgens ¹⁹	
UGT2A2	Bile acids, small phenols ¹⁸	
UGT2A3	Bile acids ^{18,20}	
UGT2B4	Aliphatic alcohols ^{2,3} , bile acids ^{2,3} , estrogens ⁴ , opioids ²²	
UGT2B7	Aliphatic alcohols ^{2,3} , carboxylic acids ^{2,3} , estrogens ⁴ , androgens ¹⁹ , bile acids ^{2,3} , opioids ²³	Zidovudine ²² , epitestosterone (liver) ¹⁹ , morphine (partially) ²²⁻²⁴ , denopamine ²⁵
UGT2B10	Nicotine ²⁶ , medetomidine ²⁷ , tricyclic antidepressants ²⁸	Nicotine ²⁶ , levomedetomidine (partially) ²⁷
UGT2B11	Fatty acid metabolites ³³ (results are not confirmed by independent laboratory)	
UGT2B15	Estrogens ⁴ , aliphatic alcohols ^{2,3} , various phenols ^{2,3}	<i>S</i> -Oxazepam ²⁹
UGT2B17	Androgens ¹⁹ , estrogens ⁴ , phenols ³	Testosterone (liver) ¹⁹
UGT2B28	Steroids (poor activity) ³⁰	

¹Ritter *et al.*, 1992; ²King *et al.*, 2000; ³Tukey and Strassburg, 2000; ⁴Itäaho *et al.*, 2008; ⁵Bosma *et al.*, 1994; ⁶Watanabe *et al.*, 2003, Wen *et al.*, 2007; ⁷Kaivosaaari *et al.*, 2011; ⁸*N*2-glucuronidation; Alonen *et al.*, 2008; ⁹*N*-glucuronidation, Zhu *et al.*, 2008; ¹⁰Uchaipichat *et al.*, 2006; ¹¹Krishnaswamy *et al.*, 2003a; ¹²Benoit-Biancamano *et al.*, 2009; ¹³Lautala *et al.*, 2000; ¹⁴phenol glucuronide, Picard *et al.*, 2005, Bernard and Guillemette, 2004; ¹⁵*C*-glucuronidation Nishiyama *et al.*, 2006; ¹⁶Soars *et al.*, 2004; ¹⁷Itäaho *et al.*, 2009; ¹⁸Sneitz *et al.*, 2009; ¹⁹Sten *et al.*, 2009; ²⁰Court *et al.*, 2008; ²¹Jedlitschky *et al.*, 1999; ²²Court *et al.*, 2003; ²³Stone *et al.*, 2003; ²⁴Ohno *et al.*, 2008; ²⁵Kaji and Kume, 2005; ²⁶Kaivosaaari *et al.*, 2007; ²⁷Kaivosaaari *et al.*, 2008; ²⁸Zhou *et al.*, 2010; ²⁹Court *et al.*, 2002; ³⁰Levesque *et al.*, 2001; ³¹Finel and Miners, unpublished results; ³²Hyland *et al.*, 2009; ³³Turgeon *et al.*, 2003.

As a general tendency, phenolic substrates are mainly glucuronidated by enzymes from UGT1A and UGT2A subfamilies, whereas aliphatic alcohols are substrates to enzymes of the UGT2B subfamily (Wu *et al.*, 2011, Dong *et al.*, 2012, King *et al.*, 2000, Tukey and Strassburg, 2000, Sorich *et al.*, 2006). Carboxylic acids, however, may be substrates to numerous UGT enzymes. UGTs 1A1, 1A9, 2B4, and 2B7, for example, proved to be the main enzymes responsible for glucuronidation of commonly prescribed non-steroidal anti-inflammatory drugs (NSAID; King *et al.*, 2001, Kuehl *et al.*, 2005, Zhang *et al.*, 2012b), whereas UGT1A1 exclusively glucuronidates bilirubin, a breakdown product of heme catabolism (Bosma *et al.*, 1994). The glucuronidation of bilirubin is a major detoxification pathway necessary for survival (reviewed by Strassburg, 2010). In contrast to bilirubin detoxification, the glucuronidation of some carboxylic acids may lead to chemically reactive products involved in a number of adverse drug reactions (reviewed by Regan *et al.*, 2010). Amines and nitrogen-containing heterocycles are mainly glucuronidated by UGTs 1A4 and 2B10 (Kaivosaaari *et al.*, 2008, Kaivosaaari *et al.*, 2007, Zhou *et al.*, 2010), although other enzymes, such as UGTs 1A3, 1A9, and 2B7 may also play significant roles in *N*-glucuronidation (reviewed by Kaivosaaari *et al.*, 2011).

2.2.1 Glucuronidation of drugs of abuse

Glucuronidation represents a significant metabolic pathway for the elimination of drugs of abuse and their phase I metabolites (Table 3). The list of abused drugs eliminated through glucuronidation consists of anabolic steroids, benzodiazepines, cannabinoids, opioids, hallucinogens, and widely abused substances such as nicotine and ethanol. As a result, the detection and analysis of glucuronides is becoming increasingly important in both forensic and antidoping studies (for examples, see Meyer and Maurer, 2012, French *et al.*, 2011, Kamata *et al.*, 2006). In addition, identifying the individual UGT enzymes involved in the metabolism of drugs of abuse may contribute to a better understanding of the tissue localization of metabolism, drug-drug interactions, and interindividual variability (Schwaninger *et al.*, 2009, Kaivosaaari *et al.*, 2007, Mazur *et al.*, 2009).

Table 3. The list of drugs of abuse eliminated by glucuronidation (in alphabetical order).

Drugs of abuse	Metabolism by UGTs	References
Anabolic steroids and their phase I metabolites	Glucuronidated by UGTs 1A1, 1A3, 1A4, 1A8, 1A9, 1A10, 2B4, 2B7, and 2B15.	(Kuuranne <i>et al.</i> , 2003) (Hintikka <i>et al.</i> , 2008) (Hyland <i>et al.</i> , 2009)
Benzodiazepines	Midazolam, lorazepam, and oxazepam are glucuronidated.	(Turfus <i>et al.</i> , 2011) (Court <i>et al.</i> , 2002)
Cannabinoids (classical and synthetic)	Phase I metabolites of classical cannabinoids are glucuronidated by UGTs 1A1, 1A3, 1A8, 1A9, 1A10, and 2B7. Synthetic cannabinoids are glucuronidated mainly by UGTs 1A1, 1A3, 1A9, 1A10, and 2B7	(Mazur <i>et al.</i> , 2009) (Chimalakonda <i>et al.</i> , 2011)
Codeine	Codeine 6-glucuronide was reported as the main metabolite in urine. Codeine is glucuronidated by UGTs 2B4 and 2B7.	(Yue <i>et al.</i> , 1991) (Court <i>et al.</i> , 2003) (Raungrut <i>et al.</i> , 2010)
Ethanol	Ethyl-glucuronide is a biomarker of ethanol intoxication. Ethanol is glucuronidated mainly by UGTs 1A1 and 2B7.	(Walsham and Sherwood, 2012) (Foti and Fisher, 2005)

Lysergic acid diethylamide (LSD)	14-Hydroxy-LSD glucuronide is detected in urine.	(Canezin <i>et al.</i> , 2001)
MDMA (3,4-methylenedioxy- <i>N</i> -methylamphetamine, Ecstasy)	Metabolites are glucuronidated by UGTs 1A1, 1A3, 1A8, 1A9, 2B4, 2B7, 2B15, and 2B17.	(Schwaninger <i>et al.</i> , 2009, Shoda <i>et al.</i> , 2009)
5-Methoxy- <i>N,N</i> -diisopropyltryptamine (Foxy-methoxy)	Phase I metabolites are excreted as glucuronides.	(Kamata <i>et al.</i> , 2006)
Morphine	UGTs 2B7, 2B4, 1A1, and many others form morphine 3- and 6-glucuronides, the latter of which, is a potent analgesic.	(Stone <i>et al.</i> , 2003) (Court <i>et al.</i> , 2003) (Ohno <i>et al.</i> , 2008)
Nicotine	Glucuronidated by UGTs 2B10 and 1A4.	(Kaivosaaari <i>et al.</i> , 2007) (Chen <i>et al.</i> , 2007)
Oxymorphone	Oxymorphone 3-glucuronide is reported in urine.	(French <i>et al.</i> , 2011) (Dickerson <i>et al.</i> , 2012)
Psilocin	Psilocin glucuronide is the main metabolite in serum and urine.	(Hasler <i>et al.</i> , 2002) (Kamata <i>et al.</i> , 2003) (Kamata <i>et al.</i> , 2006)
Testosterone	Glucuronidated mainly by UGT2B17.	(Sten <i>et al.</i> , 2009)
Tramadol	<i>O</i> -Desmethyltramadol is glucuronidated by UGTs 1A7, 1A8, 1A9, 1A10, 2B7, and 2B15.	(Lehtonen <i>et al.</i> , 2010)

For some drugs of abuse, glucuronidation represents a major route of elimination, such as in the cases of morphine (Court *et al.*, 2003, Stone *et al.*, 2003, Ohno *et al.*, 2008), MDMA phase I metabolites (Schwaninger *et al.*, 2009, Pirnay *et al.*, 2006), psilocin (Kamata *et al.*, 2006, Hasler *et al.*, 2002, Kamata *et al.*, 2003), or even nicotine and its phase I metabolites (Kaivosaaari *et al.*, 2007, Chen *et al.*, 2007). On the other hand, as in the cases of ethanol (Walsham and Sherwood, 2012, Foti and Fisher, 2005), calassical cannabinoids (Mazur *et al.*, 2009), or lysergic acid diethylamide (LSD; Canezin *et al.*, 2001), the relative contribution of glucuronidation to the overall drug metabolism appears small. However, even if they are relatively minor metabolites, glucuronides may still serve as valuable markers of substance abuse in forensic or antidoping studies. Good examples are provided by glucuronides of ethanol (Walsham and Sherwood, 2012) and testosterone isomers (Sten *et al.*, 2009) used in the analyses of alcohol intoxication and testosterone doping, respectively.

2.2.2 Glucuronidation of psilocin

Psilocybin and its dephosphorylated active metabolite, psilocin, are hallucinogenic indole alkaloids present in mushrooms of the genus *Psilocybe*, colloquially referred to as “magic mushrooms” (Stamets, 2003). The Swiss chemist Albert Hofmann first isolated psilocybin in 1958 from *Psilocybe mexicana* (Hofmann *et al.*, 1958). Although prohibited in most countries, “magic mushrooms” are commonly used as recreational drugs (Tsujikawa *et al.*, 2003, Halpern, 2004, Bjornstad *et al.*, 2009). Following ingestion, psilocybin is quickly dephosphorylated to psilocin (Hasler *et al.*, 1997), an active metabolite that acts as an agonist of serotonin presynaptic 5-hydroxytryptamine_{2A} (5-HT_{2A}) receptors (Gonzalez-Maeso *et al.*, 2007). Psilocin is eliminated mainly by glucuronidation, and psilocin glucuronide proved to be the major fraction of administered dose in both serum and urine (Kamata *et al.*, 2006, Hasler *et al.*, 2002, Kamata *et al.*, 2003, Hasler *et al.*, 1997, Sticht and Kaferstein, 2000, Grieshaber *et al.*, 2001). Alternative

metabolic routes include oxidation *via* an assumed intermediate, 4-hydroxyindole-3-acetaldehyde, to yield 4-hydroxyindole-3-acetic acid and 4-hydroxytryptophol (Hasler *et al.*, 1997, Holzmann, 1995) (Figure 11).

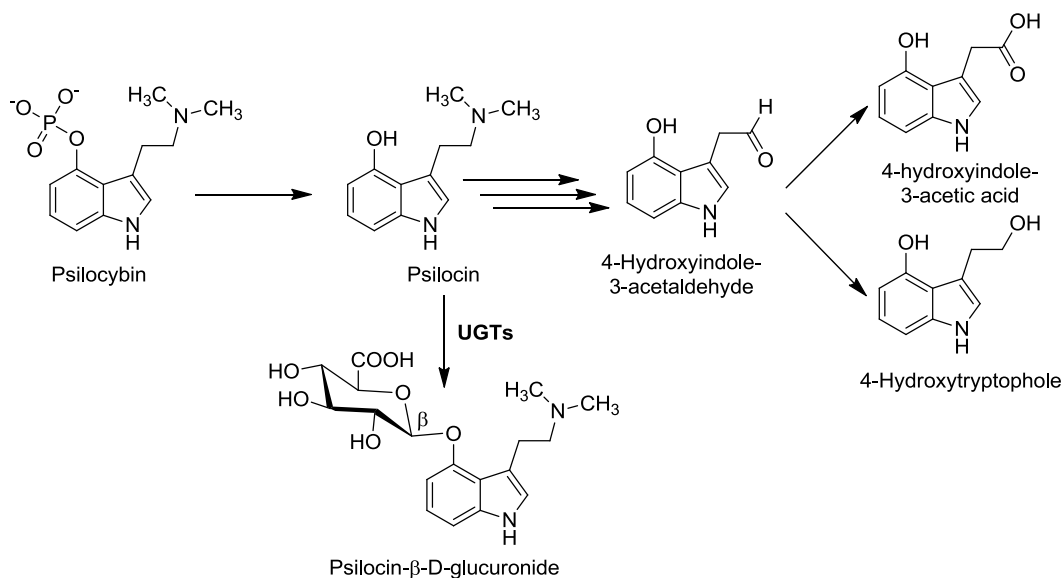


Figure 11. Metabolic pathways of psilocybin and psilocin in humans. The enzymes of oxidoreductive (phase I) metabolism are omitted for clarity.

2.2.3 Glucuronidation of endo- and xenobiotics with the indole scaffold

The indole scaffold is present in endogenous molecules, therapeutic and abused drugs, and natural products. Due to the high prevalence of the indole structure in a broad range of molecules with different pharmacodynamic effects, the indole scaffold is commonly referred to as the “privileged structure” (Welsch *et al.*, 2010, de Sa Alves *et al.*, 2009). In the body, the essential amino acid L-tryptophan is precursor for the synthesis of the neurotransmitter serotonin and hormone melatonin, as well as for a number of intermediates and downstream metabolites (Figure 13). Serotonin is exclusively glucuronidated by UGT1A6 (Krishnaswamy *et al.*, 2003a, King *et al.*, 1999), although the measured affinity toward the enzyme is very low ($K_m \approx 5\text{--}9$ mM). *N*-Acetylserotonin and 5-hydroxytryptophol, two endogenous metabolites of serotonin, are also predominantly glucuronidated by UGT1A6, even though there is a smaller contribution from UGTs 1A9 and 1A10 (Krishnaswamy *et al.*, 2004). In contrast to these results, 6-hydroxymelatonin, a degradation product of melatonin, is mainly glucuronidated by UGTs 1A9 and 1A10, whereas the activity of UGT1A8 was much lower (Krishnaswamy *et al.*, 2004). Two endogenous indoles with a carboxylic acid functional group, 5-hydroxytryptophan and 5-hydroxyindoleacetic acid, exhibited no glucuronidation activity in the preliminary assays with HLM (Krishnaswamy *et al.*, 2004). Structural analysis of the serotonin glucuronide by nuclear magnetic resonance (NMR) revealed that glucuronidation occurs exclusively on the hydroxyl group of the indole ring; no *N*-glucuronides were detected (Krishnaswamy *et al.*, 2003b).

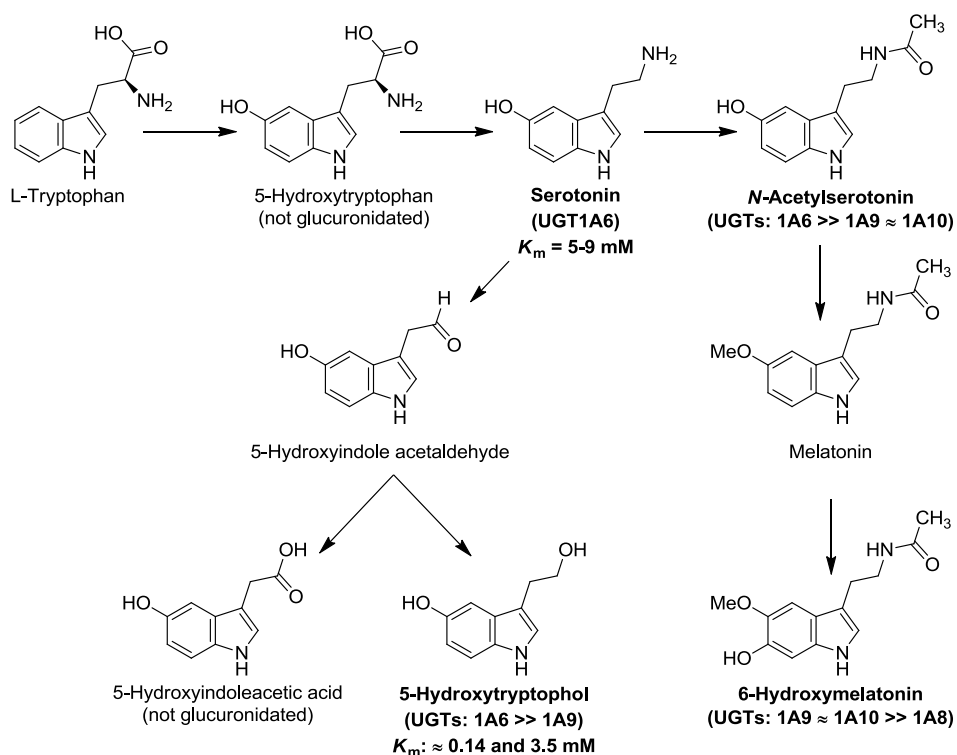


Figure 12. Metabolism of endogenous indoles in the human body. For clarity, this figure omits individual enzymes involved in the interconversion of metabolites. Serotonin (Krishnaswamy *et al.*, 2003a, King *et al.*, 1999, Krishnaswamy *et al.*, 2003b), N-acetylserotonin (Krishnaswamy *et al.*, 2004), 5-hydroxytryptophol (Krishnaswamy *et al.*, 2004), and 6-hydroxymelatonin (Krishnaswamy *et al.*, 2004) are substrates for UGT enzymes (indicated in bold; if known, K_m values are presented below the name of the UGT enzyme).

The indole scaffold is also widely present in both therapeutic drugs and drugs of abuse (Figure 13). The relative contribution of glucuronidation to the overall metabolism of these drugs and their phase I metabolites varies considerably, however. Indomethacin, a prescription NSAID commonly used for the treatment of pain and fever, is subject to extensive acyl glucuronidation and is a substrate mainly for UGTs 1A9, 1A10, 2B7, and 2A1, although many other UGT enzymes may also offer a significant contribution (Kuehl *et al.*, 2005, Zhang *et al.*, 2012b). Triptans are agonists of serotonin 5-HT_{1B} and 5-HT_{1D} receptors that are used to treat acute migraine (for a review, see Johnston and Rapoport, 2010). After phase I metabolic reactions, indoleacetic acid metabolites of sumatriptan (Dixon *et al.*, 1993) and almotriptan (McEnroe and Fleishaker, 2005) are glucuronidated and excreted into the urine. “Setrons” are antagonists of serotonin 5-HT₃ receptors used mainly to treat nausea and vomiting, especially in cancer patients undergoing chemotherapy (for a review, see Thompson and Lummis, 2007). Ondansetron is predominantly oxidized by CYPs to 8-hydroxyondansetron, which is glucuronidated further (Musshoff *et al.*, 2010). Alosetron, a 5-HT₃ antagonist predominantly used for the treatment of irritable bowel syndrome, is similarly oxidized to 6-hydroxyalosectron and is glucuronidated further (Lotronex[®] prescribing information, Prometheus Laboratories Inc., San Diego, CA, USA). Dolasetron undergoes stereoselective reduction of the carbonyl group in the octahydro quinolizin ring to yield predominantly (*R*)-reduced dolasetron (Reith *et al.*, 1995). Both (*R*)- and (*S*)-reduced dolasetron are glucuronidated further to form the major metabolites excreted in urine; the glucuronidation apparently favors the (*S*)-isomer (Reith *et al.*, 1995). Similar to the

metabolism of ondansetron and alosetron, tropisetron is first oxidized to 5-hydroxytropisetron and further glucuronidated to the major metabolite 5-hydroxytropisetron glucuronide (Fischer *et al.*, 1992).

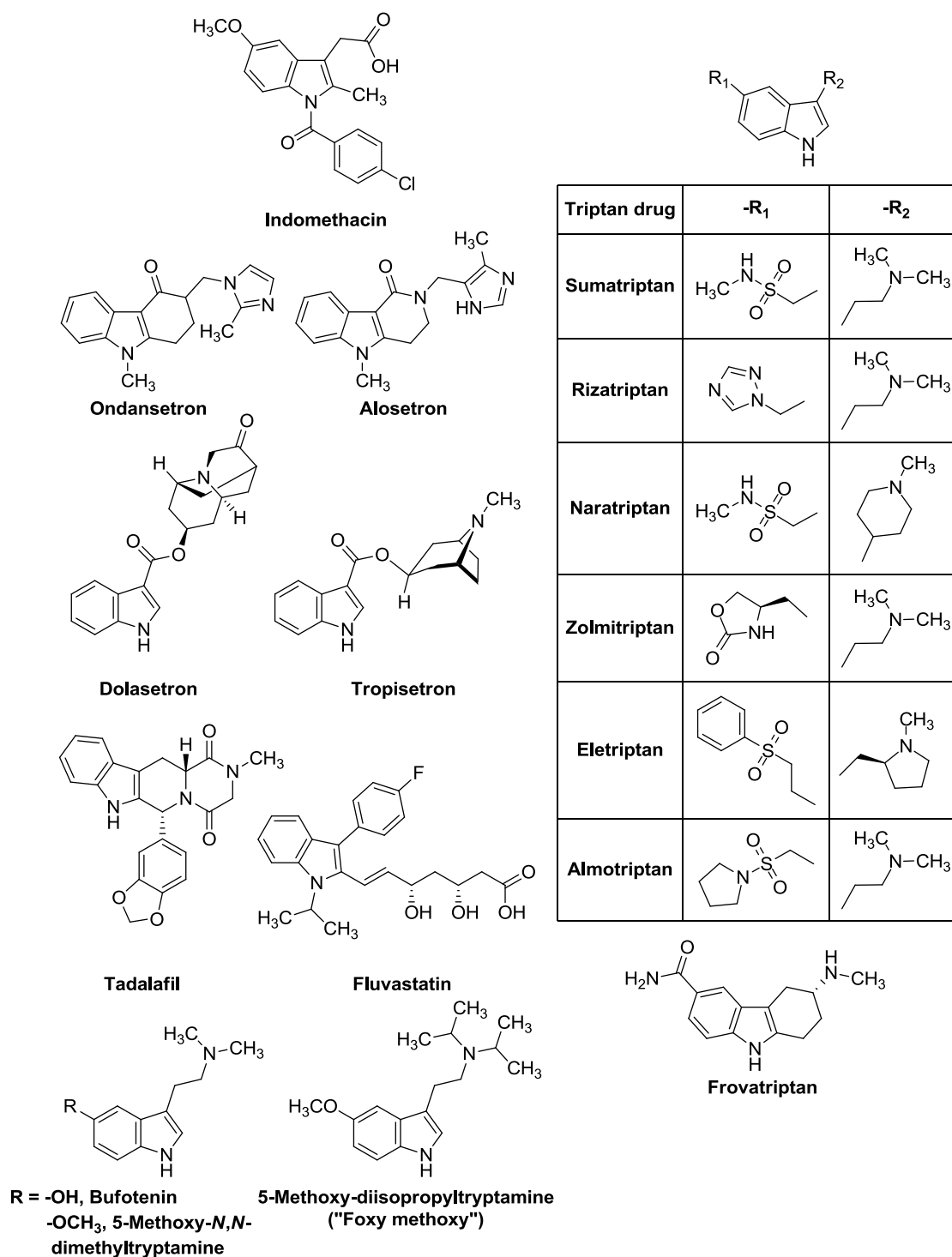


Figure 13. Chemical structures of therapeutic and abused drugs with indole scaffold.

Tadalafil, a selective inhibitor of phosphodiesterase type 5 used to treat erectile dysfunction, is sequentially metabolized by CYPs and UGTs to form a major metabolite, methylcatechol glucuronide (Forgue *et al.*, 2007). Glucuronides were identified as minor metabolites of

fluvastatin, a drug used to lower cholesterol levels by inhibiting 3-hydroxy-3-methyl-glutaryl-CoA reductase, an important enzyme in the biosynthesis of cholesterol (Dain *et al.*, 1993).

Bufotenin, 5-methoxy-*N,N*-dimethyltryptamine, and 5-methoxy-*N,N*-diisopropyltryptamine (Foxy-methoxy) are hallucinogenic indoles that occasionally serve as recreational drugs (Kamata *et al.*, 2006, Shen *et al.*, 2010, McBride, 2000) (Figure 13). These compounds are subjected to glucuronidation either directly (bufotenin) or after *O*-demethylation reaction (5-methoxy derivatives) (Kamata *et al.*, 2006, Shen *et al.*, 2010, Raisanen, 1984).

2.3 Measurement and prediction of UGT activity based on *in vitro* assays

Studies of UGT function and structure frequently use *in vitro* activity and inhibition assays. Most notably, *in vitro* UGT assays are employed in preclinical drug development to estimate drug glucuronidation *in vivo*, both qualitatively and quantitatively, as well as to investigate possible drug-drug interactions (Miners *et al.*, 2010). These requirements are also reflected in recent regulatory guidelines from EMA and FDA on drug interactions (see Section 1 for document links). Moreover, *in vitro* assays should provide reliable answers to questions about UGT substrate selectivity, catalytic mechanisms, or the activity of polymorphic enzymes. Therefore, careful optimization of *in vitro* assay conditions is not only an integral part of the drug discovery and development process, but also a crucial step in successful studies of UGT structure and function.

In vitro UGT assay are usually performed with either human microsomal fractions, recombinant human enzymes, or, more recently, with hepatocytes. Microsomal fractions, such as human liver microsomes (HLM), intestinal microsomes (HIM), or kidney microsomes (HKM), contain several UGT enzymes (see Table 1) and commonly serve to determine whether or not the compound of interest undergoes glucuronidation, and if so, what types of glucuronides are produced, if more than one is detected. If a compound undergoes glucuronidation, enzyme kinetic assays are employed to quantitatively determine the rate of glucuronidation. Next, the reaction rate measured *in vitro* is extrapolated to estimate the glucuronidation *in vivo* (Miners *et al.*, 2010). Though highly helpful in the initial phases of the study, the complex composition of the microsomal fractions makes them less useful in mechanistic studies of glucuronidation, especially in identifying individual UGT enzymes responsible for the reaction (reaction phenotyping), and in estimating the effects of polymorphic mutations in the enzymes on their activity. Recombinant human enzymes, most commonly expressed in insect *Sf9* or human HEK293 cells, are used to examine the activity of individual UGTs and their mutants (reviewed by Radomska-Pandya *et al.*, 2005a).

Despite the widespread use of microsomal fractions and recombinant UGT enzymes, several studies have reported that *in vitro* glucuronidation assays often result in large underestimations of UGT activity *in vivo* (Soars *et al.*, 2002, Boase and Miners, 2002, Mistry and Houston, 1987). Variability in experimental conditions, nonspecific microsomal binding, inappropriate physiological scaling factors, and unsuitable kinetic modeling may all influence the reliability of *in vitro*–*in vivo* extrapolation. Some researchers have suggested isolated hepatocytes as a superior model for studies of glucuronidation (Engtrakul *et al.*, 2005), even despite their greater complexity, technical difficulties, and higher cost (Hewitt *et al.*, 2007). The poor *in vitro*–*in vivo*

correlation for drugs eliminated by glucuronidation prompted intensive research seeking a detailed understanding, improvement, and standardization of UGT assays. Numerous experimental factors were found to affect *in vitro* UGT enzyme activity, including buffer type, pH, ionic strength, UGT latency, organic solvent, glucuronide stability, atypical kinetics, and the nonspecific binding of substrates. Recent studies, however, have found that the addition of purified fatty acid-free bovine serum albumin (BSA) significantly enhances the *in vitro* activities of several human UGTs and CYPs and improves the *in vitro–in vivo* extrapolation. This phenomenon, commonly referred to as the “Albumin effect”, is becoming increasingly important in drug metabolism studies and will be described in further detail in Section 2.3.2.

2.3.1 Experimental conditions of the *in vitro* UGT assay

In vitro UGT assays are typically performed in 50- to 100-mM phosphate or TRIS [tris(hydroxymethyl)aminomethane] buffer at pH 7.4. Although these two buffers are generally interchangeable, some studies have reported higher UGT activity with TRIS buffer (Boase and Miners, 2002, Mutlib *et al.*, 2006, Walsky *et al.*, 2012) or, alternatively, bicarbonate buffer (Engtrakul *et al.*, 2005). Lower pH values (pH < 7.4) proved beneficial in assays with acidic substrates such as diclofenac, indomethacin, or mycophenolic acid (Zhang *et al.*, 2012b, Chang *et al.*, 2009), whereas higher pH values (pH > 7.4) stimulate the glucuronidation of basic substrates such as raloxifene (Chang *et al.*, 2009). Divalent metal ions increase UGT activity, and 1–10 mM of Mg²⁺ ions is typically added to *in vitro* UGT incubations (Fisher *et al.*, 2000, Boase and Miners, 2002, Walsky *et al.*, 2012). Since β -glucuronidase, a mammalian enzyme that hydrolyzes β -D-glucuronides could be present in microsomal fractions or hepatocytes (Levy, 1952), an inhibitor of this enzyme, D-saccharic acid 1,4-lactone (saccharolactone), was commonly added to UGT incubations. The tetrameric intraluminal β -glucuronidase was located in the endoplasmic reticulum and shown to hydrolyze bilirubin monoglucuronides *in vivo*, thus potentially contributing to the futile cycling of glucuronides (see Bock and Kohle, 2009 and references therein). However, due to observations of only minute β -glucuronidase activity *in vitro* and the potential inhibition of UGTs by saccharolactone, a recent study has suggested that the addition of saccharolactone offers no real benefit in assays with microsomal fractions (Oleson and Court, 2008).

DMSO (1–10%) is commonly included in glucuronidation assays in order to improve the aqueous solubility of substrates and inhibitors. Although some studies have found that the inclusion of a low concentration of DMSO benefits certain glucuronidation assays (Uchaipichat *et al.*, 2004, Zhang *et al.*, 2011), preliminary tests are recommended for best results, especially with respect to the fine balance between the substrate solubility and potential inhibition of UGTs. The use of other organic solvents such as methanol, ethanol, and acetonitrile has been tested as well (Kuuranne *et al.*, 2003, Uchaipichat *et al.*, 2004).

The active site of UGTs is on the luminal side of the endoplasmic reticulum membrane and is therefore enclosed behind a lipid bilayer (see Section 2.1.3). *In vivo*, this luminal membrane location requires a number of transporters for the proper catalytic function of UGTs, most notably to actively transport UDPGA (for a reviews, see Csala *et al.*, 2007, Bock and Kohle, 2009). In microsomal fractions, however, these transporters are not fully active, and the UGTs show reduced activity, sometimes referred to as “UGT latency”. As a result, microsomal fractions require disruption of the membrane *in vitro*, or “activation”, to facilitate the access of

UDPGA to the active site. The pore-forming peptide antibiotic alamethicin is currently the preferred activator of UGTs, as it inhibits neither UGT nor CYP activity (Little *et al.*, 1997, Fisher *et al.*, 2000, Walsky *et al.*, 2012). On the other hand, available evidence suggests that alamethicin does not stimulate the activity of recombinant UGT enzymes (Kaivosaaari *et al.*, 2008, Walsky *et al.*, 2012, Zhang *et al.*, 2011), possibly due to the higher permeability to UDPGA of the membranes in such preparations.

2.3.2 Albumin effect in human UGTs and CYPs

Numerous recent studies have found that the addition of albumin significantly enhances the activities of some human UGTs and CYPs, regardless of whether microsomal fractions or recombinant enzymes serve as an enzyme source. The selection of the albumin purity grade is important, because only the use of fatty acid-free BSA or HSA led to maximal activation (Rowland *et al.*, 2007, Rowland *et al.*, 2008a, Rowland *et al.*, 2008b). To reduce the high nonspecific binding of drugs to BSA and HSA, human intestinal fatty acid binding protein (IFABP) was proposed as a suitable alternative (Rowland *et al.*, 2009). Since only the free fraction of the drug is available for interaction with the enzyme, the nonspecific binding of substrates to macromolecules should always be measured and taken into account, regardless of whether BSA, HSA, or IFABP are used for activation (see Section 2.3.5). The reported optimal concentration of albumin in assays is 1–2% (Rowland *et al.*, 2007), although concentrations as low as 0.1% proved sufficient (Shiraga *et al.*, 2012). The enhancement of activity observed in the presence of BSA manifests mainly through apparent increases in the substrate affinity for the enzyme (decrease of the reaction K_m) and, to a lesser extent, changes in V_{max} . Moreover, the addition of albumin leads to more potent inhibition of the enzymes affected, which manifests as apparently lower IC_{50} or K_i values. If substrate depletion assays are used, the albumin effect is observed as an increase in the apparent intrinsic clearance (CL_{int}) (Kilford *et al.*, 2009, Gill *et al.*, 2012).

Although albumin effects in UGTs and CYPs are usually discussed separately, these two phenomena share similar manifestation and mechanistic backgrounds. Therefore, to provide greater clarity and a better understanding of these phenomena, I present an integrated overview of the albumin effects in both UGTs and CYPs together. The effects of albumin on glucuronidation enzyme kinetics in microsomal fractions and recombinant UGTs appear in Table 4 and Table 5, respectively. The consensus result of these studies is that the addition of albumin significantly enhances the glucuronidation rates of UGTs 1A9, 2B4, and 2B7, mainly through a decrease in apparent K_m or S_{50} and mostly regardless of the source of the enzyme (Raungrut *et al.*, 2010, Walsky *et al.*, 2012, Rowland *et al.*, 2007, Rowland *et al.*, 2008a, Shiraga *et al.*, 2012, Kilford *et al.*, 2009, Gill *et al.*, 2012, Uchaipichat *et al.*, 2006). On the other hand, the activities of UGTs 1A1, 1A4, and 1A6 are generally less affected despite some changes in the enzyme kinetic model (Walsky *et al.*, 2012, Rowland *et al.*, 2008a, Kilford *et al.*, 2009, Rowland *et al.*, 2006). In addition, a few UGT studies included albumin in the glucuronidation assays, but failed to account for the non-specific binding of substrates, thus yielding inconclusive results (Loureiro *et al.*, 2011, Trdan Lusin *et al.*, 2011, Ma *et al.*, 2012, Klecker and Collins, 1997, Trapnell *et al.*, 1998).

Table 4. Albumin effects on glucuronidation enzyme kinetics in human microsomal fractions.

Enzyme source	Substrate (principle UGT enzyme)	Observed effects of albumin addition	References	
HLM	17 β -Estradiol (1A1)	K_m moderate increase, V_{max} moderate increase	(Walsky <i>et al.</i> , 2012)	
	Buprenorphine (1A1)	CL_{int} unaffected ^a	(Kilford <i>et al.</i> , 2009)	
	Ezetimibe (1A1)	CL_{int} moderate increase ^a	(Gill <i>et al.</i> , 2012)	
	Lamotrigine (1A4, 2B7)	S_{50} decrease, V_{max} unaffected ^b	(Rowland <i>et al.</i> , 2006)	
	Trifluoperazine (1A4)	K_m decrease, V_{max} moderate decrease	(Walsky <i>et al.</i> , 2012)	
	5-Hydroxytryptophol (1A6)	K_m unaffected, V_{max} moderate decrease	(Walsky <i>et al.</i> , 2012)	
	Raloxifene (1A9, 1A1)	CL_{int} increase ^a	(Kilford <i>et al.</i> , 2009) (Rowland <i>et al.</i> , 2008a)	
	Propofol (1A9)	K_m decrease, V_{max} increase	(Walsky <i>et al.</i> , 2012)	
	Darexaban (1A9)	CL_{int} increase ^a	(Gill <i>et al.</i> , 2012)	
	Mycophenolic acid (1A9)	K_m decrease, V_{max} unaffected	(Shiraga <i>et al.</i> , 2012)	
			CL_{int} increased ^a	(Gill <i>et al.</i> , 2012)
		Zidovudine (2B7)	K_m decrease, V_{max} unaffected	(Uchaipichat <i>et al.</i> , 2006) (Rowland <i>et al.</i> , 2007) (Rowland <i>et al.</i> , 2009) (Kilford <i>et al.</i> , 2009)
			K_m decrease, V_{max} increase	(Walsky <i>et al.</i> , 2012)
		Codeine (2B4, 2B7)	K_m decrease, V_{max} unaffected	(Raungrut <i>et al.</i> , 2010)
HKM	Diclofenac (1A9/2B7), gemfibrozil, ketoprofen, naloxone, zidovudine (2B7)	CL_{int} increase ^a	(Kilford <i>et al.</i> , 2009) (Gill <i>et al.</i> , 2012)	
	Ezetimibe (1A1), telmisartan (1A3), mycophenolic acid (1A9), propofol (1A9), diclofenac (1A9, 2B7), naloxone (1A8, 2B7), gemfibrozil (2B7)	CL_{int} increase ^a	(Gill <i>et al.</i> , 2012)	
HIM	Ezetimibe (1A1), telmisartan (1A3), mycophenolic acid (1A8, 1A9, 1A10), propofol (1A8, 1A9), diclofenac (1A9, 1A10, 2B7), naloxone (1A8/2B7), gemfibrozil (2B7)	CL_{int} increase ^a	(Gill <i>et al.</i> , 2012)	

^a Substrate depletion assays; ^b Data were analyzed with a hybrid of the Michaelis-Menten and the Hill equations.

Table 5. Albumin effects on the glucuronidation enzyme kinetics in recombinant human UGTs.

Enzyme source	Substrate	Observed effects of albumin addition	References
UGT1A1	4-MU	No activation. Change in the enzyme kinetic model.	(Rowland <i>et al.</i> , 2008a)
	17 β -Estradiol	K_m increase, V_{max} unaffected	(Walsky <i>et al.</i> , 2012)
UGT1A4	Lamotrigine	K_m increase, V_{max} increase	(Rowland <i>et al.</i> , 2006)
	Trifluoperazine	K_m increase, V_{max} increase	(Walsky <i>et al.</i> , 2012)

UGT1A6	4-MU	No activation. Change in the enzyme kinetic model.	(Rowland <i>et al.</i> , 2006)
	5-Hydroxytryptophol	No activation. K_m unaffected, V_{max} unaffected	(Walsky <i>et al.</i> , 2012)
UGT1A9	4-MU, propofol	K_m decrease, V_{max} unaffected	(Rowland <i>et al.</i> , 2008a) (Walsky <i>et al.</i> , 2012)
	Derexaban	K_m decrease, V_{max} unaffected	(Shiraga <i>et al.</i> , 2012)
UGT2B4	Codeine	S_{50} decrease, V_{max} decrease ^c	(Raungrut <i>et al.</i> , 2010)
UGT2B7	Zidovudine	K_m decrease, V_{max} unaffected	(Uchaipichat <i>et al.</i> , 2006) (Rowland <i>et al.</i> , 2007)
	4-MU	K_m decrease, V_{max} increase	(Walsky <i>et al.</i> , 2012)
	Codeine	S_{50} decrease, V_{max} unaffected ^c	(Rowland <i>et al.</i> , 2007) (Raungrut <i>et al.</i> , 2010)

^a Substrate depletion assays; ^b Data were analyzed with a hybrid of the Michaelis-Menten and the Hill equations; ^c Data were analyzed with the Hill equation.

The inclusion of albumin in UGT inhibition assays yielded lower apparent K_i or IC_{50} values when substrates for UGTs 2B4 and 2B7 were used (Raungrut *et al.*, 2010, Uchaipichat *et al.*, 2006, Rowland *et al.*, 2006, Uchaipichat *et al.*, 2011) (Table 6). Changes observed in the inhibitory parameters reflect the increased apparent affinity of tested inhibitors for UGTs 2B4 and 2B7. These results, together with an increased apparent substrate affinity (lower K_m), indicate that both substrates and inhibitors of UGTs 2B4 and 2B7 exhibit an apparently higher affinity in the presence of albumin. In addition, Walsky *et al.* (2012) tested the inhibition of a number of UGT enzymes in the presence of 2% BSA, but unfortunately failed to account for the nonspecific binding of the inhibitors to BSA.

Table 6. Albumin effects on the inhibition of glucuronidation in HLM and recombinant UGTs.

Enzyme source	Substrate (Principle UGT enzyme)	Inhibitor	Albumin effects	References
HLM	Zidovudine (2B7)	Fluconazole	K_i decrease	(Uchaipichat <i>et al.</i> , 2006)
	Codeine (2B4/2B7)	Many	K_i or IC_{50} decrease	(Raungrut <i>et al.</i> , 2010)
	Codeine and morphine (2B4/2B7)	Ketamine	K_i decrease	(Uchaipichat <i>et al.</i> , 2011)
	Lamotrigine (1A4/2B7)	Valproic acid	K_i decrease	(Rowland <i>et al.</i> , 2006)
UGT2B7	Zidovudine	Fluconazole	K_i decrease	(Uchaipichat <i>et al.</i> , 2006)

The effects of albumin on CYP-catalyzed reactions in HLM and recombinant CYPs appear in Table 7. In general, the addition of albumin enhanced the rate of reactions catalyzed by CYPs 1A2, 2C8, and 2C9, mainly through a K_m decreases and irrespective of the source of the enzyme (Rowland *et al.*, 2008b, Ludden *et al.*, 1997, Carlile *et al.*, 1999, Tang *et al.*, 2002, Zhou *et al.*, 2004, Wattanachai *et al.*, 2011, Wattanachai *et al.*, 2012). The reaction V_{max} was usually less affected.

Table 7. Albumin effects on the enzyme kinetics of CYP-catalyzed reactions in HLM and recombinant CYPs.

Enzyme source	Substrate (principle CYP enzyme)	Observed effects of albumin addition	References
HLM	Phenacetin (mainly 1A2)	K_{m1} decrease, V_{max1} unaffected K_{m2} unaffected, V_{max2} moderate increase ^a	(Wattanachai <i>et al.</i> , 2012)
	Lidocaine (mainly 1A2)	K_{m1} decrease, V_{max1} unaffected K_{m2} unaffected, V_{max2} unaffected ^a	(Wattanachai <i>et al.</i> , 2012)
	Paclitaxel (2C8)	K_m decrease, V_{max} unaffected	(Wattanachai <i>et al.</i> , 2011)
	Phenytoin (2C9)	K_m decrease, V_{max} unaffected	(Ludden <i>et al.</i> , 1997)
			(Carlile <i>et al.</i> , 1999) (Tang <i>et al.</i> , 2002) (Rowland <i>et al.</i> , 2008b)
Tolbutamide (2C9)	K_m decrease, V_{max} slight decrease K_m decrease, V_{max} unaffected	(Carlile <i>et al.</i> , 1999) (Tang <i>et al.</i> , 2002) (Zhou <i>et al.</i> , 2004)	
CYP1A2	Phenacetin	K_m decrease, V_{max} unaffected	(Wattanachai <i>et al.</i> , 2012)
	Lidocaine	K_m decrease, V_{max} moderate decrease	(Wattanachai <i>et al.</i> , 2012)
CYP2C8	Paclitaxel	K_m modest decrease, V_{max} moderate increase	(Wattanachai <i>et al.</i> , 2011)
CYP2C9	Phenytoin	K_m decrease, V_{max} unaffected	(Rowland <i>et al.</i> , 2008b)

^a Data were analyzed with the two-enzyme model.

2.3.3 Significance of the albumin effect for *in vitro*–*in vivo* extrapolation

The addition of albumin to UGT and CYP *in vitro* assays led to more accurate predictions of metabolic elimination *in vivo*, usually because of elevated apparent CL_{int} *in vitro*, which reduced the underprediction bias. For UGT substrates, including albumin improved the *in vitro*–*in vivo* extrapolation mainly for drugs that are glucuronidated by UGTs 1A9 and 2B7. In the case of UGT1A9 substrates, the addition of albumin improved the *in vitro*–*in vivo* extrapolation for propofol (Rowland *et al.*, 2008a, Gill *et al.*, 2012), raloxifene (Kilford *et al.*, 2009), and mycophenolic acid (Gill *et al.*, 2012). In the case of UGT2B7 substrates, *in vitro*–*in vivo* extrapolation was enhanced for zidovudine (Rowland *et al.*, 2007, Kilford *et al.*, 2009, Uchaipichat *et al.*, 2006), codeine (Kilford *et al.*, 2009), diclofenac (Kilford *et al.*, 2009, Gill *et al.*, 2012), ketoprofen (Kilford *et al.*, 2009), and naloxone (Kilford *et al.*, 2009, Gill *et al.*, 2012). Adding albumin, however, resulted in overestimation of the *in vivo* CL_{int} for gemfibrozil (substrate of UGT2B7), perhaps due to errors related to high nonspecific binding to albumin or the instability of gemfibrozil acyl glucuronide (Kilford *et al.*, 2009, Gill *et al.*, 2012).

The addition of albumin also enhanced the accuracy of predictions of drug-drug interactions for the fluconazole inhibition of zidovudine glucuronidation (Uchaipichat *et al.*, 2006), the valproic acid inhibition of lamotrigine glucuronidation (Rowland *et al.*, 2006), the inhibition of codeine glucuronidation by several drugs (Raungrut *et al.*, 2010), and the ketamine inhibition of codeine and morphine glucuronidation (Uchaipichat *et al.*, 2011) (see Table 6).

For drugs that are metabolized by CYP-catalyzed reactions, the addition of albumin to HLM incubations enhanced *in vitro*–*in vivo* extrapolation for the substrates of CYPs 1A2, 2C8, and 2C9. Specifically, the *in vivo* CL_{int} of phenacetin *O*-deethylation and lidocaine *N*-deethylation by CYP1A2 (Wattanachai *et al.*, 2012), paclitaxel 6 α -hydroxylation by CYP2C8 (Wattanachai *et*

al., 2011), and phenytoin hydroxylation by CYP2C9 (Rowland *et al.*, 2008b, Ludden *et al.*, 1997, Carlile *et al.*, 1999) were better predicted in the presence of albumin. In addition, including albumin and using cofactors for both UGT and CYP-catalyzed reactions in HLM incubations reduced the bias for *in vivo* CL_{int} estimates for ketoprofen and diclofenac, most likely due to the simultaneous activation of UGT2B7- and CYP2C9-mediated pathways (Kilford *et al.*, 2009). However, the inclusion of albumin in tolbutamide hydroxylation by HLM resulted in the overprediction of *in vivo* CL_{int} (Carlile *et al.*, 1999).

2.3.4 Mechanism of the albumin effect

Initial studies of the albumin effect focused on phenytoin and tolbutamide hydroxylation by HLM, a reaction catalyzed almost exclusively by CYP2C9 (Ludden *et al.*, 1997, Carlile *et al.*, 1999, Tang *et al.*, 2002, Zhou *et al.*, 2004). The observed K_m decrease was hypothesized to be a result of albumin effects on the ternary and quaternary structure of CYP2C9 (Ludden *et al.*, 1997, Tang *et al.*, 2002), or on the albumin-mediated removal of CYP2C9 internal inhibitors, such as fatty acids present in the microsomal preparation (Carlile *et al.*, 1999, Tang *et al.*, 2002). The latter alternative was in line with the result that fatty acid-free HSA, but not crude HSA, can stimulate tolbutamide hydroxylation in HLM (Zhou *et al.*, 2004). For drugs eliminated by glucuronidation, initial reports of the albumin effect found that including 2% BSA significantly increases the rates of zidovudine and fenoldopam glucuronidation by HLM (Kleckner and Collins, 1997, Trapnell *et al.*, 1998), even without accounting for the substrate binding to BSA. Some authors have proposed that BSA disrupts the membranes of the endoplasmic reticulum, thereby eliminating UGT latency (Trapnell *et al.*, 1998).

More recent studies have found that albumin enhances UGT and CYP activities by removing internal inhibitors from *in vitro* assays, a mechanism that both UGT- and CYP-catalyzed reactions share, independently of the source of the enzyme (Raungrut *et al.*, 2010, Rowland *et al.*, 2007, Rowland *et al.*, 2008a, Rowland *et al.*, 2008b, Wattanachai *et al.*, 2011, Wattanachai *et al.*, 2012). The inhibitors that are removed by albumin were identified as long-chain unsaturated fatty acids, most notably oleic (18:1 n -9; 18:1- Δ^9), linoleic (18:2 n -6; 18:2- $\Delta^{9,12}$), and arachidonic acid (20:4 n -6; 20:4- $\Delta^{5,8,11,14}$) (Rowland *et al.*, 2007, Rowland *et al.*, 2008a, Rowland *et al.*, 2008b) (Figure 14). These fatty acids proved to be potent inhibitors of UGTs 1A9 and 2B7 (Rowland *et al.*, 2007, Rowland *et al.*, 2008a, Tsoutsikos *et al.*, 2004), as well as of CYPs 1A2, 2C8, and 2C9 (Rowland *et al.*, 2008b, Wattanachai *et al.*, 2011, Wattanachai *et al.*, 2012). Although the inhibition studies were not comprehensive, the inhibitory potencies of fatty acids toward UGTs and CYPs are generally in the low- μ M range. For example, linoleic was a competitive inhibitor of 4-MU glucuronidation by UGT1A9 with K_i value of 4.1 μ M (Tsoutsikos *et al.*, 2004). Arachidonic acid exhibited even more potent inhibition of UGT1A9, but displayed “atypical inhibition behavior” which prevented the authors from determining the K_i (Tsoutsikos *et al.*, 2004). Moreover, arachidonic acid competitively inhibited phenytoin hydroxylation by HLM and *E. coli*-expressed CYP2C9 with K_i values of 3.8 and 1.6 μ M, respectively (Rowland *et al.*, 2008b), whereas the K_i values for arachidonic acid, linoleic acid, and oleic acid inhibition of CYP1A2-catalyzed phenacetin *O*-deethylation were 4.7, 13.6, and 16.7 μ M, respectively (Wattanachai *et al.*, 2012).

In addition to being inhibitors, oleic, linoleic, and arachidonic acid are also substrates for UGT2B7 (Turgeon *et al.*, 2003, Rowland *et al.*, 2007) and CYP2C9 (Rowland *et al.*, 2008b),

suggesting a competition between the fatty acids and the drugs tested for binding to the active sites of the enzymes. As shown by the radiometric thin layer chromatography method, UGT2B7 glucuronidated a broad variety of fatty acids, both saturated and unsaturated, with average glucuronidation rate of 10–100 pmol·min⁻¹·mL⁻¹ (Rowland *et al.*, 2007). On the other hand, in incubations with NADPH-generating system, as measured by tandem mass spectrometry, CYP2C9 produced mono- and dihydroxylated metabolites of several fatty acids (Rowland *et al.*, 2008b).

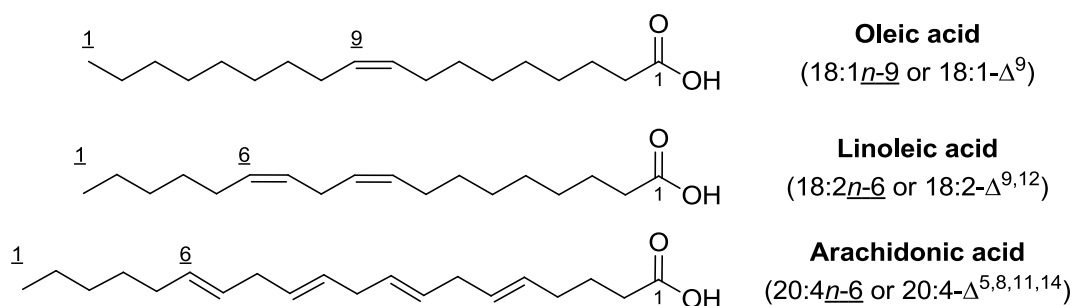


Figure 14. Chemical structures of fatty acids identified as principal inhibitors of UGTs and CYPs.

The inhibitory fatty acids are presumably released from disrupted cell membranes during the preparation of microsomal fractions or recombinant UGTs and CYPs (Rowland *et al.*, 2007, Rowland *et al.*, 2008b). This hypothesis is supported by the fact that apparent K_m value for zidovudine glucuronidation by UGT2B7 was high in HLM (760 μM) but low in isolated hepatocytes (87 μM) (Engtrakul *et al.*, 2005). If fatty acid-free BSA or HSA is added to *in vitro* assays, the effective concentration of fatty acids decreases, leading to a reversal of the inhibitory effect (Rowland *et al.*, 2007, Rowland *et al.*, 2008a, Rowland *et al.*, 2008b). The structures of both BSA and HSA have at least 2–3 high affinity and 4–5 intermediate affinity fatty acid-binding sites (recently reviewed by Van der Vusse, 2009). The comparable removal of fatty acid inhibitors can also be achieved if UGT2B7 and HSA are coexpressed in HEK293 cells (Rowland *et al.*, 2007).

Since inhibitory fatty acids originate from disrupted cell membranes, differences in lipid composition between different enzyme sources may affect the magnitude of the albumin effect. Available data suggests that the relative abundance of fatty acids is highest in HLM (Rowland *et al.*, 2007), lower in HEK293 cells expressing UGT enzymes (Rowland *et al.*, 2007), and lowest in *Escherichia coli* (*E. coli*) cells expressing CYP enzymes (Rowland *et al.*, 2008b). Measured concentrations of inhibitory fatty acids in these enzyme sources were approximately 10–60 μM (Rowland *et al.*, 2007), 1–8 μM (Rowland *et al.*, 2007), and 0.1–5 μM (Rowland *et al.*, 2008b), for HLM, HEK293 cells expressing UGTs, and *E. coli* cells expressing CYPs, respectively, all assayed at enzyme source concentration of 1 mg/mL. The activity data in the presence of albumin corresponds fairly well with fatty acid abundance, as the highest relative decrease in K_m occurred in HLM (Rowland *et al.*, 2007, Rowland *et al.*, 2008a, Rowland *et al.*, 2008b), a smaller decrease occurred in UGTs 1A9 and 2B7 expressed in HEK293 cells (Rowland *et al.*, 2007, Rowland *et al.*, 2008a), and the lowest decrease occurred in CYPs 1A2, 2C8, and 2C9 expressed in *E. coli* cells (Rowland *et al.*, 2008b, Wattanachai *et al.*, 2011, Wattanachai *et al.*, 2012). The fatty acid composition of *Sf9* cells, the cell line that is commonly employed for

expressing recombinant UGTs, appears to be quantitatively similar to HEK293 cells, even if Sf9 cells contain comparatively less linoleic and arachidonic acid, but more oleic and palmitoleic acid (16:1n-7; 16:1-Δ⁹) (Marheineke *et al.*, 1998).

2.3.5 Drug binding to albumin and enzyme sources

Apart from interacting with the active site of UGTs, substrates may also bind to macromolecules present in the incubation mixture, most notably externally added albumin and enzyme sources, either microsomal fractions or recombinant UGTs. This process, commonly referred to as “nonspecific binding”, may significantly reduce the actual concentration of the substrate available for interaction with the enzyme. If unaccounted for, nonspecific binding may lead to the underprediction of both the substrate affinity and inhibitor potency, all leading to poor *in vitro*–*in vivo* extrapolation (Miners *et al.*, 2010, Obach, 1997, McLure *et al.*, 2000). In addition, unaccounted nonspecific binding may result in misinterpretation of the enzyme kinetic model (McLure *et al.*, 2000).

Drug binding to albumin and enzyme sources is typically measured by ultrafiltration or equilibrium dialysis. Equilibrium dialysis is considered the “gold standard” method employed by many laboratories (reviewed by Banker and Clark, 2008). Although ultrafiltration is a rapid method suitable for automation, the non-specific adsorption of drugs to the ultrafiltration membrane may limit its practical usefulness (Lee *et al.*, 2003). Rapid equilibrium dialysis (RED) was recently been introduced as a faster and high-throughput alternative to classical equilibrium dialysis (Waters *et al.*, 2008).

2.3.6 Principles of *in vitro*–*in vivo* extrapolation

HLM or hepatocytes are typically used as the enzyme source for *in vitro*–*in vivo* extrapolation. The *in vitro* intrinsic clearance ($CL_{int, in vitro}$), the principle *in vitro* parameter used for *in vitro*–*in vivo* extrapolation, can be calculated as the V_{max}/K_m ratio (Eq. 1) or, alternatively, determined from substrate depletion assays at low concentrations of substrate ($[S] \ll K_m$) (Jones and Houston, 2004) (Eq. 2):

$$(1) CL_{int, in vitro} = \frac{V_{max}}{K_m}; \text{ or } (2) CL_{int, in vitro} = \frac{kV}{m_p}$$

where V_{max} is the reaction limiting velocity, K_m is the Michaelis-Menten constant, k is the substrate depletion rate constant, V is the volume of incubation, and m_p is the amount of microsomal protein in the assay. Usually, $CL_{int, in vitro}$ is expressed in $\mu\text{L}\cdot\text{min}^{-1}\cdot\text{mg}^{-1}$ of microsomal protein. Next, $CL_{int, in vitro}$ is scaled-up to the whole-liver intrinsic clearance ($CL_{int, liver}$) by using the published values of HLM protein abundance (approx. $40 \text{ mg}\cdot\text{g}^{-1}$) or hepatocellularity per gram of liver (approx. $10^8 \text{ cells}\cdot\text{g}^{-1}$ liver), as well as the average weight of the human liver (approx. $20 \text{ g}\cdot\text{kg}^{-1}$) (Barter *et al.*, 2007, Houston and Galetin, 2008). The use of microsomal fractions from other organs, such as HKM or HIM, will require specific scaling factors. $CL_{int, liver}$ is extrapolated to hepatic clearance (CL_H) with physiologically-based models of hepatic clearance, most commonly the well-stirred model (Eq. 3):

$$(3) CL_H = \frac{Q_H f_u CL_{int, liver}}{Q_H + (f_u CL_{int, liver})}$$

where Q_H is the liver-blood flow (approx. $20 \text{ ml}\cdot\text{min}^{-1}\cdot\text{kg}^{-1}$), f_u is the fraction of unbound drug in the blood, and $CL_{\text{int, liver}}$ is the whole-liver intrinsic clearance. To simulate the *in vivo* situation, the well-stirred model assumes that (1) distribution into the liver is limited only by the perfusion rate and has no diffusion barriers, (2) only unbound drug crosses the cell membrane and interacts with the enzymes, (3) metabolic enzymes are homogeneously distributed in the liver, and (4) the concentration of the drug in the liver is equal to the outflow concentration (Houston and Galetin, 2008). Additional physiologically-based models of hepatic clearance, such as the parallel-tube model and the dispersion model, may offer an advantage in the prediction of CL_H (Houston and Galetin, 2008). The hepatic extraction ratio (E_H), the percentage of the dose that is metabolized during the first pass through the liver, is calculated as CL_H/Q_H . Other clearance terms, such as intestinal, renal, or biliary metabolism and excretion, may be required in order to obtain the total body clearance of the drug.

2.3.7 Prediction of inhibitory drug-drug interactions

The inhibition potency of the drug is usually quantified through the inhibitory dissociation constant K_i , which is determined experimentally (see Section 2.4.3). Alternatively, assuming the inhibition modality is known, measured IC_{50} values can be converted to their corresponding K_i values (Cheng and Prusoff, 1973). The magnitude of drug-drug interactions *in vivo* is estimated by the ratio of the area under the *plasma drug concentration vs. time curve* in the presence (AUC_i) and absence of an inhibitor (AUC) (Miners *et al.*, 2010):

$$(4) \frac{AUC_i}{AUC} = \frac{1}{\frac{f_m}{1 + \frac{[I]}{K_i}} + (1 - f_m)}$$

where $[I]$ is the concentration of the inhibitor at the enzyme site (usually the unbound concentration in plasma or the hepatic input concentration), K_i is the inhibitory dissociation constant, and f_m is the fraction of the dose metabolized by the enzyme of interest. The high numerical value of AUC_i/AUC ratio indicates that significant drug-drug interaction is likely to be observed *in vivo*. The review by Williams *et al.* (2004) suggests that the AUC_i/AUC ratios observed in the presence of UGT inhibitors are typically less than two, indicating the relatively modest significance of drug-drug interactions for drugs metabolized by UGTs. Generally, similar modestly elevated AUC_i/AUC ratios were recently obtained in the fluconazole inhibition of zidovudine glucuronidation (Uchaipichat *et al.*, 2006), the valproic acid inhibition of lamotrigine glucuronidation (Rowland *et al.*, 2006), the inhibition of codeine glucuronidation by several drugs (Raungrut *et al.*, 2010), and the ketamine inhibition of codeine and morphine glucuronidation (Uchaipichat *et al.*, 2011). The possible risk for drug-drug interactions (high AUC_i/AUC ratios), however, rises if a drug is glucuronidated by a single UGT enzyme, the E_H is high, and the inhibitor $[I]/K_i$ ratio is high (Williams *et al.*, 2004). The extensive list of clinically observed and *in vitro* proposed UGT drug-drug interactions is compiled by Kiang *et al.* (2005).

2.4 Enzyme kinetics of UGT-catalyzed reactions

Enzyme kinetic assays are widely used to estimate the substrate affinity and enzyme activity of UGT-catalyzed reactions. Although UGTs catalyze a two-substrate two-product reaction (see Figure 1), enzyme kinetic assays are commonly performed at a saturating concentration of UDPGA (2–5 mM), essentially simplifying the system to a single substrate analysis (Luukkanen *et al.*, 2005). UGT enzyme kinetic assays are usually performed by measuring the initial rates of

glucuronidation under steady-state conditions, under the assumption that the concentrations of intermediate enzyme • substrate complexes are constant over the time period of the assay ($d[E\cdot S]/dt = 0$). In order to fulfill these criteria, the concentrations of substrates should be much higher than the enzyme concentration ($[S] \gg [E]$), and both enzyme concentration and incubation time should be optimized in order to minimize both substrate depletion and product formation (because products of the enzyme reaction often act as inhibitors of the enzyme). In practice, in order to measure the initial rates, $\leq 10\%$ of substrate depletion or product formation is usually acceptable.

Initial glucuronidation rates, measured and plotted over the range of different aglycone substrate concentrations, are usually fitted to the Michaelis-Menten equation *via* nonlinear regression. This equation simplifies the enzyme reaction to two distinct steps: (1) the enzyme and substrate first interact to form a non-covalent complex ($E + S \rightleftharpoons E\cdot S$) and (2) the actual catalytic step occurs and the product is released ($E\cdot S \rightarrow E + P$) (Figure 15). The first step of the reaction is described by two rate constants: the second-order rate constant k_1 for the association reaction ($E + S \rightarrow E\cdot S$) and the first-order rate constant k_{-1} for the dissociation reaction ($E\cdot S \rightarrow E + S$). The ratio of the dissociation rate constant to association rate constant is the equilibrium dissociation constant (K_s) for the first step of the enzyme reaction, the non-covalent interaction of enzyme with substrate ($E + S \rightleftharpoons E\cdot S$; $K_s = k_{-1}/k_1$). The second, catalytic, step of the reaction ($E\cdot S \rightarrow E + P$) is described by the first-order rate constant k_{cat} , usually known as the *catalytic constant* (Cornish-Bowden, 2012, Copeland, 2000).



Figure 15. A simplified scheme of the enzyme reaction used to derive the Michaelis-Menten equation.

The mathematical forms of the Michaelis-Menten equation appear in Eq. 5:

$$(5) \ v = \frac{V_{max}[S]}{K_m + [S]} = \frac{[E]k_{cat}[S]}{K_m + [S]} = \frac{[E]k_{cat}[S]}{\frac{k_{-1}k_{cat}}{k_1} + [S]}$$

where v is the initial reaction rate measured (usually $\text{nmol}\cdot\text{min}^{-1}\cdot\text{mg}^{-1}$), $[S]$ is the concentration of the aglycone substrate (corrected for nonspecific binding to albumin and the enzyme source; see Section 2.3.5), and $[E]$ is the concentration of the enzyme in the assay. V_{max} is the limiting reaction velocity asymptotically approached at high concentrations of the substrate (Figure 16A). According to the definition $k_{cat} = V_{max}/[E]$. The k_{cat} is, however, determined rarely in glucuronidation assays, mainly because the exact concentration of UGT enzymes is difficult to measure, an issue closely related to the absence of purified and fully active UGT enzymes, as well as to the lack of specific UGT antibodies (Oda *et al.*, 2012).

K_m is the Michaelis-Menten constant, graphically defined as the $[S]$ at half of the V_{max} (Figure 16A). Moreover, because $K_m = k_{-1}\cdot k_{cat}/k_1$, it serves as the pseudo-affinity constant for the substrate binding to the enzyme and is closely related to the corresponding equilibrium dissociation constant $K_s = k_{-1}/k_1$. If k_{-1} is much larger than k_{cat} , K_m is equivalent to K_s . If,

however, the magnitudes of the individual rate constants are unknown, one cannot assume that K_m will be equal K_s . Therefore, K_m is best described as an empirical quantity relating v to $[S]$ rather than as a measure of the thermodynamic stability of the enzyme • substrate complex. The ratio of V_{max}/K_m , commonly referred to as the intrinsic clearance (CL_{int}), is a second-order rate constant for the overall reaction at low concentrations of the substrate ($E + S \rightleftharpoons E + P$; $[S] \ll K_m$). This parameter widely serves as a starting point for the *in vitro*–*in vivo* extrapolation of glucuronidation activity (see Section 2.3.6).

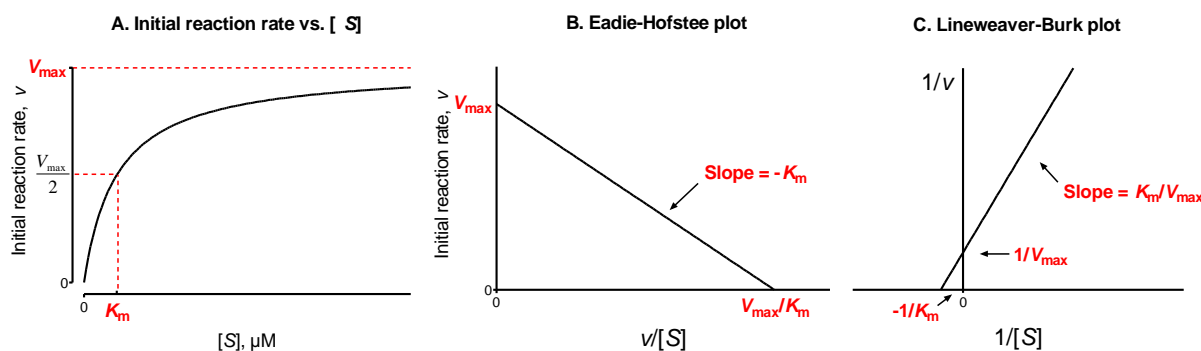


Figure 16. The theoretical saturation profile for the Michaelis-Menten equation presented as the initial rate vs. the $[S]$ plot (A), the Eadie-Hofstee plot (B), and the Lineweaver-Burk plot (C).

The linear transformations of the Michaelis-Menten equation often appear in the literature, most notably Eadie-Hofstee (Figure 16B) and Lineweaver-Burk (Figure 16C) plots. Although they offer no advantage in determining enzyme kinetic parameters, these linear plots are useful for visualizing the relationship between several enzyme kinetic experiments, especially in inhibition assays and bisubstrate kinetic studies (Cornish-Bowden, 2012). Moreover, the Eadie-Hofstee plot is commonly used to detect deviations from Michaelis-Menten kinetics.

Similar to studies of aglycone kinetics, the enzyme kinetics of UDPGA can be studied at saturating concentration of the aglycone substrate (Luukkanen *et al.*, 2005). However, since many UGT reactions exhibit substrate inhibition with respect to the aglycone substrate (Luukkanen *et al.*, 2005; see Section 2.4.2), these experiments are more complex than commonly perceived and may yield unreliable results. In addition, the aqueous solubility of many aglycone substrates may be insufficient to reach full saturation, thus leading to overestimation of the K_m for UDPGA.

2.4.1 Enzyme kinetic mechanism of UGT-catalyzed reactions

Human UGTs catalyze glucuronic acid-transfer reactions with two substrates and two products. Schematically, glucuronidation can be presented as the transfer of group X (glucuronic acid) from substrate A to substrate B: $AX + B \rightleftharpoons BX + A$, where AX stands for UDPGA, B for the aglycone substrate, BX for the glucuronide conjugate, and A for UDP. Knowledge of the enzyme kinetic mechanism is important to understand the function and structure of UGTs, especially with respect to UGT inhibition, to the design of *in vitro* assays, and for studies of substrate selectivity and the catalytic mechanism. In order to understand the enzyme kinetic mechanism of

UGT-catalyzed reactions, one must take into account both substrates and both products. In general, such reactions are classified into two distinct mechanisms: (1) the ternary-complex mechanism, which proceeds through the formation of a single ternary complex with both substrates bound to the enzyme (Figure 17A), and (2) the substituted-enzyme mechanism, which proceeds through the formation of two binary complexes (Figure 17B) (Cornish-Bowden, 2012, Copeland, 2000). According to the substrate binding order, one can further subdivide the ternary-complex mechanism into compulsory-order and random-order mechanisms. On the other hand, the substituted-enzyme mechanism is always compulsory-ordered, since reaction has only one mechanistically reasonable pathway along which to proceed (Cornish-Bowden, 2012).

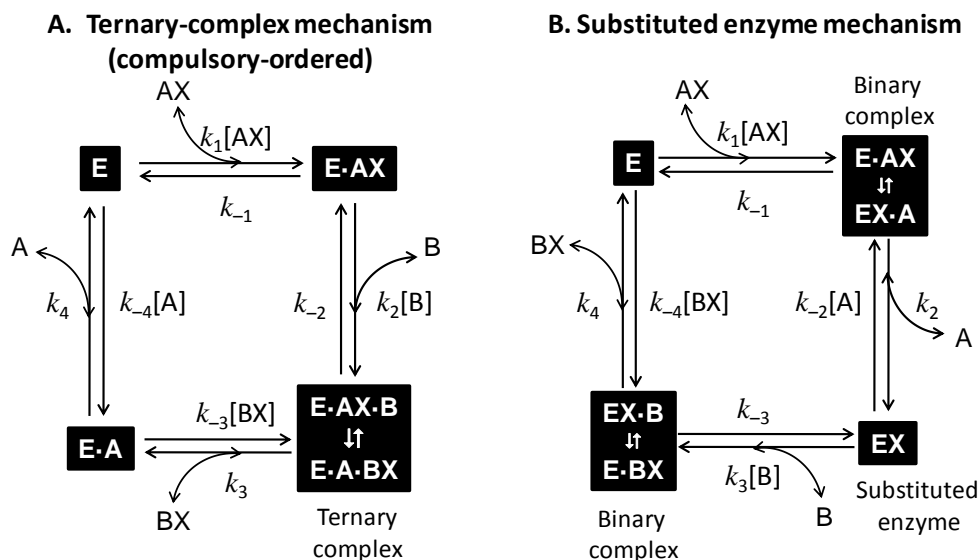


Figure 17. Hypothetical compulsory-order ternary-complex (A) and substituted-enzyme (B) kinetic mechanisms for the transfer of group X from substrate A to substrate B ($AX + B \rightleftharpoons BX + A$).

The principal tool for enzyme kinetic mechanism study is bisubstrate enzyme kinetics, an assay in which the initial reaction rate is measured as a function of simultaneous change in the concentrations of both substrates. The initial rates obtained can be fitted to appropriate equations for either a compulsory-order ternary-complex mechanism (Eq. 6; Cornish-Bowden, 2012), a random-order ternary-complex mechanism (Eq. 7; Alberty, 2011), or a substituted-enzyme mechanism (Eq. 8; Cornish-Bowden, 2012):

$$(6) v = \frac{V_{max}[AX][B]}{K_{iAX}K_{mB} + K_{mB}[AX] + K_{mAX}[B] + [AX][B]}$$

where V_{max} is the limiting velocity at the saturating concentration of both AX and B, K_{iAX} is the equilibrium dissociation constant for the $E + AX \rightleftharpoons E \cdot AX$ reaction, K_{mAX} is the limiting Michaelis constant for AX when B is saturated, and K_{mB} is the limiting Michaelis constant for B when AX is saturated. This steady-state equation assumes that substrate AX binds first and that substrate B binds second.

$$(7) v = \frac{V_{max}[AX][B]K_{iB}}{K_BK_{iAX}[B] + K_{iB}[AX][B] + K_BK_{iAX}[AX] + K_BK_{iAX}K_{iB}}$$

where K_{iAX} and K_{iB} are the equilibrium dissociation constants for the complexes $E \cdot AX$ and $E \cdot B$, respectively. K_B is the first equilibrium dissociation constant for the complex $E \cdot AX \cdot B$ ($E \cdot AX \cdot B \rightleftharpoons E \cdot AX + B$). K_A , the second equilibrium dissociation constant for the complex $E \cdot AX \cdot B$ ($E \cdot AX \cdot B \rightleftharpoons E \cdot B + AX$), is not included in this equation, but can still be calculated from the following relationship: $K_{iA}K_B = K_{iB}K_A$. Due to the complexity of the random-order ternary-complex mechanism, this equation is derived based on the rapid-equilibrium assumption, which assumes that only the interconversion of two binary complexes is rate-limiting ($E \cdot AX \cdot B \rightleftharpoons E \cdot A \cdot BX$), whereas all other steps are much faster.

$$(8) v = \frac{V_{max}[AX][B]}{K_{mAX}[B] + K_{mB}[AX] + [AX][B]}$$

where K_{mAX} and K_{mB} are the limiting Michaelis constants for AX and B, as in Eq. 6. This steady-state equation also implicitly assumes a mechanistically reasonable compulsory-order mechanism, where AX and B are the first and second binding substrates, respectively.

Based on the goodness-of-fit and characteristic intersection patterns of the primary linear plots, one can clearly distinguish between ternary-complex and substituted-enzyme mechanisms. If the reaction follows a ternary-complex mechanism, however, the bisubstrate kinetics alone are insufficient to discriminate between the compulsory- and random-order of substrate binding; both Eqs. 6 and 7 are likely to fit ternary-complex data well, regardless of binding order. Product and dead-end inhibition studies, together with the nature of substrate inhibition, are commonly used to elucidate the order of substrate binding (Cornish-Bowden, 2012, Bisswanger, 2002). If the kinetic parameters can be measured in both the forward and reverse directions of the enzyme reaction, one may use the Haldane relationship to determine the thermodynamic equilibrium constant of the overall reaction (Cornish-Bowden, 2012). Moreover, for reactions following the compulsory-order ternary-complex mechanism, a unique relationship exists between the enzyme kinetic parameters and individual rate constants, thus offering a possibility to quantify the rate of each individual reaction step (Cornish-Bowden, 2012).

The past 40 years witnessed the extensive investigation of the UGT enzyme kinetic mechanism, but with variable results (Table 8). The majority of such studies found that UGT-catalyzed reactions follow a ternary-complex mechanism, regardless of the enzyme source or experimental conditions. The formation of ternary complex is also supported by evidence that glucuronidation resembles an S_N2 -type nucleophilic substitution reaction, with the inversion of the glucuronic acid anomeric carbon from the α -configuration in UDPGA to the β -configuration in the resultant glucuronide (Axelrod *et al.*, 1958, Johnson and Fenselau, 1978; see Section 2.1.4 and Figure 8). Retention of the configuration is expected, but unnecessary in substituted-enzyme mechanisms (Cornish-Bowden, 2012). Despite broad agreement on the formation of ternary complex, previous studies disagree about whether or not the two substrates (the aglycone substrate and the UDPGA) bind in a random or compulsory order (Table 8). Disagreements over the order of substrate binding may have arisen from the use of liver microsomal preparations that contain multiple UGT enzymes (Potrepka and Spratt, 1972, Vessey and Zakim, 1972, Sanchez and Tephly, 1975, Rao *et al.*, 1976, Koster and Noordhoek, 1983), or of partially purified UGT enzymes (Yin *et al.*, 1994, Matern *et al.*, 1982, Matern *et al.*, 1991, Falany *et al.*, 1987) that may have been inactivated by detergents during the purification process (Kurkela *et al.*, 2003).

Table 8. Previous studies that investigated the enzyme kinetic mechanism of UGTs.

Enzyme source	Aglycone substrate	Reaction mechanism	Reference
Guinea pig liver microsomes	Bilirubin	Compulsory-order ternary-complex (UDPGA first, aglycone second) or <i>iso</i> -Theorell-Chance	(Potrepka and Spratt, 1972)
Beef and guinea pig liver microsomes	<i>p</i> -Nitrophenol	Rapid equilibrium random-order ternary-complex	(Vessey and Zakim, 1972)
Rat liver microsomes	Morphine	Compulsory-order ternary-complex (UDPGA first, aglycone second)	(Sanchez and Tephly, 1975)
Pig kidney microsomes	Estrone	Ternary-complex mechanism, <i>iso</i> -Theorell-Chance (aglycone first, UDPGA second)	(Rao <i>et al.</i> , 1976)
Purified UGT from rat liver	Chenodeoxycholic acid and testosterone	Ternary-complex mechanism	(Matern <i>et al.</i> , 1982)
Rat intestinal microsomes	1-Naphthol	Compulsory-order ternary-complex (aglycone first, UDPGA second)	(Koster and Noordhoek, 1983)
Two purified UGTs from rat liver	Androsterone and testosterone	Rapid equilibrium random-order ternary-complex	(Falany <i>et al.</i> , 1987)
Purified UGT from human liver	Hyodeoxycholic acid	Ternary-complex mechanism	(Matern <i>et al.</i> , 1991)
Purified UGT from rat liver microsomes	Substituted phenols	Random-order ternary-complex	(Yin <i>et al.</i> , 1994)
Recombinant human UGTs from 1A family	Entacapone, scopoletin, umbelliferone, 1-naphthol, 4-hydroxyestrone, ethinylestradiol	Compulsory-order ternary-complex (UDPGA first, aglycone second)	(Luukkanen <i>et al.</i> , 2005)
Recombinant human UGT1A6	Scopoletin	Compulsory-order ternary-complex (UDPGA first, aglycone second)	(Patana <i>et al.</i> , 2007)

Until now, only two studies have used recombinant enzymes to investigate the enzyme kinetic mechanism of UGTs (Patana *et al.*, 2007, Luukkanen *et al.*, 2005). Luukkanen *et al.* (2005) concluded that UGTs follow a compulsory-order ternary-complex mechanism in which UDPGA binds first. It should be noted, however, that this study was performed in the absence of BSA and focused on UGT1A9, an enzyme recently found to be activated by BSA (Rowland *et al.*, 2008a). Earlier enzyme kinetic studies were also performed without BSA.

2.4.2 Substrate inhibition in UGT-catalyzed reactions

A higher aglycone substrate concentration often lowers the reaction rate of UGT-catalyzed reactions and may lead to the underestimation of reaction's V_{max} and the erroneous determination of K_m (Figure 18; recently reviewed by Wu, 2011). Substrate inhibition is usually modeled with an empirical equation that is based on a mechanism in which a second molecule of substrate acts as an uncompetitive inhibitor of the reaction (Eq. 9; Figure 19A):

$$(9) v = \frac{V_{max}[S]}{K_m + [S](1 + \frac{[S]}{K_{si}})}$$

where K_{si} is the constant describing the substrate inhibition interaction.

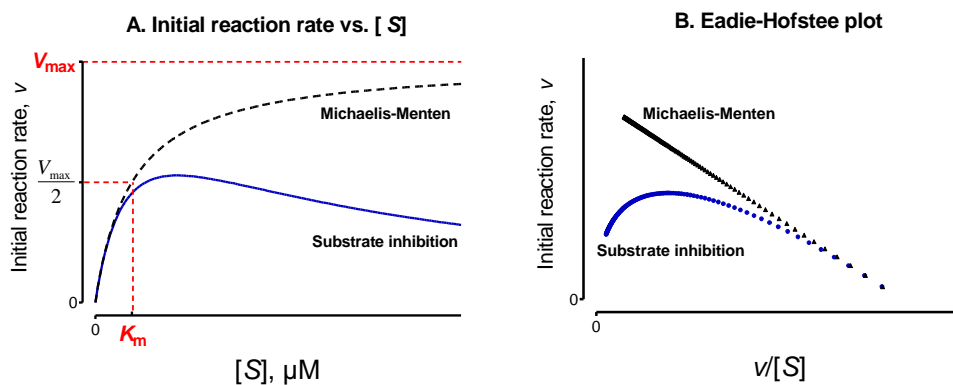


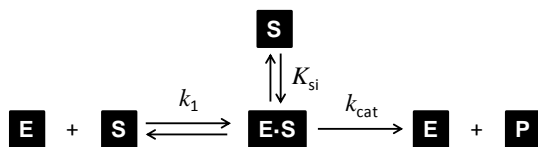
Figure 18. Theoretical saturation profiles of substrate inhibition (solid line) and the Michaelis-Menten equation (dotted line) presented on an initial rate vs. $[S]$ plot (A) and an Eadie-Hofstee plot (B).

A mechanistic model with two equivalent binding sites was proposed as an alternative to the empirical model of substrate inhibition (Houston and Kenworthy, 2000) (Eq. 10; Figure 19B):

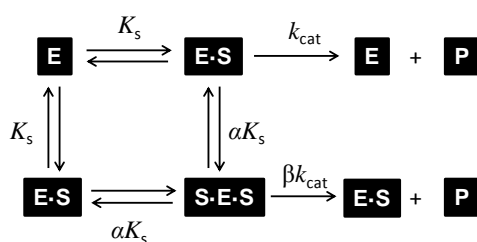
$$(10) v = \frac{V_{\max} \left(\frac{[S]}{K_s} + \frac{\beta[S]^2}{\alpha K_s^2} \right)}{1 + \frac{2[S]}{K_s} + \frac{[S]^2}{\alpha K_s^2}}$$

where K_s is a substrate dissociation constant, α describes the change in substrate binding affinity for the second enzyme site, and β describes the change in the rate of product formation from $S \cdot E \cdot S$ complex in comparison to that from $E \cdot S$ complex. Substrate inhibition occurs if $\beta < 1$, which means that product formation rate from the ternary $S \cdot E \cdot S$ complex is decreased compared to formation rate from the binary $S \cdot E$ complex. This model, however, does not distinguish between the binding of two substrates to two separate active sites or, alternatively, to a single large binding cavity.

A. Empirical model of substrate inhibition



B. Two-site model



C. Substrate inhibition in compulsory-order ternary-complex mechanism

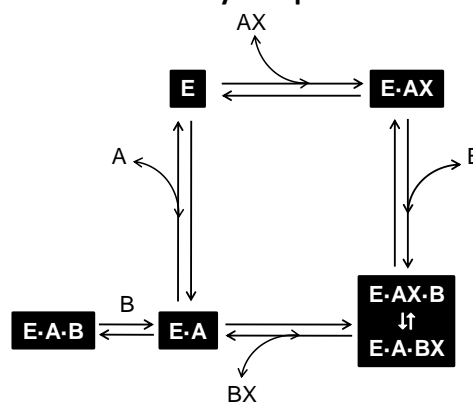


Figure 19. Enzyme kinetic models that describe substrate inhibition in UGT-catalyzed reactions.

Substrate inhibition may also occur due to the compulsory-order ternary-complex reaction mechanism of UGT-catalyzed reactions (Luukkanen *et al.*, 2005). In the case of a general group transfer reaction $AX + B \rightleftharpoons BX + A$, the second substrate B may bind to the “wrong” binary-complex E•A to form an unproductive ternary-complex E•A•B (Cornish-Bowden, 2012) (Figure 19C). Thus, substrate inhibition in the UGT-catalyzed reaction may occur if the second substrate (the aglycone) binds to the enzyme • UDP complex to form an unproductive enzyme • UDP • aglycone complex (Luukkanen *et al.*, 2005). The following equation models this mechanism of substrate inhibition well, assuming a steady state (Cornish-Bowden, 2012):

$$(11) v = \frac{V_{max}[A][B]}{K_{iAX}K_{mB} + K_{mB}[AX] + K_{mAX}[B] + [AX][B](1 + \frac{[B]}{K_{siB}})}$$

where K_{siB} is a constant that describes the substrate inhibition interaction. This model assumes that AX and B are the first and second substrates in the enzyme reaction, respectively.

2.4.3 Inhibition of UGT-catalyzed reactions

Figure 20 presents the most common types of reversible enzyme inhibitors. Inhibitor potency is usually indicated by the descriptive IC_{50} value, the concentration of inhibitor required to inhibit the reaction by 50%, or the mechanistic K_i value, an equilibrium dissociation constant for the enzyme-inhibitor (E•I) complex (Copeland, 2005). Competitive inhibitor binds only to the free enzyme E, uncompetitive inhibitor binds exclusively to the E•S complex, and mixed-type inhibitor binds to both free E and E•S complexes, albeit with different affinities ($K_i \neq \alpha K_i$). Noncompetitive inhibitor is a special case of mixed-type inhibitor that binds with equal affinity to both the free E and the E•S complexes ($\alpha = 1$; $K_i = \alpha K_i$). In order to determine the K_i value, the substrate enzyme kinetics is performed in the presence of several concentrations of inhibitor and the data are fitted to equations for competitive (Eq. 12), mixed-type (Eq. 13), noncompetitive (Eq. 14), and uncompetitive inhibition (Eq. 15) (Copeland, 2000):

$$(12) v = \frac{V_{max}[S]}{[S] + K_m(1 + \frac{[I]}{K_{ic}})}; (13) v = \frac{V_{max}[S]}{[S](1 + \frac{[I]}{\alpha K_{im}}) + K_m(1 + \frac{[I]}{K_{im}})}; (14) v = \frac{V_{max}[S]}{([S] + K_m)(1 + \frac{[I]}{K_{in}})}$$

$$(15) v = \frac{V_{max}[S]}{[S](1 + \frac{[I]}{\alpha K_{iu}}) + K_m}$$

where K_{ic} , K_{im} , K_{in} , and K_{iu} are the competitive, mixed-type, noncompetitive, and uncompetitive inhibition constants, respectively. The coefficient α in Eqs. 13 and 15 represents the relative difference in the inhibitor’s binding affinity between the free enzyme (competitive modality) and the E•S complex (uncompetitive modality).

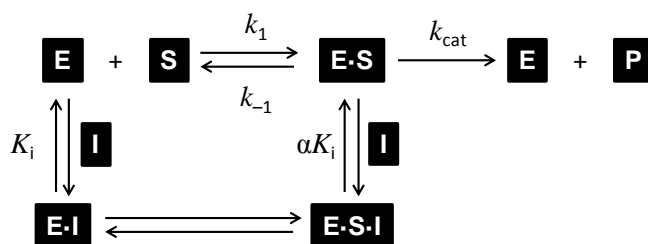


Figure 20. Modalities of reversible enzyme inhibition. If $K_i \ll \alpha K_i$, the inhibitor is mainly competitive; if $K_i \gg \alpha K_i$, the inhibitor is mainly uncompetitive; if $K_i \approx \alpha K_i$, the inhibitor is mixed-type; and if $K_i = \alpha K_i$, the inhibitor is noncompetitive.

However, because UGTs catalyze the two-substrate two-product reaction, the inhibition modality will differ with respect to both substrates. For example, Luukkanen *et al.* (2005) found that 1-naphthol is a competitive inhibitor with respect to the aglycone substrate entacapone, but is uncompetitive with respect to UDPGA. In addition, it is important to notice that the products of the UGT-catalyzed reactions, glucuronide conjugates and UDP, may also inhibit UGTs; this type of inhibition is known as product inhibition. For instance, UDP proved to be a competitive inhibitor with respect to UDPGA, and a noncompetitive inhibitor with respect to the aglycone substrates (Luukkanen *et al.*, 2005, Fujiwara *et al.*, 2008). Moreover, as mentioned in Section 2.4.2, substrate inhibition may be considered as an uncompetitive inhibition by aglycone substrate with respect to itself (Figure 19A).

2.4.4 Atypical enzyme kinetics of UGT-catalyzed reactions

Atypical enzyme kinetics generally refers to saturation profiles that differ from Michaelis-Menten or substrate inhibition. Despite common occurrence, however, some authors also consider substrate inhibition to be “atypical” saturation profile (for examples, see review by Wu, 2011). In UGT-catalyzed reactions, the most commonly observed atypical saturation profiles are sigmoidal and biphasic kinetics (Figure 21). Possible experimental artifacts, most notably the nonspecific binding of substrates (McLure *et al.*, 2000), enzyme inactivation, or the presence of multiple enzymes within the assay, should be excluded before performing a detailed analysis of atypical kinetics. If confirmed, the presence of atypical kinetics may suggest the existence of multiple substrate binding sites or, at least, multiple binding domains within a single large binding cavity (Uchaipichat *et al.*, 2008, Zhou *et al.*, 2010, Zhou *et al.*, 2011, Uchaipichat *et al.*, 2004). Reports of atypical kinetics in glucuronidation could be closely related to the oligomeric state of UGTs (Lewis *et al.*, 2011, Finel and Kurkela, 2008), since the binding of substrate to one enzyme unit may affect the binding of the next substrate to another unit within the same oligomeric complex.

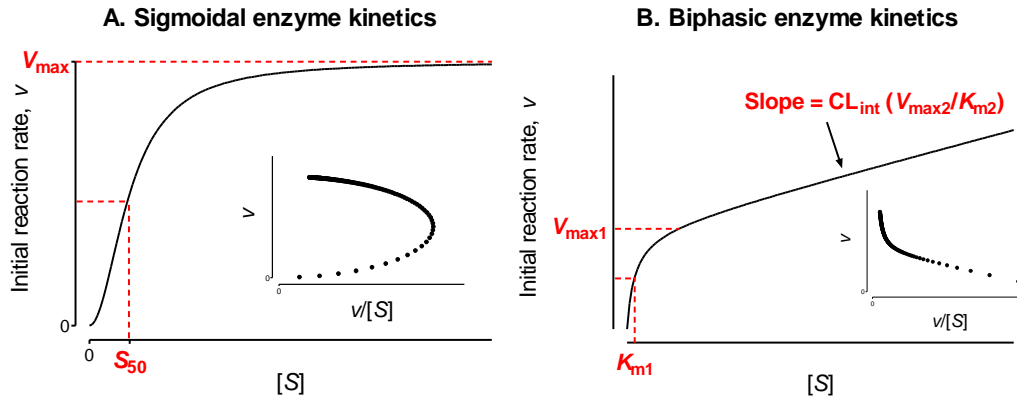


Figure 21. Theoretical saturation profiles for sigmoidal (A) and biphasic (B) enzyme kinetics. Eadie-Hofstee plots appear as insets.

Sigmoidal kinetics results in an *S*-shaped curve which, compared to the Michaelis-Menten hyperbolic profile, is steeper and approaches V_{\max} faster (Figure 21A). This saturation profile usually indicates positive cooperativity, a phenomenon that is frequently present in enzymes with multiple substrate binding sites. The binding of the first substrate induces a conformational change in the enzyme and enhances the binding affinity for the second substrate, thus resulting in sigmoidal kinetics. If the substrate enhances its own reaction (autoactivation), the cooperativity is homotropic; if, however, another molecule enhances the binding of the substrate, the cooperativity is heterotropic. Positive cooperativity presumably plays an important role in the physiological control of enzyme activity (Cornish-Bowden, 2012). This behavior is usually modeled with the empirical Hill equation:

$$(16) v = \frac{V_{\max}[S]^h}{S_{50}^h + [S]^h}$$

where S_{50} is the concentration of the substrate at half of the V_{\max} (analogous to K_m in the Michaelis-Menten model), and h is the Hill coefficient describing the degree of cooperativity. If $h > 1$, the reaction is sigmoidal and exhibits positive cooperativity. One should note, however, that enzymes may also exhibit negative cooperativity ($h < 1$), although the physiological role of this phenomenon is less understood (Cornish-Bowden, 2012). In addition to the Hill equation, Eq. 10 may also be used to model positive cooperativity (see Section 2.4.2). In that case, sigmoidal kinetics takes place if either $\alpha < 1$ or $\beta > 1$, or both. Several UGT substrates, such as 4-methylumbelliferone (4-MU) and 1-naphthol with UGT2B7 (Uchaipichat *et al.*, 2004, Rowland *et al.*, 2008a) and midazolam with UGT1A4 (Hyland *et al.*, 2009), are known to exhibit sigmoidal kinetics. Heterotropic cooperativity also occurred in several other UGT reactions, most notably in UGT1A1 (Zhou *et al.*, 2011), UGT1A4 (Zhou *et al.*, 2010), and UGT2B7 (Uchaipichat *et al.*, 2008). In addition, in contrast to Michaelis-Menten kinetics, the CL_{int} for sigmoidal kinetics, expressed as the V_{\max}/S_{50} ratio, depends heavily on the concentration of substrate and is unsuitable for *in vitro*–*in vivo* extrapolation. The maximum clearance CL_{max} , an alternative parameter that expresses the clearance of a fully activated enzyme before saturation, was suggested as a suitable replacement (Houston and Kenworthy, 2000):

$$(17) CL_{\text{max}} = \frac{V_{\max}}{S_{50}} \frac{(h-1)}{h(h-1)^{1/h}}$$

The biphasic saturation profile is characterized by the presence of two distinct phases: (1) the high affinity–low turnover phase at low concentrations of the substrate and (2) the low affinity–high turnover phase at high concentrations of the substrate (Figure 21B). This saturation profile often occurs in microsomal fractions, where a drug may be a substrate to multiple enzymes with different affinities and turnover rates (for an example, see Rowland *et al.*, 2006, Bowalgaha *et al.*, 2005). On the other hand, if the assay contains a single enzyme, biphasic kinetics may indicate the existence of multiple substrate binding sites. Biphasic kinetics is usually modeled with the following equation (Korzekwa *et al.*, 1998):

$$(18) v = \frac{V_{max1}[S] + \frac{V_{max2}}{K_{m2}}[S]^2}{K_{m1} + [S]} = \frac{V_{max1}[S] + CL_{int}[S]^2}{K_{m1} + [S]}$$

where K_{m1} and V_{max1} describe the high affinity–low turnover phase, and K_{m2} and V_{max2} describe the low affinity–high turnover phase of the reaction. Since the low affinity–high turnover phase is rarely saturated, the accurate determination of V_{max2} may be difficult. For this reason, the V_{max2}/K_{m2} ratio is often replaced with a single parameter, CL_{int} , which represents the slope of the low affinity–high turnover phase (Figure 21B). Alternatively, biphasic kinetics can be modeled with the Hill equation (Eq. 16), assuming negative cooperativity ($h < 1$) (Gaganis *et al.*, 2007).

2.4.5 Substrate depletion assays

In addition to the more common studies of metabolite formation, substrate depletion assays serve as an alternative method to estimate the glucuronidation rate (Kilford *et al.*, 2009, Gill *et al.*, 2012, Jones and Houston, 2004). This approach may prove especially useful if glucuronide standards are unavailable or when the substrate is consumed in several concomitant metabolic pathways, for example if one employs both CYP and UGT cofactors in assays with HLM (Kilford *et al.*, 2009). In order to estimate the CL_{int} with this method (Figure 22), substrate disappearance is monitored over time, and the resulting data points are fitted to the following exponential decay equation:

$$(19) [S]_t = [S]_0 e^{-kt}$$

where $[S]_t$ is the concentration of substrate at time t , $[S]_0$ is the initial concentration of the substrate, and k is the substrate depletion rate constant. The substrate depletion half-life may be calculated as $t_{1/2} = \ln 2/k = 0.693/k$. If monoexponential decay inadequately describes the data, one may use the alternative biexponential decay equation (Jones and Houston, 2004). The resultant substrate depletion rate constant k , together with the incubation volume and microsomal amount, is used to calculate CL_{int} according to Eq. 2 (see Section 2.3.6).

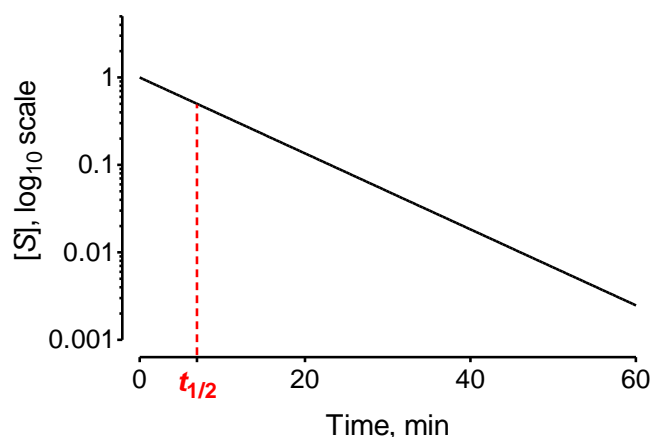


Figure 22. The theoretical representation of the substrate depletion assay ($[S]_0 = 1$; $k = 0.1 \text{ min}^{-1}$; $t_{1/2} = 6.93 \text{ min}$)

The potential problem in substrate depletion assays is that, although product inhibition is usually negligible in the initial-rate studies, one can rarely ignore it during the time course assay. Both UDP and glucuronide conjugates proved to be potent UGT inhibitors (Luukkanen *et al.*, 2005, Fujiwara *et al.*, 2008). Moreover, other problems such as the loss of enzyme activity during the assay, the nonspecific binding of substrates, and analytical sensitivity should be taken into account (Jones and Houston, 2004).

2.4.6 Key statistical concepts used in enzyme kinetics

The standard deviation of the sample (S.D.) quantifies the variability (i.e. scatter) of the data (Motulsky, 1995). If the data are sampled from a Gaussian distribution, 68% and 95% of the values are expected to lie within one and two S.D. from the mean value, respectively (Figure 23). The S.D. is usually calculated according to Eq. 20:

$$(20) \text{ S.D.} = \sqrt{\frac{\sum_{i=1}^N (x_i - x_m)^2}{N-1}}$$

where N is the sample size, x_m is the sample mean value, and x_1, x_2, \dots, x_i are the values of the individual replicates.

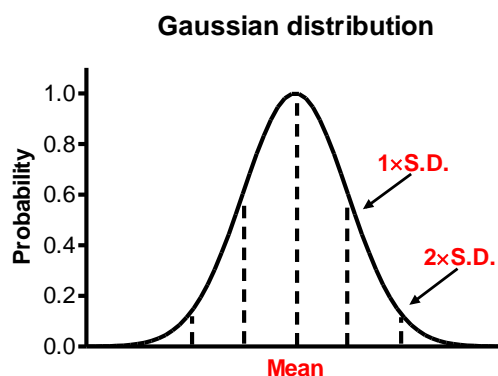


Figure 23. Theoretical representation of data with a Gaussian distribution.

The standard error of the mean (S.E.) quantifies the precision of the mean (Motulsky, 1995) and is a measure of how far the sample mean is likely to be from the true population mean. The S.E. is calculated according to Eq. 21:

$$(21) S.E. = \frac{S.D.}{\sqrt{N}}$$

where S.D. is the standard deviation of the sample, and N is the sample size.

The confidence interval of the mean (CI) quantifies how precisely the mean value was determined (Motulsky, 1995, Motulsky and Christopoulos, 2004). The 95% CI describes the interval with a 95% chance that the true population mean lies within it. In other words, there is a 95% chance that the 95% CI includes the true population mean, and a 5% chance that it does not. The CI is centered on the sample mean and extends symmetrically in both directions. That distance is equal the S.E. multiplied by a constant from the t distribution tables ($p = 0.05$; two-tailed); the value of this constant depends only on the sample size (N). For a large sample size ($N > 10$), the 95% CI is approximately equal to the mean value plus or minus two S.E.

The goal of **nonlinear regression** is to minimize the sum-of-squares of the vertical deviations (distances) of the data points from the fitted curve (Cornish-Bowden, 2012, Motulsky and Christopoulos, 2004) (Figure 24A). The sum-of-squares in nonlinear regression is calculated by:

$$(22) SS_{reg} = \sum_{i=1}^n e_i^2$$

where e_i is the vertical deviation of the data point from the fitted curve, and n is the number of data points. The best-fit values of the enzyme kinetic parameters are those that jointly minimize the sum-of-squares of the deviation. Several methods serve to adjust the parameters in order to minimize the SS_{reg} , most notably the Marquardt-Levenberg, linear descent, and Gauss-Newton method (Motulsky and Christopoulos, 2004). The **coefficient of determination**, r^2 , is commonly used to estimate the goodness-of-fit in nonlinear regression (Motulsky and Christopoulos, 2004). This parameter is expressed as:

$$(23) r^2 = 1 - \frac{SS_{reg}}{SS_{tot}}$$

where SS_{tot} is the total sum-of-squares of the vertical deviations (distances) of the data points from the horizontal line that passes through the mean of all the data points (Figure 24B). A numerical value of r^2 that approaches one indicates that the fitted curve passes closely to the data points. On the other hand, a low or even negative value of r^2 indicates a poor fit (r^2 is not the “square” of anything and can be negative). One should note, however, that r^2 cannot serve to compare models of different complexities. Due to its higher number of parameters, the more complex model will usually have a higher r^2 , even if it is incorrect.

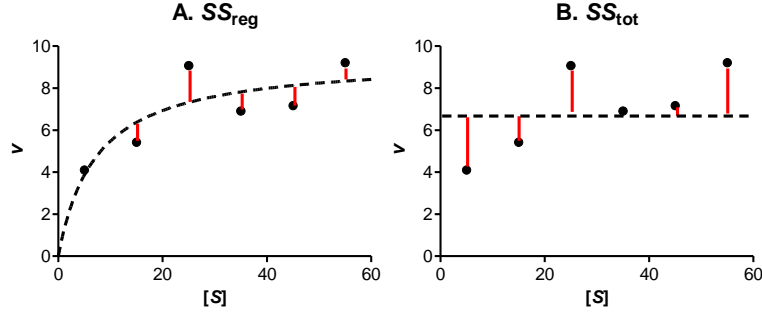


Figure 24. Theoretical representation of SS_{reg} (A) and SS_{tot} (B) in the analysis of the enzyme kinetic data fitted by the Michaelis-Menten equation.

A successful comparison between a simpler and a more complex model in enzyme kinetics should balance: (1) the decrease in SS_{reg} and (2) the increase in the number of parameters (or a decrease in the degrees of freedom). Such a comparison is usually performed by the **extra sum-of-squares F-test** and the **corrected Akaike's information criterion** (Motulsky and Christopoulos, 2004). The F-test is based on hypothesis testing where the null hypothesis states that the simpler model (model 1) is correct, whereas the alternative hypothesis supports the more complex model (model 2). First, the F-ratio is calculated as follows:

$$(24) F_{ratio} = \frac{\frac{SS_{reg1} - SS_{reg2}}{DF_1 - DF_2}}{\frac{SS_{reg2}}{DF_2}}$$

where SS_{reg1} and SS_{reg2} are the sum-of-squares, and DF_1 and DF_2 are the degrees of freedom for the simpler and more complex models, respectively. The degrees of freedom equal the number of data points minus the number of parameters in the model. If the simpler model is correct, the F-ratio is close to one; if, however, the F-ratio is much greater than one, the complex model is more probable. The p value is calculated from the F-ratio using the F-distribution tables. Usually, if the p value is less than 0.05, the simpler model is rejected and the more complex model is accepted as a better fit to the data. The F-test can only be used if kinetic models are “nested”, however, meaning that one model is a special case of another model (for example, Michaelis-Menten model is a special case of substrate inhibition model where K_{si} is infinitely large) (Motulsky and Christopoulos, 2004). The values of the corrected Akaike's information criterion (for both the simpler and more complex models) are calculated according to the following equation:

$$(25) AIC_c = N \ln \left(\frac{SS_{reg}}{N} \right) + 2K + \frac{2K(K+1)}{N-K-1}$$

where N is the number of data points, and K is the number of parameters in the equation, plus one. Next, the difference in AIC_c between the two models is calculated as follows: $\Delta AIC_c = AIC_c^1 - AIC_c^2$ where AIC_c^1 and AIC_c^2 are the corrected Akaike's information criteria for the simpler and more complex models, respectively. If $\Delta AIC_c < 0$, the complex model is more probable, whereas if $\Delta AIC_c > 0$, the simpler model is more probable. In other words, the model with higher numerical value of AIC_c is more probable. One can calculate the probability of the correct decision as follows: $Probability = \frac{e^{-0.5\Delta AIC_c}}{1 + e^{-0.5\Delta AIC_c}}$ (Motulsky and Christopoulos, 2004).

3 Aims of the Study

The aims of this study were:

1) To examine the glucuronidation of psilocin, a hallucinogenic indole alkaloid isolated from mushrooms of the genus *Psilocybe*, by HLM, HIM, and a set of recombinant human UGT enzymes that includes all the members of subfamilies 1A, 2A, and 2B (**I**). With the aim of deepening out insight into the substrate specificity of human UGTs, we also studied the glucuronidation of 4-hydroxyindole (4-HI), a simpler analog of psilocin that lacks the side chain in position 3 of the indole. Considering potential chemical degradation of psilocin during the *in vitro* assays, we investigated suitable methods for improving the stability of psilocin in buffered aqueous solutions. Another goal of this study was to specify the human tissues in which psilocin glucuronidation takes place. For this purpose, in collaboration with Dr. Michael H. Court from Tufts University School of Medicine, we used real-time qRT-PCR to examine the expression levels of UGTs that were most active in psilocin glucuronidation.

2) To investigate the scope and mechanism of albumin effects in HLM, HIM, and recombinant human UGTs expressed in *Sf9* insect cells (**II**, **III**, and **IV**). We aimed to identify the human UGTs affected by the addition of albumin, to quantify those effects, and to examine whether or not the albumin effects depend on the substrate. Moreover, our goal was to carefully optimize the assays conditions of *in vitro* UGT assays, especially with respect to the nonspecific binding of substrates and the optimal concentration of albumin.

3) To investigate the enzyme kinetic mechanism of UGT1A9 in the absence and presence of albumin (**IV**). Our main goals were to examine whether or not UGT1A9-catalyzed reactions proceed through the formation of ternary-complex, what is the order of substrate binding, and how the addition of albumin influences the mechanism and enzyme kinetic parameters of these reactions. Another aim of this part of the study was to determine both the individual rate constants and the equilibrium constant of the overall reaction (K_{eq}) by carrying out the reverse reaction in the presence of albumin.

4 Materials and Methods

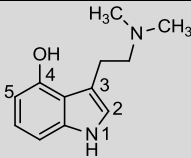
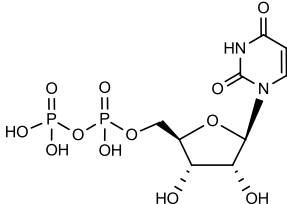
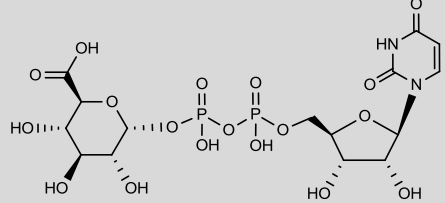
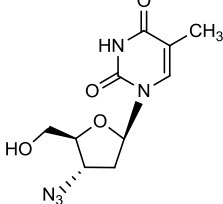
A detailed description of the materials, chemicals, synthetic, analytical, and biochemical methods is presented in publications **I–IV**. This section only briefly summarizes the most important chemicals and methods used in this study.

4.1 Chemicals

In general, we used chemicals and solvents of the highest available purity. The chemical structures of the UGT substrates and inhibitors used in this study appear in Table 9. Psilocin [3-(*N,N*-dimethylaminoethyl)-4-hydroxyindole] and 6-hydroxyindole (6-HI) were synthesized in our laboratory (for a description, see *Materials and Methods* in publications **I** and **III**).

Table 9. UGT substrates and inhibitors used in this study (in alphabetical order). The *logP* and *logD* (pH 7.0) values were calculated by ACD/Labs Software V11.02 (Toronto, Canada)

Substrate (abbreviation)	Structure	M (g/mol)	<i>logP</i> (log <i>D</i> , pH 7)	Study
17 α -Estradiol		272.38	4.15 (4.15)	III
17 β -Estradiol		272.38	4.15 (4.15)	I and III
Entacapone		305.29	2.12 (0.47)	II and III
4-Hydroxyindole (4-HI)		133.15	1.95 (1.95)	I and III
6-Hydroxyindole (6-HI)		133.15	1.95 (1.95)	III
4-Methylumbelliferone (4-MU)		176.17	2.43 (2.43)	II , III , and IV
4-Methylumbelliferone- β -D-glucuronide (4-MUG)		352.29	-0.51 (-4.18)	II , III , and IV
1-Naphthol		144.17	2.72 (2.72)	I , III , and IV

Psilocin		204.27	1.46 (-0.68)	I
UDP		404.16	-2.95 (-7.76)	III
UDP- α -D-glucuronic acid (UDPGA)		580.29	-3.90 (-9.65)	I, II, III, and IV
Zidovudine (AZT)		267.24	-0.58 (N.A.)	II

4.2 *In vitro* glucuronidation assays

The recombinant UGT enzymes used in this study were expressed as His-tagged proteins in baculovirus-infected *Sf9* insect cells (Sneitz *et al.*, 2009, Kurkela *et al.*, 2007). In order to better compare the glucuronidation rates of different UGT enzymes, we employed immunodetection to measure the relative expression levels of each recombinant UGT enzyme by using tetra-His antibodies (QIAGEN, Hilden, Germany) as the primary antibody (Kurkela *et al.*, 2007). The relative expression levels obtained served to “normalize” the measured activities of the recombinant UGTs (**I** and **III**). Insect cell membranes without any human UGT, prepared by infecting insect cells with baculovirus that encodes no human UGT, were used as a negative control for all glucuronidation assays. Control insect cell membranes also served to determine the nonspecific binding of substrates to UGT enzymes expressed in insect cells (**II**, **III**, and **IV**). We obtained the HLM and HIM, as well as the recombinant UGT1A9 (BD Supersomes[®] also expressed in *Sf9* insect cells) used in study **II**, from commercial sources (BD Biosciences; Woburn, MA, USA). Due to the lack of UGT-specific antibodies (see Section 2.1.5), we did not compare the expression levels of our in-house prepared UGTs to expression levels of UGTs present in HLM, HIM, or commercial BD Supersomes[®]. In publication **II**, we measured the nonspecific binding of substrates and inhibitors to the externally added albumin and enzymes sources using ultrafiltration (Amicon Ultra[®] filters with 10-kDa regenerated cellulose membrane; Millipore Corporation, Billerica, MA, USA). In publications **III** and **IV**, we performed binding assays with rapid-equilibrium dialysis (RED, Thermo Scientific, Rockford, IL, USA).

Glucuronidation assays were performed in 50-mM phosphate buffer (pH 7.4, 50 mM) supplemented with 10 mM of MgCl₂. The glucuronidation reactions contained 0.02–1.50 mg/mL of enzyme source (total protein content). Aglycone substrates and inhibitors were added as

methanol or ethanol solutions, and the organic solvent was evaporated *in vacuo*. Assays with HLM and HIM also contained alamethicin in order to eliminate UGT latency (Little *et al.*, 1997, Fisher *et al.*, 2000) (**I** and **II**). No alamethicin was added to the assays with recombinant UGTs, as it does not increase the activity in such samples (Kaivosari *et al.*, 2008, Walsky *et al.*, 2012, Zhang *et al.*, 2011). Assays with psilocin also contained 1 mM of dithiothreitol (DTT), a reducing agent that served to prevent the oxidative degradation of the substrate (**I**). We generally avoided using organic solvents; exceptions were assays with 17 α - and 17 β -estradiol, as well as assays with high concentrations of 4-MU and 1-naphthol ($[S] > 1$ mM), where 1% DMSO was added to the incubations (**I** and **III**). Based on the preliminary assays, this concentration of organic solvent produced a minimal inhibitory effect on the UGT enzymes ($\leq 20\%$). The assays with albumin contained 0.01–2% of fatty acid-free BSA (essentially fatty acid free, $\leq 0.004\%$, Sigma-Aldrich, St. Louis, MO; **II**, **III**, and **IV**). First, we prewarmed the UGT reaction mixtures at 37 °C for 5 min, initiated reactions by the addition UDPGA, and then incubated them at 37 °C for 10–120 min protected from light. Reactions were stopped by adding either 4 M perchloric acid, 4 M perchloric acid/methanol (1:5) mix, 5% acetic acid in methanol, or pure methanol, depending on the preliminary assays. After reaction stopping, we kept the tubes at –20 °C for 30–60 min and centrifuged at 16000g. Aliquots of the supernatants were transferred to dark vials and directly submitted to HPLC, UPLC, or LC–MS analyses.

4.3 Enzyme kinetic assays

Prior to the enzyme kinetic assays, we carried out preliminary assays in order to optimize the concentration range of substrates, the protein amount, and the incubation time. With the aim of preventing excessive nonspecific binding and consumption of substrates ($\leq 10\%$ allowed), we generally performed enzyme kinetic assays with low amounts of microsomal fractions or recombinant UGTs (0.02–0.2 mg/mL) and shorter incubation times (10–60 min). Exceptions included screening assays with psilocin and 4-HI, where we used higher concentrations of the enzyme (0.5–1 mg/mL). The linearity of product formation with respect to the protein amount and the incubation time was tested for each enzyme-substrate pair at low concentration of substrate ($[S] < K_m$). The concentrations of substrates were corrected for nonspecific binding prior to data analysis.

4.4 Analytical methods

Substrates and glucuronides were generally analyzed with HPLC and UPLC equipped with UV, fluorescent, or radio flow detectors (**I**, **II**, **III**, and **IV**). In addition, we used LC–MS to qualitatively analyze the psilocin and 4-HI glucuronides (**I**). When available, authentic standards served for quantification. In the case of psilocin- β -D-glucuronide and 4-hydroxyindole- β -D-glucuronide, however, such glucuronide standards were unavailable and the quantification was achieved with radiolabeled [14 C] UDPGA and the combination of radiochemical and UV detection (**I**). In the combined radioactive-UV analysis of psilocin, a glucuronidation reaction containing 1.5 mg/mL recombinant UGT1A10 in a final volume of 360 μ L was carried out in the presence of 1 mM psilocin. For this purpose the cosubstrate mixture contained 15.4 μ M radiolabeled [14 C] UDPGA and 500 μ M unlabeled UDPGA, and the incubation time was 120 min at 37 °C (**I**). In the case of 17 α -estradiol- β -D-glucuronide and 6-hydroxyindole- β -D-glucuronide, quantification was achieved based on the standard curves that we constructed using UV absorption of the corresponding substrates (**IV**). For this purpose, to

verify whether the substrates and glucuronides differ in their spectral properties, we compared the UV spectra of 17 α -estradiol and 6-HI to the UV spectra of the corresponding glucuronides and found no significant differences in the UV absorption maxima (not shown).

4.5 Data analysis

The enzyme kinetic parameters were obtained by fitting the kinetic models to the experimental data using GraphPad Prism version 5.04 (GraphPad Software Inc., San Diego, CA, USA), SigmaPlot 11 (Systat Software, San Jose, CA, USA), or MATLAB version R2010a (MathWorks, Natick, MA, USA). We selected the most appropriate kinetic model for each reaction based on a visual inspection of the Eadie-Hofstee and Lineweaver-Burk plots (Section 2.4), residuals graphs, parameter S.E. and estimates of the 95% confidence intervals (95% CI), the calculated r^2 values, the corrected Akaike's information criterion, and the extra sum-of-squares F-test (see Section 2.4.6). In assays containing BSA, we corrected the free substrate or inhibitor concentrations (f_u , or fraction unbound) according to the drug binding to BSA measured under the specific conditions of each glucuronidation assay. In other words, the concentrations of substrates and inhibitors were corrected for total drug binding in UGT specific assay (BSA + UGT enzyme source + buffer etc.).

5 Results and Discussion

5.1 Glucuronidation of psilocin and 4-HI by human UGTs (I)

Psilocin is an active metabolite responsible for the hallucinogenic effects of “magic mushrooms” (see Section 2.2.2). Forensic and pharmacokinetic studies identified psilocin glucuronide as the major metabolite of psilocin in both serum and urine (Kamata *et al.*, 2006, Hasler *et al.*, 2002, Kamata *et al.*, 2003, Hasler *et al.*, 1997, Sticht and Kaferstein, 2000, Sticht and Kaferstein, 2000, Grieshaber *et al.*, 2001, Grieshaber *et al.*, 2001). In order to gain mechanistic insight into the metabolism of psilocin, we studied the glucuronidation of psilocin HLM, HIM, and the 19 recombinant human UGTs of subfamilies 1A, 2A, and 2B that were expressed in insect *Sf9* cells. Moreover, to examine the substrate selectivity of human UGTs, we studied the glucuronidation of 4-HI, the simplified analogue of psilocin that lacks the *N,N*-dimethylaminoethyl side chain in position 3 (see Table 9 for chemical structures).

5.1.1 Prevention of psilocin degradation *in vitro*

Our preliminary experiments confirmed that psilocin is unstable in aqueous buffer solutions, especially in the presence of light, heat (37 °C), DMSO, and high concentrations of protein (Anastos *et al.*, 2006). The degradation of psilocin, presumably due to oxidative processes, resulted in pronounced darkening of the solution and the appearance of numerous additional peaks in the HPLC-UV chromatograms. To overcome this problem, we tested the effects of two reducing agents (or antioxidants), ascorbic acid and DTT, on psilocin glucuronidation by UGT1A10 (Figure 25A). The 4-HI, on the other hand, was chemically stable under assays conditions.

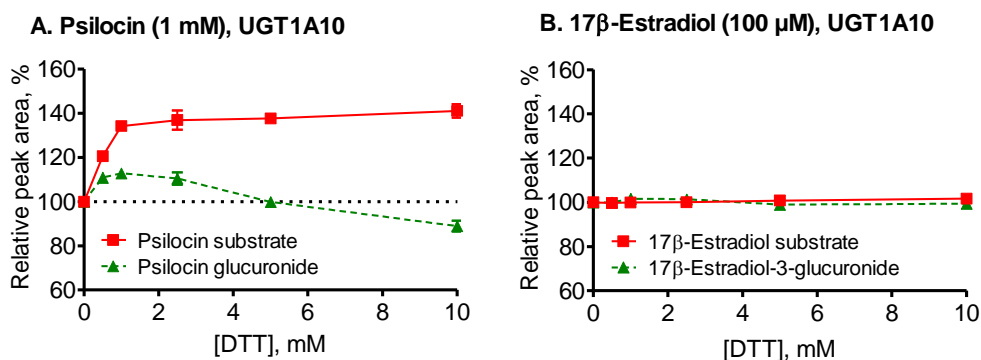


Figure 25. The influence of DTT on the glucuronidation of psilocin (A) and 17β-estradiol (B) by UGT1A10. The results (mean ± S.E.) appear as the relative peak area (in %), for both substrate and glucuronide peaks, compared to control samples without DTT.

The addition of up to 2.5 mM of DTT enhanced the glucuronidation rate, increased the peak area of the psilocin substrate, and prevented both the visual darkening and the appearance of additional chromatographic peaks. On the other hand, the effects of ascorbic acid were less favorable. Although the addition of ascorbic acid prevented the visual darkening of the solution, significant chromatographic interferences persisted. With an aim to verify whether or not the

addition of DTT modulates UGT activity, we tested the influence of DTT on the glucuronidation of a chemically stable substrate, 17 β -estradiol, by UGT1A10 (Figure 25B), and detected no significant inhibition or stimulation. We obtained a similar absence of a DTT effect in the 4-HI glucuronidation by UGTs 1A6, 1A7, 1A8, 1A9, 1A10, and 2A1 (data now shown). Although these results are in close agreement with those of a previous report that DTT does not affect the bilirubin glucuronidation by UGT1A1 (Ghosh *et al.*, 2005), they somewhat disagree with earlier reports that DTT activates UGTs from rat liver microsomes (El-Bacha *et al.*, 2000, Ikushiro *et al.*, 2002). Taken together, our results suggest that DTT may serve as an efficient antioxidant in glucuronidation studies of substrates prone to oxidative degradation.

5.1.2 Screening assays with HLM, HIM, and recombinant UGTs

The incubation of psilocin and 4-HI with HLM and HIM, as HPLC and LC–MS analyses show, resulted in the formation of single glucuronide products. Although we did not perform the complete structural analysis of the products, the comparative analysis of serotonin glucuronide (Krishnaswamy *et al.*, 2003b), a close structural analog of psilocin, suggests that *O*-glucuronides form. The rates of psilocin glucuronidation by HLM and HIM were approximately equal for all three concentrations of substrate tested, namely 100, 500, and 1000 μ M (Figure 26A). On the other hand, the rates of 4-HI glucuronidation in HLM were 10-fold higher compared to corresponding 4-HI rates in HIM, and almost 20-fold higher than the psilocin glucuronidation rates in either HLM or HIM (Figure 26B).

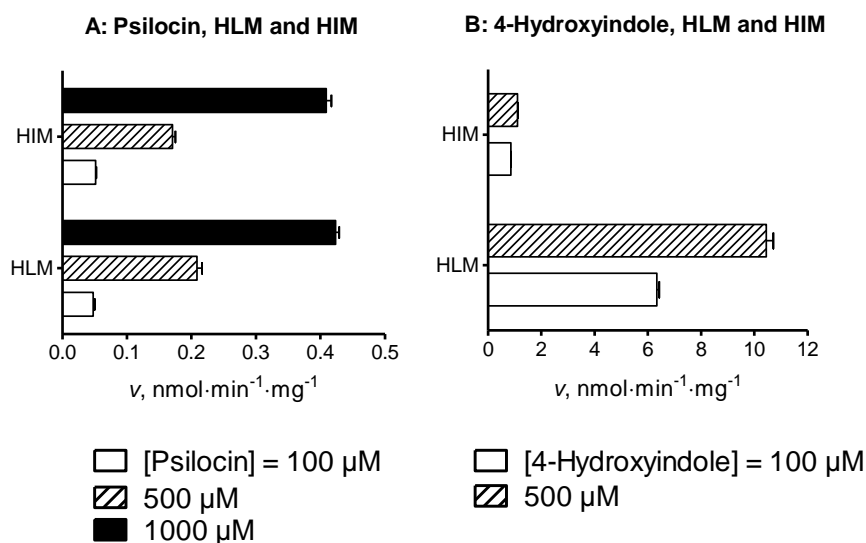


Figure 26. Glucuronidation of psilocin (A) and 4-HI (B) by HLM and HIM. We performed assays at three psilocin concentrations (100, 500, and 1000 μ M) and two 4-HI concentrations (100 and 500 μ M). The bars represent an average of three samples \pm S.E.

The screening assay with the recombinant UGTs revealed that psilocin is glucuronidated mainly by UGTs 1A10, 1A9, 1A8, 1A7, and, to a minor extent, by UGT1A6 (Figure 27A). The UGT enzymes from the subfamilies UGT2A and UGT2B proved inactive. In contrast to the psilocin results, 4-HI glucuronidation screening showed that UGT1A6 is by far the most active enzyme, whereas the glucuronidation rates of UGTs 1A7–1A10 closely resembled their respective

psilocin glucuronidation activities (Figure 27B). In addition, 4-HI was glucuronidated by UGT2A1, an enzyme expressed in the nasal epithelium (see Section 2.1.5). The lack of glucuronidation activity by UGTs 1A4 and 2B10, the main enzymes involved in *N*-glucuronidation reactions, suggests that only *O*-glucuronides form from both psilocin and 4-HI.

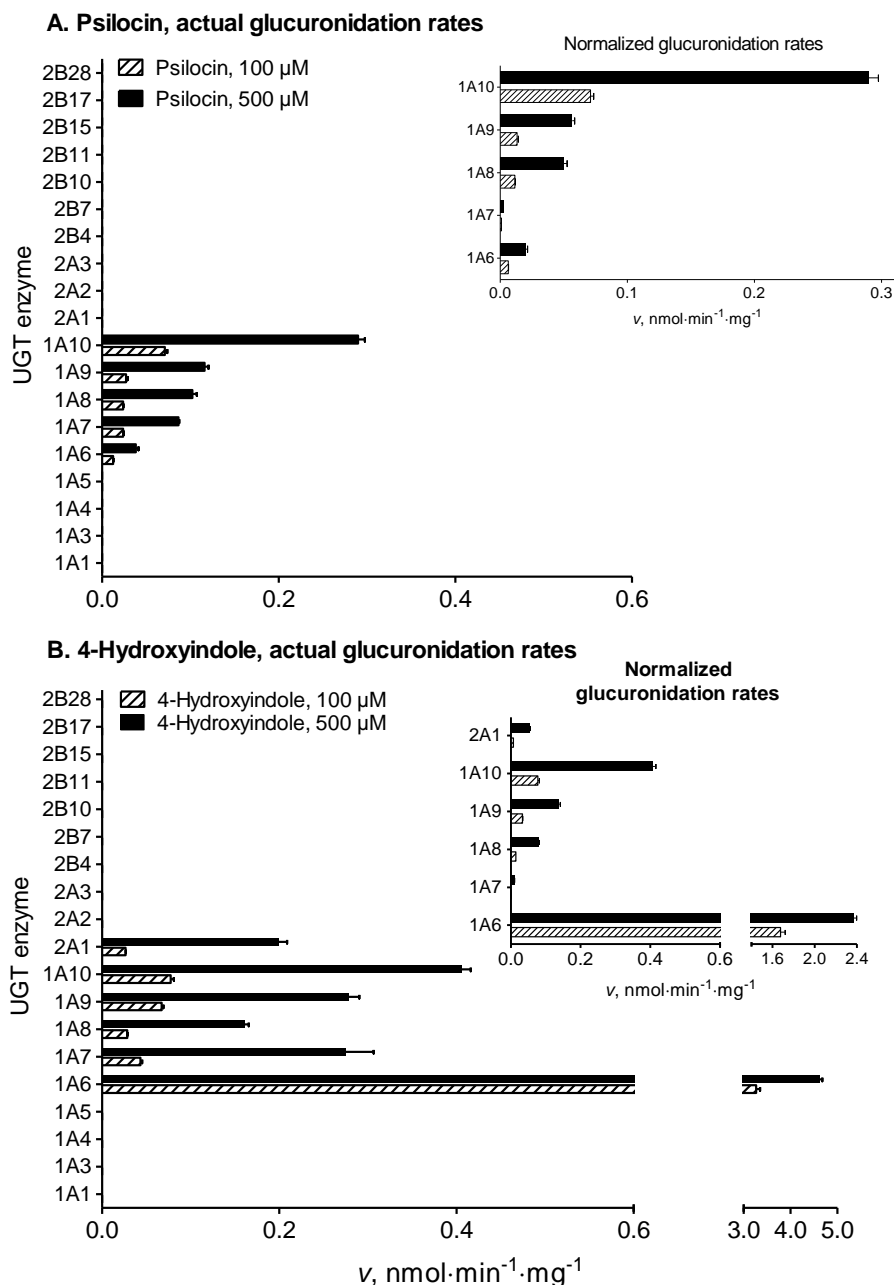


Figure 27. Glucuronidation of psilocin (A) and 4-HI (B) by 19 human recombinant UGTs. The screening assays appear at two concentrations of substrate: 100 and 500 µM. The bars represent mean ± S.E. ($n = 3$). The results appear as actual glucuronidation (measured) rates. For the active UGTs, the results also appear as normalized rates (corrected for the relative expression level). The expression level of UGT1A10 was set to 1.0 for normalization. See publication I for additional details.

The glucuronidation of psilocin by UGTs 1A7–1A10, as well as its poor activity with UGT1A6, are surprising in view of the previous reports of serotonin and 5-hydroxytryptophol glucuronidation, close structural analogs predominantly glucuronidated by UGT1A6 (Krishnaswamy *et al.*, 2003a, Krishnaswamy *et al.*, 2004). Such differences in the substrate selectivity of human UGTs may be attributed to structural and physicochemical differences between psilocin and serotonin, especially with respect to the bulkiness of the side chain, the position of the phenol group, and the difference in lipophilicity. Moreover, compared to psilocin, the 100-fold higher glucuronidation activity of 4-HI by UGT1A6, but relatively similar activities of UGTs 1A7–1A10, may suggest that the *N,N*-dimethylaminoethyl side chain of psilocin hinders the activity of UGT1A6, but affects UGTs 1A7–1A10 only slightly.

5.1.3 Enzyme kinetics of psilocin and 4-HI glucuronidation

We performed the enzyme kinetics assays of psilocin glucuronidation by UGTs 1A10 and 1A9, the two enzymes that exhibited the highest normalized glucuronidation rates in the screening assay (Figure 28). Psilocin glucuronidation by UGT1A10 followed low affinity–high turnover Michaelis-Menten kinetics (Figure 28). The substrate affinity for the enzyme was low, as the very high K_m value (over 3 mM) indicates, whereas the estimated V_{max} value was the highest among tested recombinant UGTs (Table 10). The enzyme kinetics of psilocin glucuronidation by UGT1A9 exhibited an atypical biphasic profile, and the data were fitted to Eq. 18 (see Section 2.4.4). The K_{m1} for this reaction (estimated value: 1 mM) was also high, whereas the K_{m2} and V_{max2} values were determined only as a ratio ($V_{max2}/K_{m2} = CL_{int}$; Table 10) because no saturation was achieved.

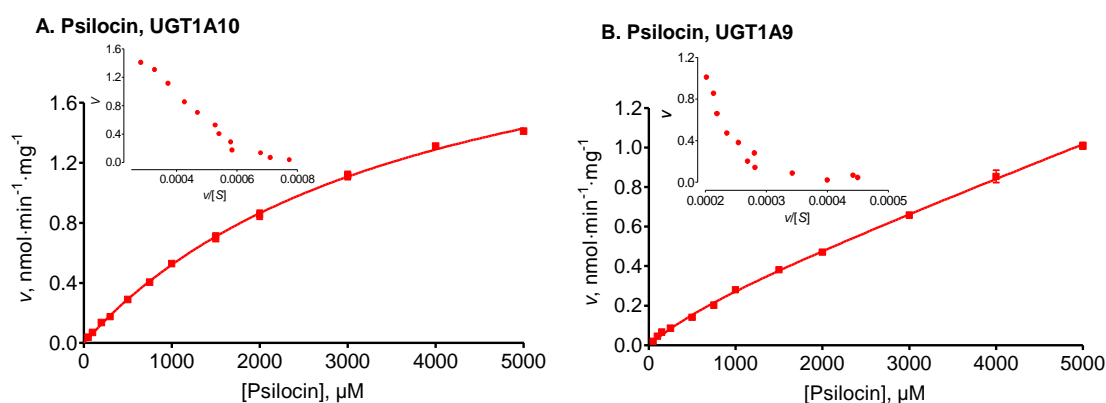


Figure 28. Enzyme kinetics of psilocin glucuronidation by UGT1A10 (A) and UGT1A9 (B). The points represent an average of three samples \pm S.E. Glucuronidation rates appear as actual (measured) rates in $\text{nmol}\cdot\text{min}^{-1}\cdot\text{mg}^{-1}$ of recombinant protein. The derived kinetic constants and normalized glucuronidation values appear in Table 10. The Eadie-Hofstee transforms of the data appear as insets.

In the case of 4-HI, we performed enzyme kinetic assays with UGTs 1A6, 1A10, and 2A1. The glucuronidation of 4-HI by UGT1A6 showed pronounced substrate inhibition kinetics (Figure 29A). This substrate exhibited a relatively high affinity for UGT1A6 ($K_m < 200 \mu\text{M}$) with fast glucuronidation rates in the lower concentration range (Table 10). UGT1A10, on the other hand,

displayed atypical kinetics with 4-HI, revealed by possible sigmoidal kinetics at the lower concentration range (50–500 μM) and substrate inhibition at high concentrations of the substrate (Figure 29B, see Eadie-Hofstee plot; Table 10). For this reason, we fitted the data to both the empirical substrate inhibition equation (Eq. 9) and the Hill equation (Eq. 16). The Hill equation provided an arguably more accurate description of the data, since the estimated S_{50} is a more realistic value than the K_m obtained with the substrate inhibition equation (Table 10). Moreover, we tried to fit the data from 4-HI glucuronidation by UGT1A10 to the two-site model (Eq. 10, see Section 2.4.2). This resulted in the poor estimate of enzyme kinetic parameters, perhaps partly due to the insufficiently defined substrate inhibition section of the curve, mainly caused the limited aqueous solubility of the substrate. The Michaelis-Menten equation most accurately described the kinetics of 4-HI glucuronidation by UGT2A1 (Figure 29C), and the analysis revealed a low affinity, as indicated by the very high K_m value ($> 3 \text{ mM}$), and a moderate V_{max} value (Table 10).

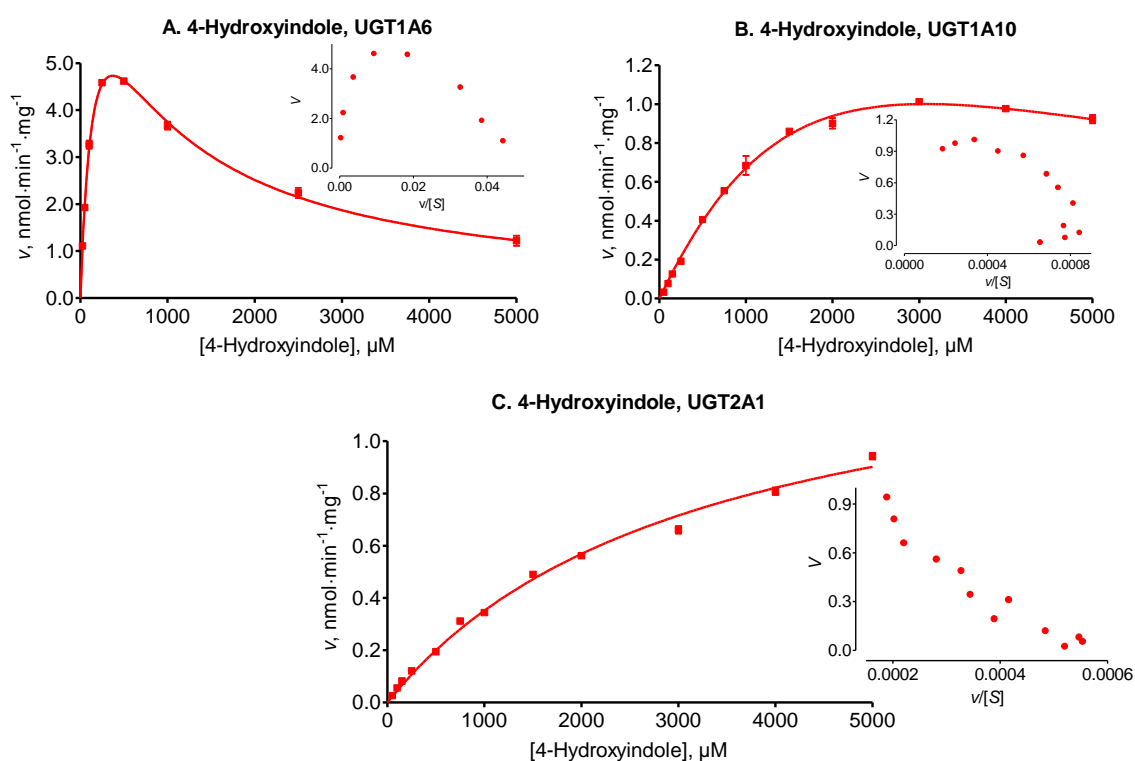


Figure 29. Enzyme kinetics of 4-HI glucuronidation by UGT1A6 (A), UGT1A10 (B), and UGT2A1 (C). The points represent an average of three samples \pm S.E. Glucuronidation rates appear as actual (measured) rates in $\text{nmol}\cdot\text{min}^{-1}\cdot\text{mg}^{-1}$ of recombinant protein. The derived kinetic constants and normalized glucuronidation values appear in Table 10. The Eadie-Hofstee transforms of the data appear as insets.

Table 10. Psilocin and 4-HI glucuronidation enzyme kinetic data. The values represent the best fit results \pm S.E. The reaction velocity appears both as actual rates and as rates normalized to the expression level of UGT1A10 (for UGT1A10, the actual and normalized rates are identical).

Substrate	Enzyme	K_m	V_{max} (actual rates)	V_{max} (normalized rates)	K_{is}	Kinetic model (r^2)
		μM	$nmol \cdot min^{-1} \cdot mg^{-1}$	$nmol \cdot min^{-1} \cdot mg^{-1}$		
Psilocin	UGT1A10	3851.0 ± 166.6	2.53 ± 0.06	—	—	Michaelis-Menten (0.997)
	UGT1A9	$K_{m1} = 1017.0 \pm 249.9^a$	$V_{max1} = 0.38 \pm 0.14^a$	$V_{max1} = 0.19 \pm 0.04^a$	—	Biphasic (0.996)
4-HI	UGT1A10	3624.0 ± 839.7	3.36 ± 0.63	—	2603.0 ± 744.8	Substrate Inhibition (0.992)
		$S_{50} = 631.6 \pm 32.7$	1.03 ± 0.02	—	—	Hill equation (0.986); $h = 1.6 \pm 0.1$
	UGT1A6	178.7 ± 14.8	9.31 ± 0.45	4.78 ± 0.23	765.1 ± 65.5	Substrate Inhibition (0.991)
	UGT2A1	3210.0 ± 235.7	1.48 ± 0.06	0.39 ± 0.02	—	Michaelis-Menten (0.992)

^a The calculated CL_{int} is $1.69 \times 10^{-4} \pm 1.04 \times 10^{-5} \text{ mL} \cdot \text{min}^{-1} \cdot \text{mg}^{-1}$ (normalized, $8.29 \times 10^{-5} \pm 5.12 \times 10^{-6} \text{ mL} \cdot \text{min}^{-1} \cdot \text{mg}^{-1}$) and represents the linear portion of the biphasic curve (ratio V_{max2}/K_{m2}). Data were also fitted to the Michaelis-Menten equation, $K_m = 12047 \pm 1428 \mu M$, $V_{max} = 3.41 \pm 0.31$ (normalized, 1.66 ± 0.15) $\text{mL} \cdot \text{min}^{-1} \cdot \text{mg}^{-1}$, $r^2 = 0.996$.

One of the main findings of this study was that UGT1A10 appears to interact with psilocin and 4-HI similarly, whereas UGT1A6 exhibits a clear preference for 4-HI (Figure 27). The low activity of psilocin glucuronidation by UGT1A6 may stem from poor binding, low enzyme turnover (nonproductive binding), or both. In order to determine whether or not psilocin binds to UGT1A6 with significant affinity, we tested psilocin as the inhibitor of 4-HI glucuronidation by UGT1A6 (see Figure 8 in publication I). The results showed that even high concentrations of psilocin only slightly inhibited 4-HI glucuronidation of UGT1A6, thus indicating poor binding affinity. In contrast to psilocin, 1-naphthol, a high-affinity substrate for UGT1A6, was a good inhibitor of 4-HI glucuronidation by UGT1A6 ($IC_{50} = 57 \mu M$; K_i estimate is $27 \mu M$).

5.1.4 Expression of UGT enzymes that glucuronidate psilocin

To investigate the possible locations of psilocin glucuronidation in the human body, this study also examined the expression levels of the genes encoding UGTs 1A6–1A10 by qRT-PCR (Table 11). This work was performed in collaboration with Dr. Michael H. Court of the Tufts University School of Medicine, Boston, Massachusetts. UGT1A6 is abundantly expressed in the liver, trachea, kidneys, and intestine (stomach, small intestine, and colon); UGT1A9 was found in the liver, kidneys, and intestine, whereas expression of UGT1A10 is limited mainly to the intestine. On the other hand, the expression levels of UGTs 1A7 and 1A8 were markedly lower in all the tissues studied. The gene expression results also revealed that none of the UGTs examined is expressed in the brain, implying that in humans, neither psilocin nor serotonin is glucuronidated inside this organ. These results agree closely with those of studies published on UGT expression in human tissues (see Section 2.1.5).

Table 11. Expression of UGTs 1A6, 1A7, 1A8, 1A9, and 1A10 mRNA in human tissues. The data appear as mRNA copies per 10^9 copies of 18S rRNA, mean \pm S.E.

Tissue	UGT enzymes				
	1A6	1A7	1A8	1A9	1A10
	<i>copies per 10⁹ copies of 18S rRNA, mean \pm S.E.</i>				
Adipose	28 \pm 8	18 \pm 6	8 \pm 2	86 \pm 15	313 \pm 57
Adrenal gland (<i>n</i> = 62)	3.0 \pm 0.3	43 \pm 9	—	3.0 \pm 0.4	—
Brain	—	—	—	—	—
Brain, cerebellum (<i>n</i> = 24)	—	—	—	—	—
Colon (<i>n</i> = 3)	215 \pm 22	79 \pm 22	25 \pm 8	188 \pm 55	1210 \pm 299
Kidney	226 \pm 19	104 \pm 12	—	2157 \pm 269	—
Liver, adult (<i>n</i> = 47)	923 \pm 9	40 \pm 11	—	3239 \pm 42	6.0 \pm 0.2
Lung	2 \pm 1	—	—	—	—
Ovary	—	—	—	—	—
Pancreas	—	—	—	—	—
Placenta	4.0 \pm 0.3	3.0 \pm 0.1	—	3.0 \pm 0.2	—
Prostate (<i>n</i> = 47)	68 \pm 2	9 \pm 1	1 \pm 1	8 \pm 1	6 \pm 1
Small intestine (<i>n</i> = 5)	334 \pm 77	80 \pm 33	12 \pm 2	319 \pm 109	660 \pm 254
Stomach	184 \pm 59	7 \pm 1	—	4 \pm 1	21 \pm 3
Testis (<i>n</i> = 19)	14 \pm 2	2.0 \pm 0.3	1.0 \pm 0.3	13 \pm 3	6 \pm 1
Thyroid (<i>n</i> = 65)	11 \pm 1	3 \pm 1	—	1.0 \pm 0.1	—
Trachea	693 \pm 76	26 \pm 9	7.0 \pm 0.5	32 \pm 7	27 \pm 8
Uterus (<i>n</i> = 10)	53 \pm 13	—	—	—	—

—, Not detected

The differential expression of UGTs 1A9 and 1A10, in combination with the screening and kinetics results for psilocin glucuronidation (Figure 27A and Figure 28), supports our finding that the psilocin glucuronidation rate in HIM is very similar to the rate in HLM (Figure 26A). In the case of 4-HI, the glucuronidation rate in HLM was much higher than in HIM (Figure 26B), as expected from the higher expression levels of UGT1A6 in the liver. In this study, we examined the glucuronidation of psilocin by the human UGTs of subfamilies 1A, 2A, and 2B. While UGT1A10 is the most active enzyme in psilocin glucuronidation, UGT1A9, due to its high expression levels in the liver and kidneys, is probably the main contributor to psilocin glucuronidation in humans.

Also worth noticing is that the psilocin and 4-HI glucuronidation studies were performed in the absence of albumin, a substance that later proved to significantly enhance the glucuronidation rates of many human UGTs (see Section 2.3.2, publications **II**, **III**, and **IV**, and the text below). Specifically, the addition of albumin increased the activities of UGTs 1A7, 1A8, 1A9, 1A10, and 2A1 through either a decrease in K_m or increase in V_{max} , or both (see Figure 36). For this reason, the enzyme kinetic parameters of psilocin and 4-HI glucuronidation by HLM, HIM, and recombinant UGTs would presumably differ in the presence of albumin. Our preliminary assays confirm this hypothesis but, unfortunately, we were unable to complete this study by the time this thesis was written.

5.2 Albumin effects in human UGTs (II, III, and IV)

Recent reports indicate that the inclusion of fatty acid-free albumin significantly enhances *in vitro* UGT activities and improves *in vitro*–*in vivo* extrapolation (see Section 2.3.2). Of the 19

human UGT enzymes of subfamilies 1A, 2A, and 2B, however, only six were tested for albumin effects, often with only one or two suitable substrates. Moreover, the majority of previous studies were performed with recombinant UGT enzymes expressed in HEK293 cells, but not with the commonly used and commercially available enzymes expressed in insect *Sf9* cells. In addition, our preliminary assays showed that the manifestation of albumin effects may depend on both the enzyme source and the substrate used. These factors prompted us to investigate the albumin effects in UGTs expressed in *Sf9* cells, as well as to reexamine the previous results with a more diverse set of substrates and optimized assay conditions.

5.2.1 Drug binding to albumin and enzyme sources

Due to the potential binding of drugs to macromolecules present in the *in vitro* assays, the total concentration of the drug may differ from the free concentration available for interaction with the enzyme (see Section 2.3.5). We used ultrafiltration and RED to measure the free, unbound fraction of drugs (f_u) in the presence of BSA and the enzyme source (microsomal fractions or control insect cell membranes). The combined results for all the UGT substrates or inhibitors used appear in Table 12.

Table 12. *Binding of drugs to BSA and enzyme sources (in alphabetical order).*

Compound	Method	Binding data	Publication
Entacapone	Ultrafiltration and RED	1) To 0.1% BSA: $f_u = 0.1-0.85$; increases hyperbolically in the $[S]$ range 5–750 μM 2) To 1% BSA: $f_u < 0.01$ at $[S] = 5 \mu\text{M}$ 3) To the enzyme source (up to 0.2 mg/mL): negligible 4) To both 0.1% BSA and the enzyme source: presence of the enzyme source lowers the binding of entacapone to 0.1% BSA (see Fig. 2 in II)	II and IV
17 α -Estradiol	RED	1) To 0.1% BSA: $f_u = 0.49 \pm 0.01$; independent of $[S]$ 2) To the enzyme source (up to 0.2 mg/mL): negligible	III
17 β -Estradiol	RED	1) To 0.1% BSA: $f_u = 0.48 \pm 0.01$; independent of $[S]$ 2) To the enzyme source (up to 0.2 mg/mL): negligible	III
6-HI	RED	1) To 0.1% BSA: $f_u = 0.84-0.97$; increases in the $[S]$ range 5–750 μM 2) To the enzyme source (up to 0.2 mg/mL): negligible	III
4-MU	Ultrafiltration and RED	1) To 0.1% BSA: $f_u = 0.62-0.91$; increases in the $[S]$ range 5–500 μM 2) To 1% BSA: $f_u = 0.15-0.30$; increases in the $[S]$ range 5–500 μM 3) To the enzyme source (up to 0.2 mg/mL): negligible	II and IV
4-MUG	RED	To 0.1 % BSA, and the enzyme source (up to 0.2 mg/mL): negligible	IV
1-Naphthol	RED	1) To 0.1% BSA: $f_u = 0.78 \pm 0.01$; independent of $[S]$ 2) To the enzyme source (up to 0.2 mg/mL): negligible	IV
UDP	RED	To 0.1 % BSA, and the enzyme source (up to 0.2 mg/mL): negligible	IV
UDPGA	RED	To 0.1 % BSA, and the enzyme source (up to 0.2 mg/mL): negligible	IV
Zidovudine	Ultrafiltration	1) To 0.1 and 1% BSA: negligible 2) To the enzyme source (up to 0.2 mg/mL): negligible	II

Our initial efforts were aimed at developing an ultrafiltration method for zidovudine, entacapone, and 4-MU binding to BSA (II). The preliminary assays, however, showed that the high nonspecific binding of the compounds to the filter device (NSB_f) may severely limit ultrafiltration. With 20 μ M solutions of zidovudine, entacapone, and 4-MU, the NSB_f was 20, 99, and 40%, respectively. In an effort to minimize the nonspecific binding, we pre-washed the filters with a solution of the mild detergent Tween 20 at 1% of the final concentration, followed by a phosphate buffer rinse (II). This pretreatment reduced the NSB_f of 20 μ M zidovudine, entacapone, and 4-MU solutions to the acceptable values of 1, 27, and 7%, respectively. Moreover, we evaluated the NSB_f across the concentration range of the substrates tested and subtracted it from the overall drug binding measured in the presence of BSA or the enzyme source, or both. In contrast to the ultrafiltration assays, the NSB_f in the RED assays was generally low (< 20%), except for estradiols, where it reached almost 40%. However, because the binding of estradiols to BSA was independent of estradiol concentration, the high NSB_f did not affect the final results. Due to the generally low NSB_f in RED assays, we did not perform any device pretreatment. The results obtained with the two different drug binding methods, ultrafiltration and RED, were similar for both entacapone and 4-MU, two substrates for which we applied both methods (see Figure 1 in publication IV).

The binding of entacapone, 4-MU, and 6-HI to BSA depended on the substrate concentration, whereas the binding of estradiol isomers and 1-naphthol was generally independent of the substrate concentration (Table 12). On the other hand, the binding of zidovudine, 4-MUG, UDPGA, and UDP to BSA was negligible. The results of zidovudine and 4-MU binding to BSA are in fairly close agreement with the published results of a study which used the classical equilibrium dialysis methodology (Rowland *et al.*, 2007, Rowland *et al.*, 2008a), even if our results on 4-MU binding to 0.1 and 1% BSA were somewhat higher. Specifically, at 0.1 and 1% BSA published f_u values are 0.89 and 0.49, respectively (Rowland *et al.*, 2008a), whereas our measured f_u values are 0.62–0.91 and 0.15–0.30, respectively. In contrast to BSA binding, the measured binding of drugs to the enzyme sources, either microsomal fractions or control insect cells membranes, was generally minor at up to 0.2 mg total protein per mL, the highest protein concentration we used in publications II, III, and IV. The addition of $MgCl_2$ and UDPGA to the drug binding assays did not significantly alter the drug binding to either BSA or the enzyme sources. Moreover, drug binding in the presence of both BSA and the enzyme sources (up to 0.2 mg/mL) was generally equal to drug binding only to BSA. The important exception to this rule was entacapone binding to BSA, which changed significantly in the presence of the enzyme source (Figure 30).

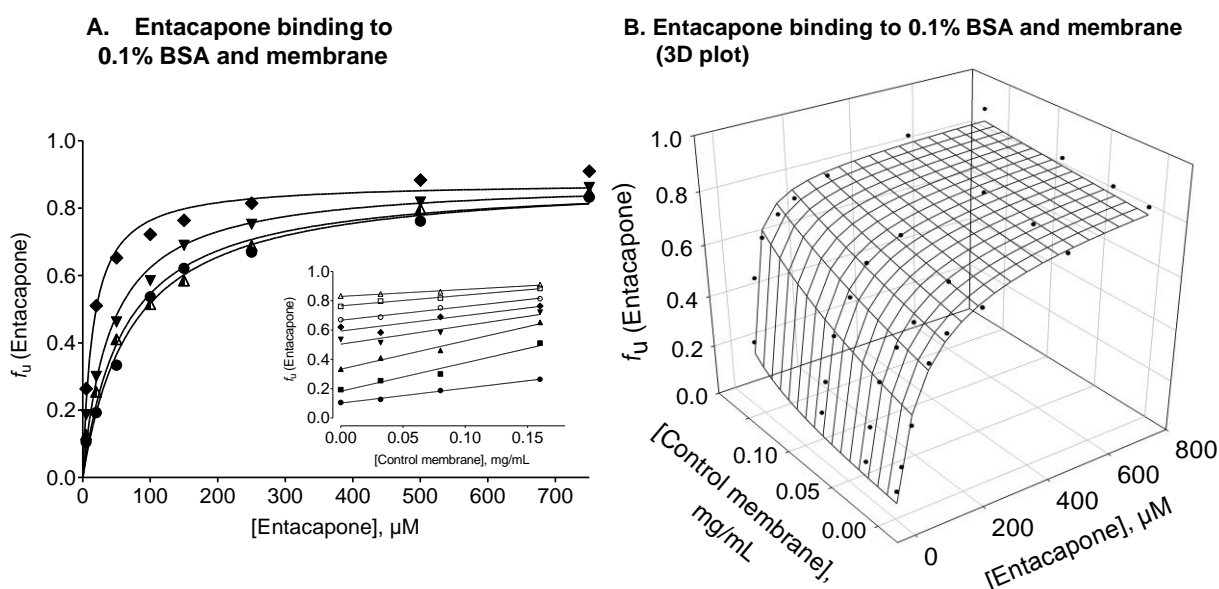


Figure 30. Binding of entacapone to 0.1% BSA in the absence of *Sf9* control membrane (●) and in the presence of 0.032 (▲), 0.080 (▼), or 0.16 (◆) mg/mL of *Sf9* control membrane (A). The results appear as f_u and represent the mean of three determinations. The S.E. was small and, for the sake of clarity in this condensed figure, we have omitted the S.E. bars. We fitted the data to an empirical hyperbolic equation (see publication II). The correlation between the measured f_u and *Sf9* control membrane concentration, at different entacapone concentrations, appears as the inset in panel A. An identical set of data appears in the form of a 3D scatter plot (B). We fitted an empirical 3D function to the data points (see the supplemental material of publication II for further details).

The addition of *Sf9* control membrane resulted in a dose-dependent decrease in entacapone binding to BSA. Similar results occurred when HLM served as the enzyme source. As a result, the f_u of entacapone in the presence of 0.1% BSA was a function of two independent variables, the entacapone concentration and the amount of the enzyme source present in the assay. Therefore, in order to solve this problem, we interpolated an empirical three-dimensional function over the experimental data points (Figure 30B) that enables us to estimate the entacapone binding to 0.1% BSA at any given concentration of entacapone and enzyme source used in the *in vitro* assay (see publication II and corresponding supplemental material for details). The entacapone binding to 0.1% BSA was similarly affected in the presence of HLM and HIM (data now shown). These results highlight the need to carefully examine the drug binding across the concentration range used in the study. Not only can substrate binding to BSA depend on the substrate concentration, but it may also vary depending on the conditions of the *in vitro* assay, especially the amount of the enzyme source used. The binding of entacapone to 1% BSA was very high, and estimated f_u at low concentration of entacapone was below 0.01%.

5.2.2 Optimization of *in vitro* assay conditions

Although the use of 2% BSA yielded good enzyme activation (Rowland *et al.*, 2007, Rowland *et al.*, 2008a), the high binding of the substrates to 2% BSA effectively prevents the assays with highly lipophilic compounds, many of which are good substrates for UGTs. Therefore, prior to

the detailed studies of the albumin effect in human UGTs, we aimed to optimize the experimental conditions of the *in vitro* assays, especially with respect to the most favorable concentration of albumin and the enzyme source used. For this purpose, we tested different BSA concentrations on 4-MU glucuronidation by UGT2A1, an enzyme that proved highly sensitive to the addition of BSA in preliminary assays.

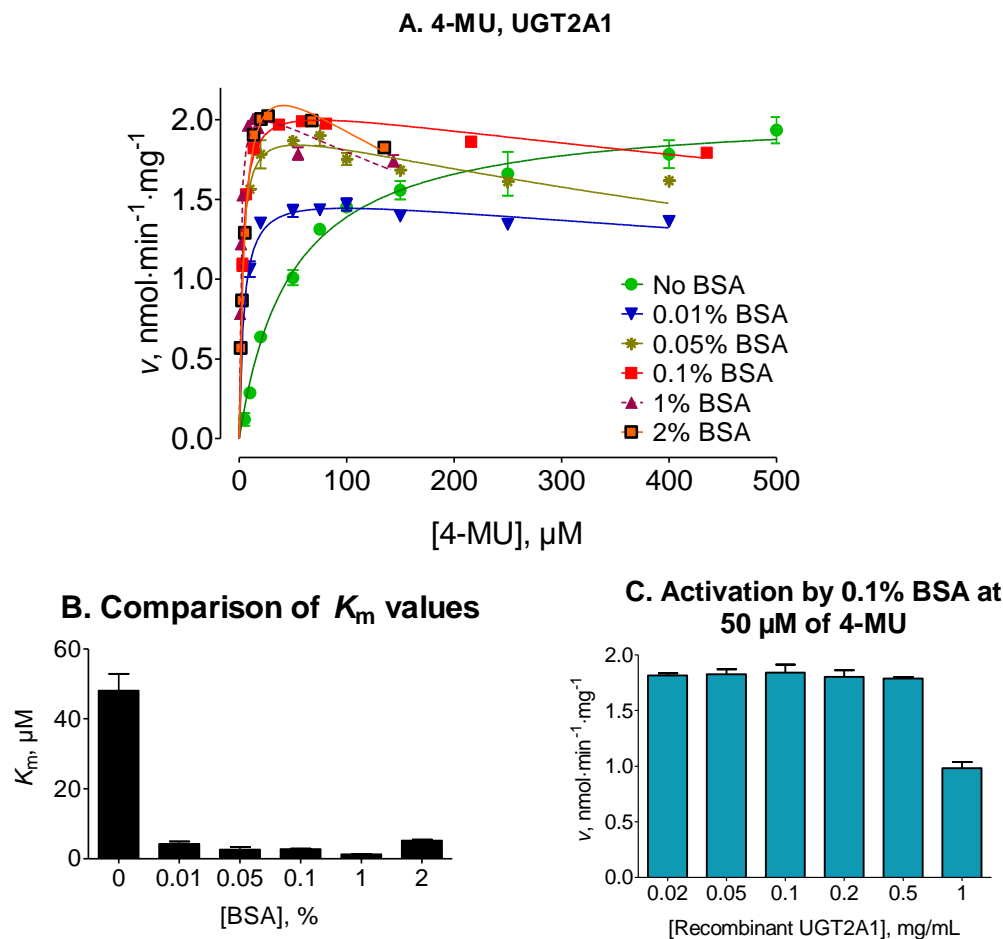


Figure 31. Panel A presents the influence of different BSA concentrations on 4-MU glucuronidation by UGT2A1. The 4-MU binding to 0.01 and 0.05% BSA was considered negligible. We fitted the data without BSA to the Michaelis-Menten equation, whereas the data in the presence of BSA were fitted to the substrate inhibition equation. Panel B presents the relationship between the apparent K_m values and the added BSA concentration. Panel C presents the relationship between the 4-MU (50 μM) glucuronidation activity in the presence of 0.1% BSA and the increasing concentration of recombinant UGT2A1. The values appear as the mean \pm S.E.

The addition of 0.01–2% BSA to 4-MU glucuronidation by UGT2A1 resulted in sharply reduced K_m value (Figure 31, panels A and B). The differences in the K_m decrease observed were relatively minor between the lowest (0.01%) and highest (2%) concentrations of BSA tested. Although the K_m decrease was most pronounced at 1% BSA, we selected 0.1% BSA as the optimal concentration for the subsequent assays because of the fine balance between the enzyme activation and the low nonspecific binding of the substrates. The reduced drug binding to 0.1%

BSA was especially important for subsequent assays with entacapone and estradiols, the compounds that bind strongly to 1 or 2% BSA (Table 12; Walsky *et al.*, 2012, Rowland *et al.*, 2009). The reactions with even lower concentrations of BSA than 0.1%, namely 0.01 and 0.05%, were excluded due to somewhat lower measured V_{\max} values (Figure 31A). The choice of 0.1% BSA was further supported by the enzyme kinetic assays of 4-MU glucuronidation by UGTs 1A9 and 1A10, performed in the presence of both 0.1 and 1% BSA (Figure 32).

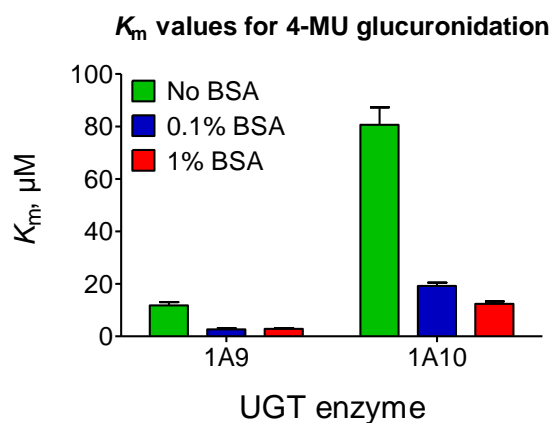


Figure 32. The effects of BSA concentration on the K_m values for 4-MU glucuronidation by UGTs 1A9 and 1A10 in the absence and presence of BSA. We fitted the data to the substrate inhibition equation (not shown). The results appear as the mean value \pm S.E.

Since the added BSA presumably removes lipophilic inhibitors that dissociate from the disrupted cell membranes (Rowland *et al.*, 2007, Rowland *et al.*, 2008a), the concentration of the enzyme source may play an important role in the magnitude of the BSA effects. For this reason, we tested the activation of 4-MU (50 μM) glucuronidation by 0.1% BSA in the presence of increasing concentrations of recombinant UGT2A1 (Figure 31C). The results showed that 0.1% BSA was able to fully activate the 4-MU glucuronidation in the presence of up to 0.5 mg/mL of UGT2A1. Based on this finding, as well as necessary safety margins, we selected 0.2 mg/mL as the highest concentration of the enzyme source for use in combination with 0.1% BSA. The safety margin was implemented because different enzyme sources, such as in-house expressed UGTs, commercial recombinant UGTs, or microsomal fractions, may have different protein to lipid ratios and, therefore, exhibit different inhibitory properties toward UGTs.

Although we generally avoided using organic cosolvents, the presence of 1% DMSO was necessary in the glucuronidation assays with estradiol isomers and high concentrations of 4-MU and 1-naphthol (>1000 μM). Addition of 1% DMSO for these substrates was required due to poor aqueous solubility of estradiols (Shareef *et al.*, 2006), as well as visually observed precipitation of substrates and poor reproducibility that we have observed in preliminary assays with high concentrations of 4-MU and 1-naphthol. To verify whether or not the inclusion of 1% DMSO changes the effects of BSA, we tested its addition on the glucuronidation of the well soluble substrate, entacapone, by UGT1A8 in both the absence and presence of albumin (Figure 33). The results showed that adding 1% DMSO has relatively little effect on the glucuronidation rates and, importantly, does not abolish the stimulatory effect of BSA. In the absence of BSA, the K_m values were $73.05 \pm 3.68 \mu\text{M}$ (no DMSO) and $95.97 \pm 5.08 \mu\text{M}$ (1% DMSO). On the

other hand, in the presence of 0.1% BSA the K_m values were $26.94 \pm 1.52 \mu\text{M}$ (no DMSO) and $30.05 \pm 1.61 \mu\text{M}$ (1% DMSO). The addition of 1% DMSO, however, reduced the V_{max} value in the presence of 0.1% BSA by 23.5%. The V_{max} value in the absence of BSA was less affected by the addition of 1% DMSO; it was reduced by only 3.3%. These findings are in close agreement with those of previous reports on the use of organic solvents in glucuronidation reactions (Uchaipichat *et al.*, 2004, Zhang *et al.*, 2011).

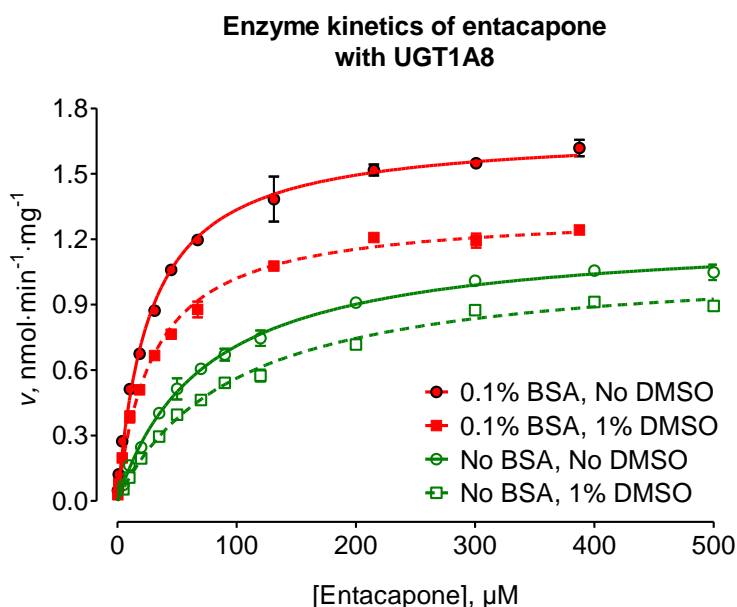


Figure 33. Enzyme kinetics of entacapone glucuronidation by UGT1A8 in the absence (solid symbols) and presence (open symbols) of 0.1% BSA. The reactions without and with DMSO appear as full and dotted lines, respectively. We fitted the data to the Michaelis-Menten equation. The data points appear as the mean value \pm S.E.

5.2.3 Differences between enzyme sources

Considering possible differences in the lipid composition of HLM, HEK293, and *Sf9* cells (see Section 2.3.4), our initial tests aimed to investigate the effects of BSA on recombinant UGTs expressed in *Sf9* cells and to compare the results to the corresponding effects on HLM and existing literature reports (Rowland *et al.*, 2007, Rowland *et al.*, 2008a). For this purpose, we used two UGT-selective substrates, zidovudine for UGT2B7 and entacapone for UGT1A9 (liver), to probe the effects of BSA on both in-house UGTs (expressed in *Sf9* cells) and HLM. In the case of zidovudine glucuronidation by UGT2B7 and HLM, the addition of BSA reduced K_m in both tested samples with no significant effect on the V_{max} of the reaction (Figure 34). These results are similar to the recently published data on zidovudine glucuronidation by UGT2B7 that was expressed in HEK293 cells and in HLM (Rowland *et al.*, 2007, Uchaipichat *et al.*, 2006). On the other hand, adding BSA to entacapone glucuronidation by UGT1A9 and HLM both reduced K_m and increased V_{max} (Figure 35, panels A and B). The enzyme kinetic parameters of entacapone glucuronidation in the absence of BSA closely agreed with previously published values (Lautala *et al.*, 2000). Although the results of the tested samples, UGT1A9 and HLM were mutually quite similar, they differed considerably from the published reports on the effects of BSA on UGT1A9 (Rowland *et al.*, 2008a), an enzyme where K_m , but not V_{max} , changed (i.e.

other researchers have found effects similar to these for the effects of BSA on UGT2B7). In order to confirm this finding, we also tested the effects of BSA on entacapone glucuronidation by commercial UGT1A9, also expressed in *Sf9* cells, but without the C-terminal fusion peptide that our locally expressed recombinant UGTs mostly carry (Figure 35C). The results with the commercial recombinant UGT1A9 agreed closely with those of our previous entacapone tests, namely that the addition of BSA both reduced K_m and increased V_{max} (see Table 1 in publication II for detailed enzyme kinetic parameters). The equivalence of BSA effects between the in-house and commercial UGT1A9, as well as the consistent increase in V_{max} in the presence of BSA, was additionally confirmed with 4-MU glucuronidation by UGT1A9 (see Figure 5 and Table 1 in publication II).

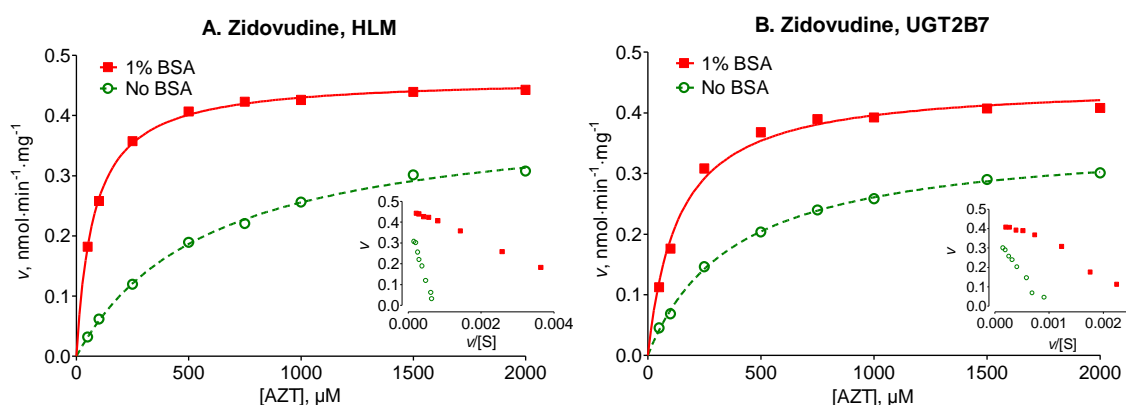


Figure 34. Enzyme kinetics of zidovudine glucuronidation by HLM (A) and UGT2B7 (B) in the absence and presence of 1% BSA. The binding of zidovudine to 1% BSA is negligible. The points represent an average of three samples \pm S.E. The Eadie-Hofstee transforms of the data appear as insets. The enzyme kinetic parameters appear in Table 1 of publication II.

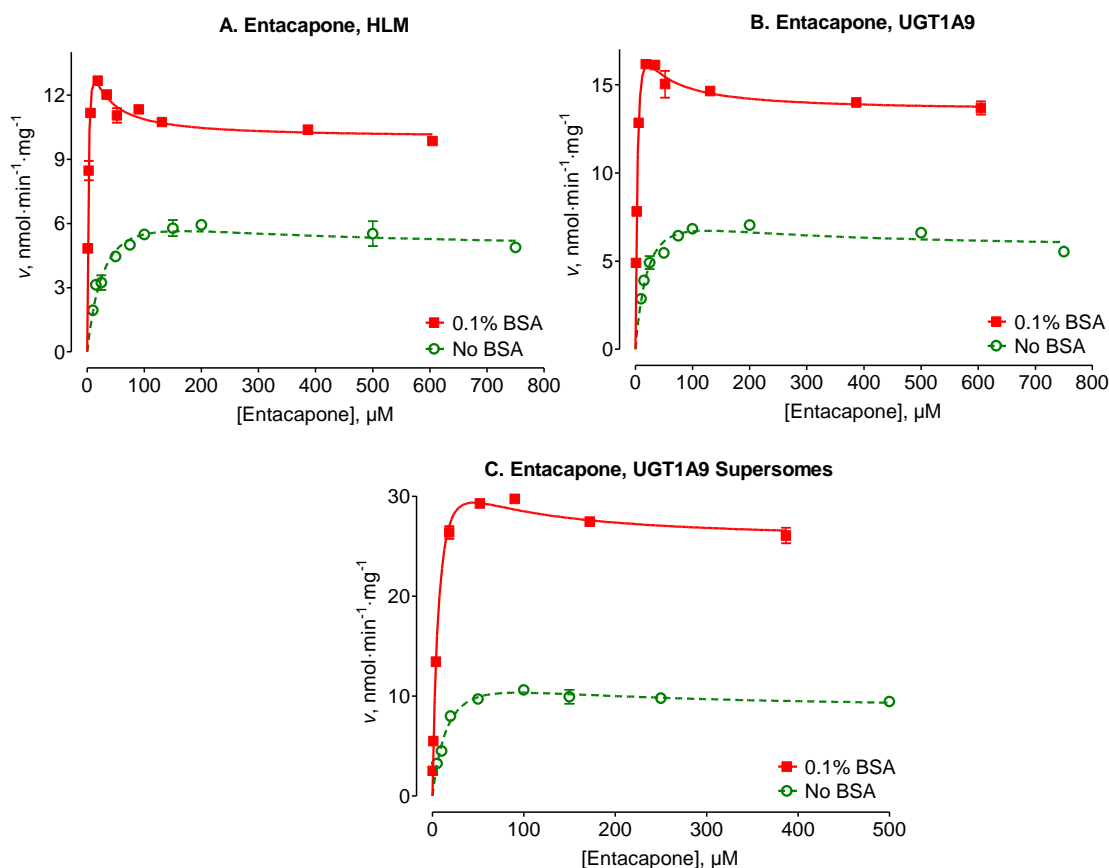


Figure 35. Enzyme kinetics of entacapone glucuronidation by HLM (A), in-house produced UGT1A9 (B), and commercial UGT1A9 (C), in the absence and presence of 0.1% BSA. The points represent an average of three samples \pm S.E. We corrected the concentrations of entacapone for nonspecific binding. We fitted the data to Eq. 10 (see Materials and Methods of publication **III** and Section 2.4.2). Enzyme kinetic parameters appear in Table 1 of publication **II**.

Taken together, our results of zidovudine and entacapone glucuronidation strongly suggest that there are no major differences in BSA effects between the HLM and recombinant UGTs expressed in *Sf9* insect cells, with or without a C-terminal fusion peptide (which includes a His-tag). In addition, even if the BSA effects on zidovudine glucuronidation by UGT2B7 are in close agreement with published reports (Rowland *et al.*, 2007, Uchaipichat *et al.*, 2006), the BSA effects on UGT1A9 differ from the published results and include changes in both the K_m and V_{max} values of the reaction (Figure 35).

5.2.4 Scope of albumin effects in human UGTs

We tested the effects of albumin on 11 recombinant human UGTs, as well as on HLM and HIM. Of the 11 UGTs tested, 5 (UGTs 1A1, 1A6, 1A9, 2B4, and 2B7) had been examined previously, whereas, to best of our knowledge, the effects of albumin remained untested on 6 enzymes: UGTs 1A7, 1A8, 1A10, 2A1, 2B15, and 2B17. In order to determine whether or not the effects of albumin are substrate dependent, we performed enzyme kinetics in the absence and presence of BSA with at least two different substrates for each enzyme source tested. Moreover, to test whether the chemical nature of the substrate governs the appearance and magnitude of the BSA

effects, we used substrates of different physicochemical properties: both small and planar molecules such as 4-MU, 1-naphthol, and 6-HI, as well as larger and more hydrophobic molecules such as entacapone, 17 α -, and 17 β -estradiol. We generally performed the assays in the absence and presence of 0.1% BSA and up to 0.2 mg/mL of enzyme source, as described previously in Section 5.2.2. The only exceptions to this rule were assays with the poor-BSA binder zidovudine and the optimization assays with 4-MU (see Section 5.2.2), which we performed in the presence of 1% BSA. A combined overview of these results appears in Figure 36. The enzyme kinetic parameters obtained appear in Table 1 of publication **II**, Tables 2 and 3 of publication **III**, and the *Results* section of publication **IV**. Corresponding enzyme kinetic curves also appear in publications **II–IV**. In most cases, the addition of BSA affected both the reaction K_m and V_{max} values. For the sake of presentation clarity, the effects of BSA on the reaction K_m and V_{max} values are initially discussed separately, even though both are manifestations of the same phenomenon.

The addition of BSA reduced the reaction K_m or S_{50} in UGTs 1A7, 1A9, 1A10, 2A1, 2B4, 2B7, and 2B15 (Figure 36A). Conversely, the K_m values of the reactions catalyzed by UGTs 1A1, 1A6, and 2B17 appear less affected. Our results with UGTs 1A1, 1A6, 1A9, 2B4, and 2B7 are in close agreement with those of respective previous reports on the effects of BSA on these human UGTs (Walsky *et al.*, 2012, Rowland *et al.*, 2007, Rowland *et al.*, 2008a, Shiraga *et al.*, 2012, Kilford *et al.*, 2009, Gill *et al.*, 2012, Uchaipichat *et al.*, 2006). The BSA-mediated decrease in K_m appears to occur mainly independently of the substrate used, although we observed large scatter of values for UGTs 1A8, 1A9, 2B7, 2B15, and 2B17. The notable exception was UGT1A8. The addition of BSA to UGT1A8-catalyzed reactions reduced K_m in the case of 17 β -estradiol and entacapone, whereas the reaction K_m remained unaffected, or even increased, if the substrates were 4-MU and 1-naphthol. Further studies are needed to answer the interesting question of whether or not the effects of BSA on UGT1A8 depend on the size of the substrate.

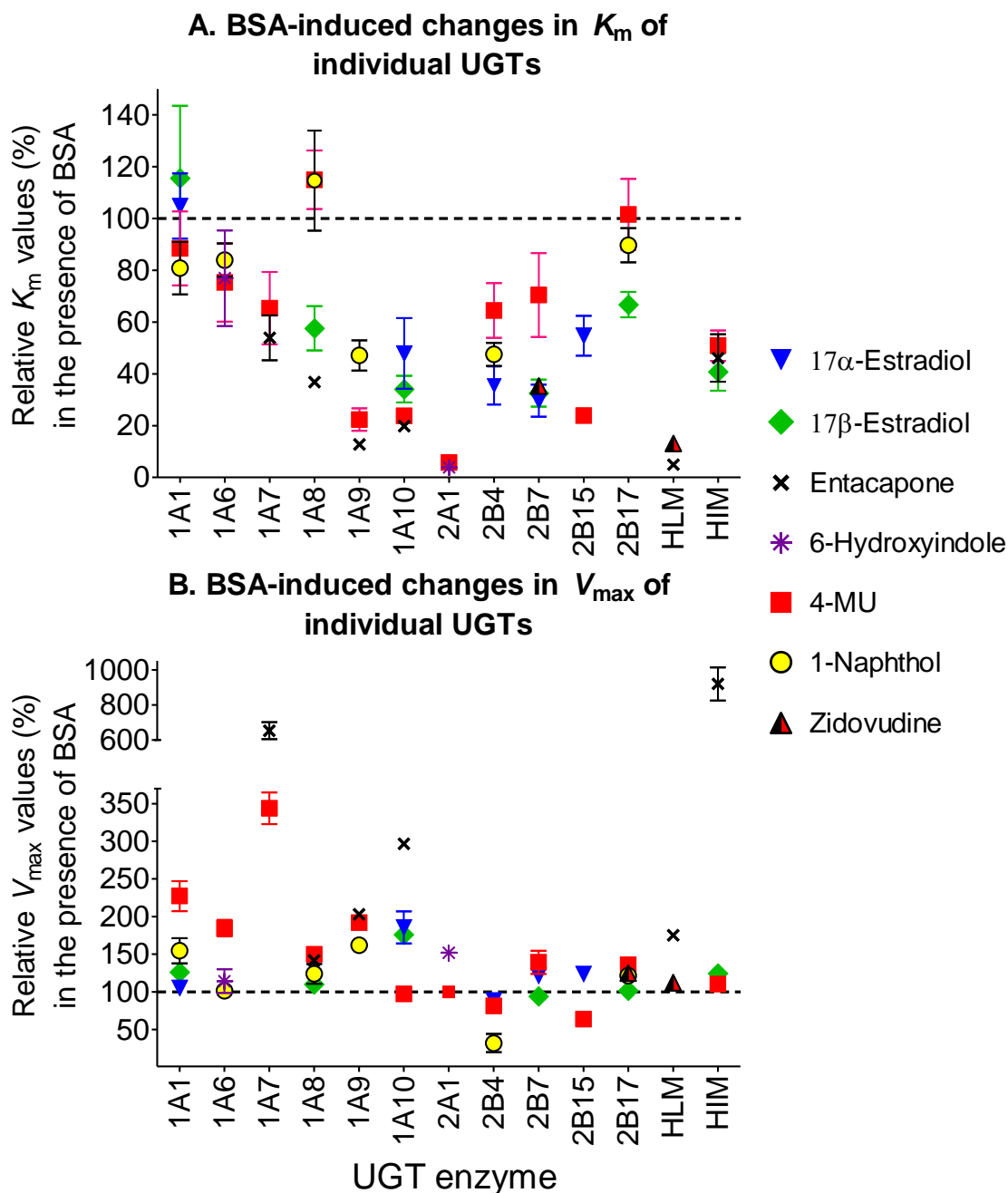


Figure 36. The combined effects of BSA on the K_m or S_{50} (A) and V_{max} (B) values in 11 recombinant human UGTs, as well as in HLM and HIM. We arbitrarily assigned the average values of the enzyme kinetic parameters, determined in the absence of BSA, to 100%. The average corresponding values of K_m and V_{max} in the presence of BSA were compared to their respective values in the absence of BSA and plotted for all the enzyme sources tested. The presented errors are propagated S.E. values that take into account the errors in the parameters determined in both the absence and presence of BSA (see publication **III** for further details about the error analysis).

The inclusion of BSA also sharply decreased the K_m values for zidovudine and entacapone glucuronidation by HLM, as one should expect for substrates that are selectively glucuronidated by UGTs 2B7 and 1A9, respectively. In addition, the K_m values for 17 β -estradiol, 4-MU, and entacapone were decreased in HIM. For 17 β -estradiol and entacapone, the substrates

for the intestinal UGTs 1A7–1A10, this decrease in K_m was well expected. On the other hand, apart from the UGT1A7–1A10 group, UGTs 1A6 and 2B7 also glucuronidate 4-MU (Uchaipichat *et al.*, 2004, Luukkanen *et al.*, 2005), making the results of 4-MU glucuronidation by HIM more difficult to interpret (see Table 1 for the expression of UGTs in intestinal tissues). While the addition of BSA significantly activates UGTs 1A7–1A10 and UGT2B7, UGT1A6 appears less affected (Figure 36).

The effects of BSA on the K_m values of some UGTs, but not all, raises an interesting question about the mechanism of albumin effects. If the apparently higher affinity for the substrates in the presence of the BSA arises from the BSA-mediated removal of lipid inhibitors, such as arachidonic or linoleic acid (Rowland *et al.*, 2007), then the lack of such effects in UGTs 1A1, 1A6, and 2B7 would suggest that the tentative inhibitors do not inhibit these enzymes, at least not in any way that compromises the binding of aglycone substrate. The lack of a BSA-mediated decrease in K_m is somewhat surprising in the case of UGT1A1, an enzyme whose active site is large enough to allow the binding of bilirubin (see Laakkonen and Finel, 2010) and several arachidonic and linoleic acid metabolites (Turgeon *et al.*, 2003). Interestingly, the inclusion of BSA also reduces the K_m value even if the substrate affinity is already very high, as with 17 α -estradiol and UGT2B7 (see Figure 8 and Table 3 in **III**), and 1-naphthol and UGT1A9 (see Figure 2 and the *Results* section in **IV**). Although unexpected at a first glance, these results are generally consistent with the theory of competitive inhibition, in particular with the fact that the K_{mI}/K_m ratio, the ratio of apparent substrate affinities in the presence (K_{mI}) and absence (K_m) of the inhibitor, depends solely on the $[I]/K_i$ ratio rather than on the absolute magnitude of the substrate affinity. In line with this, the tentative UGT inhibitors that BSA removes, such as fatty acids, may also exhibit a high affinity for the enzymes (Turgeon *et al.*, 2003, Tsoutsikos *et al.*, 2004).

In contrast to its effects on K_m values, the effects of BSA on the reaction V_{max} values were mainly substrate dependent (Figure 36B). In general, large increases in V_{max} were present mainly in the UGT1A subfamily, whereas minor to moderate increases in V_{max} also occurred in members of the UGT2A and UGT2B subfamilies. The increases in V_{max} in the presence of BSA were consistently present in UGTs 1A7, 1A9, and mostly 1A10. On the other hand, the increases in V_{max} in UGTs 1A1, 1A6, 1A8, 2A1, and 2B7 were primarily dependent on the substrate used. A two-fold increase in V_{max} also occurred in entacapone glucuronidation by HLM, a reaction almost exclusively catalyzed by UGT1A9 (Lautala *et al.*, 2000). Interestingly, a large 10-fold increase in V_{max} increase was observed in entacapone glucuronidation by HIM, a reaction catalyzed by UGTs 1A7–1A10, and mainly UGTs 1A9 and 1A10, all of which exhibited increases in V_{max} with other substrates as well.

The increase in V_{max} in the presence of BSA may be explained by the albumin-mediated removal of noncompetitive or mixed-type inhibitors with respect to the aglycone substrate (see Section 5.3). These inhibitors may be long-chain fatty acid (Turgeon *et al.*, 2003, Rowland *et al.*, 2007, Tsoutsikos *et al.*, 2004) or other lipophilic compounds that were not identified thus far. Taking into account the compulsory-order of substrate binding in UGT-catalyzed reactions, such inhibitors would also bind to the ternary enzyme • UDPGA • aglycone complex. Because structurally diverse aglycone substrates may lead to slightly different ternary complexes, these tentative UGT inhibitors may exhibit different affinities for them, which explains the variable effects of BSA inclusion on V_{max} values. Moreover, we found no correlation between the relative

K_m and V_{max} changes in this study (see supplementary Figure S5 in **III**), suggesting that the possible removal of different inhibitors causes these two independent effects. Regarding the chemical structures of these putative " V_{max} -affecting" inhibitors, no data are currently available, but it could well be one or more of the fatty acids removed by BSA. Interestingly, arachidonic acid was reportedly an "atypical inhibitor" of UGT1A9 (Tsoutsikos *et al.*, 2004), indicating behavior beyond the simple, competitive inhibition.

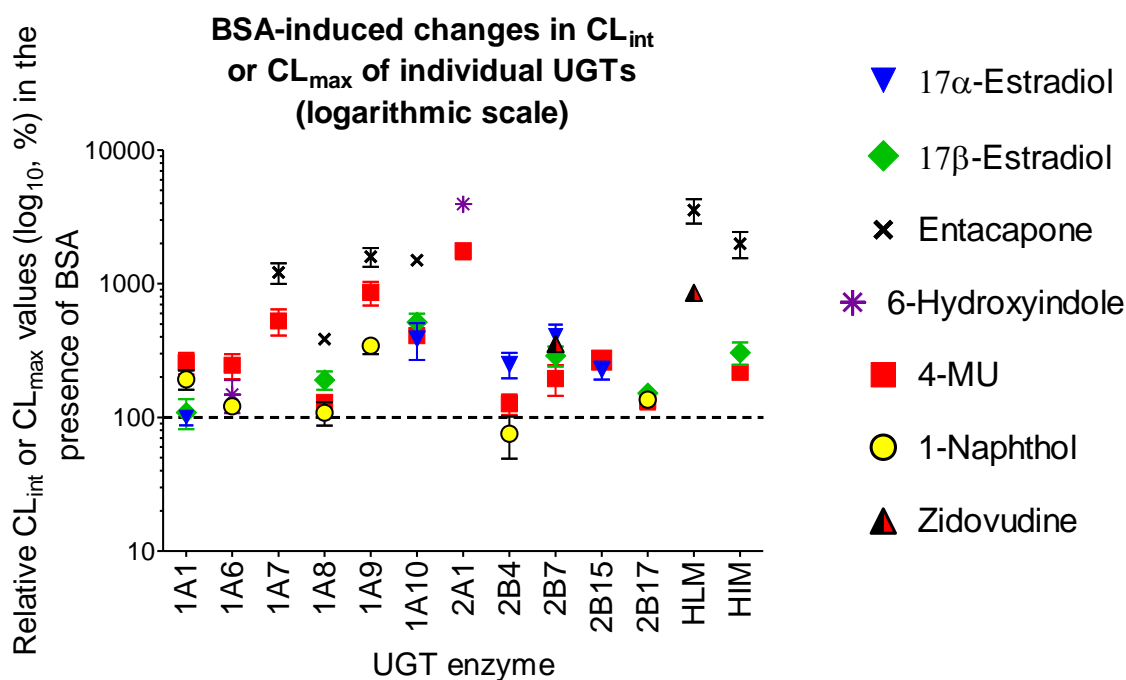


Figure 37. The combined effects of BSA on CL_{int} or CL_{max} in the 11 human recombinant UGTs, HLM, and HIM tested. We arbitrarily assigned the average values of CL_{int} or CL_{max} , determined in the absence of BSA, to 100%, and the average corresponding values of CL_{int} or CL_{max} in the presence of BSA were compared to the values in the absence of BSA and plotted for all 10 of the UGT enzymes tested. The errors presented are propagated S.E. values that take into account errors in the parameters determined in both the absence and presence of BSA (see publication **III** for further details). Due to large increases of CL_{int} or CL_{max} in the presence of BSA, the values of the y-axis appear on a \log_{10} scale.

The overall magnitude of activity enhancement in the presence of BSA, especially at low concentrations of substrate, is important for studies focusing on *in vitro*–*in vivo* extrapolation. Such activity enhancement can be expressed through relative changes in CL_{int} (Figure 37, note the \log_{10} scale along the y-axis). These changes can simply be interpreted as the combined effects of K_m and V_{max} modulation or, from a slightly different point of view, as the overall enhancement of enzyme activity at low concentrations of substrate. It should be noted, however, that in the case of substrates that follow sigmoidal kinetics we calculated the CL_{max} , the maximal clearance that results from autoactivation (Houston and Kenworthy, 2000). The results show that the inclusion of 0.1% BSA leads to large CL_{int} increases in UGTs 1A7, 1A9, 1A10, 2A1, and 2B7. The up to 400-fold increase in CL_{int} is especially striking in the case of UGT2A1, an enzyme with broad substrate selectivity and a limited tissue expression pattern. A significant

increase in CL_{int} in the presence of BSA also occurred in zidovudine glucuronidation by HLM (catalyzed by UGT2B7) and in entacapone glucuronidation by HLM (mainly UGT1A9) and HIM (UGTs 1A7, 1A8, 1A9, and 1A10).

To the best of our knowledge, we are the first to describe the effects of albumin on UGTs 1A7, 1A8, 1A10, 2A1, 2B15, and 2B17. Moreover, we used previously untested substrates to reexamine the effects of albumin on UGTs 1A1, 1A6, 1A9, 2B4, and 2B7. Altogether, our results indicate that adding BSA alters both the K_m and V_{max} values of human UGTs, although the effects are both enzyme and substrate dependent. This highlights the complexity and variability of this effect, which differs considerably from the original results with UGT2B7, where the effects of BSA were limited only to the reaction K_m value (Uchaipichat *et al.*, 2006, Rowland *et al.*, 2006). The new results significantly deepen our current knowledge of the effects of BSA on human UGTs and should raise our awareness of the experimental condition of *in vitro* UGT assays.

5.3 Enzyme kinetic mechanism of UGT1A9 (IV)

The addition of BSA to UGT1A9-catalyzed reactions substantially changed the enzyme kinetic parameters, depicted by both a decrease in K_m and an increase in V_{max} (Figure 35). These changes raise an interesting question: Will the inclusion of BSA affect the enzyme kinetic mechanism of UGT1A9-catalyzed reactions? In other words, since previous studies of the UGT enzyme kinetic mechanism were performed in the absence of albumin, will the conclusions of these studies remain valid in the presence of BSA? As described in Section 2.4.1, studies of the UGT enzyme kinetic mechanism generally agree on the formation of ternary complex (enzyme • UDPGA • aglycone), but largely disagree about the order of substrate binding. In order to resolve these issues, we investigated the bisubstrate enzyme kinetics of 4-MU and UDPGA with UGT1A9, in both the presence and absence of albumin. Moreover, with the aim to measure both the equilibrium constant (K_{eq}) of the overall reaction and the individual rate constants, we studied the bisubstrate kinetics of the reverse reaction, the formation of 4-MU and UDPGA from 4-MUG and UDP. Finally, in order to study the order of substrate binding, we performed dead-end and product inhibition studies with 1-naphthol and UDP.

5.3.1 Bisubstrate enzyme kinetics of UGT1A9-catalyzed reactions

Our initial studies focused on bisubstrate enzyme kinetics at lower concentrations of 4-MU (Figure 38), a region where the substrate inhibition by 4-MU is not apparent. The Eadie-Hofstee transforms of the primary data revealed a common intersection point in the second quadrant, a pattern characteristic of ternary-complex mechanisms (Figure 38, Eadie-Hofstee insets). If the reaction followed a substituted enzyme-mechanism, however, the expected intersection point would have been located in the first quadrant, on the x-axis (Cornish-Bowden, 2012). The formation of ternary-complex was further supported by the poor fit of the data obtained to the equation for the substituted-enzyme mechanism (Eq. 8 in Section 2.4.1). On the other hand, the bisubstrate kinetic data closely fit the equations for both compulsory-order and random-order ternary-complex mechanisms (Eqs. 6 and 7 in Section 2.4.1). Based on subsequent results from substrate inhibition, dead-end and product inhibition studies (see below), the compulsory-order ternary-complex mechanism with UDPGA binding first proved to be the most likely. The results of bisubstrate kinetic studies obtained with the equation for the compulsory-order ternary-complex mechanism appear in Table 13.

Adding BSA changed the enzyme kinetic parameters of the bisubstrate kinetics, but did not qualitatively influence the enzyme kinetic mechanism (Figure 38). In the presence of BSA, the K_m values for 4-MU decreased and the overall reaction V_{max} increased (Table 13), as observed previously in the single-substrate kinetics of UGT1A9 (Figure 35). The apparent K_m value for UDPGA, however, increased in the presence of BSA. These findings could be attributed to the BSA-mediated removal of competitive and mixed-type inhibitor(s) with respect to the aglycone substrate, 4-MU, and removal of uncompetitive inhibitor(s) with respect to UDPGA (see also Figure 41).

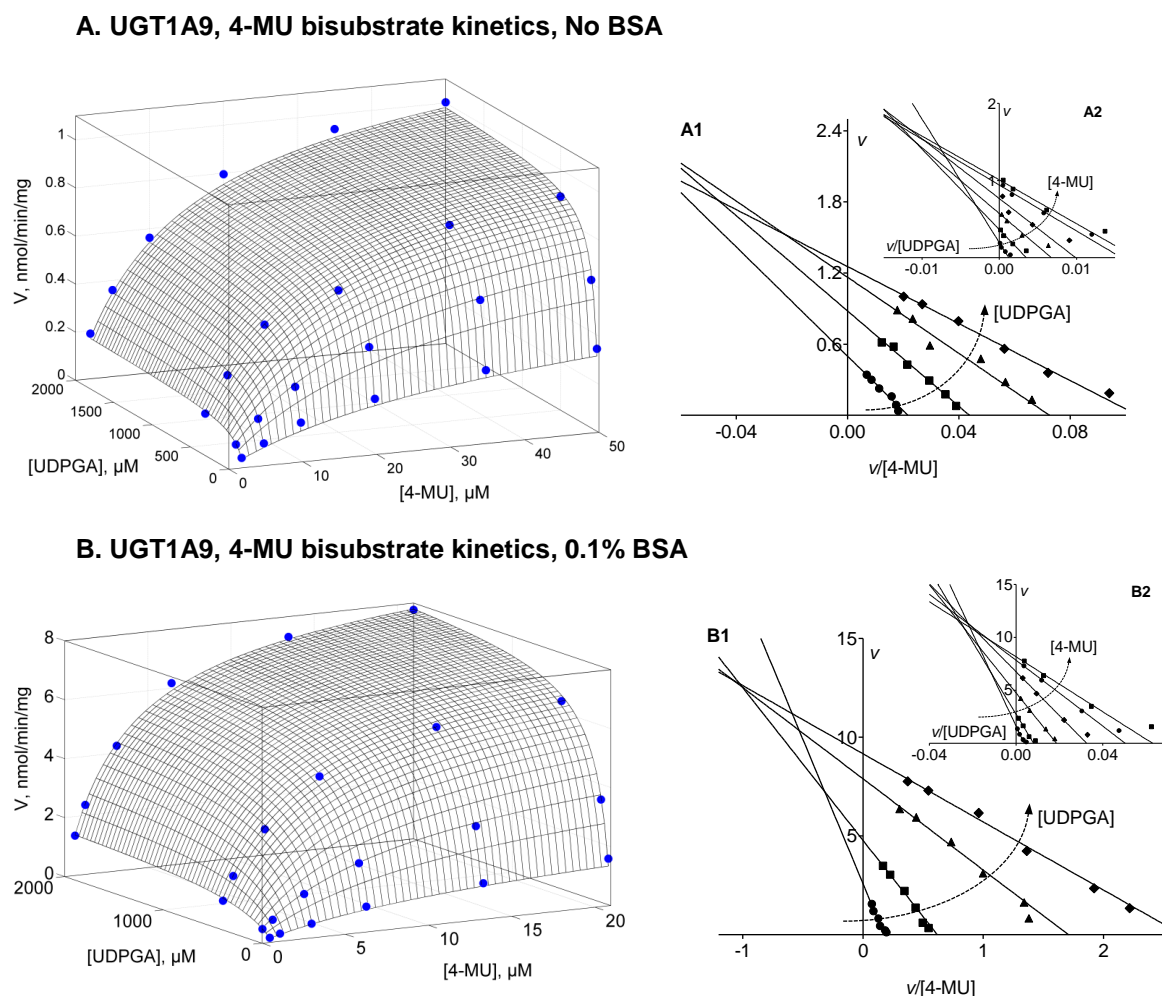


Figure 38. Bisubstrate enzyme kinetics of UGT1A9-catalyzed 4-MU glucuronidation in the absence (A) and presence of BSA (B). The points represent the average of two samples (variation between two replicates was less than 15%). Glucuronidation rates appear as measured initial rates in $\text{nmol}\cdot\text{min}^{-1}\cdot\text{mg}^{-1}$ of UGT1A9-enriched insect cell membranes. The kinetic constants derived appear in Table 13. The Eadie-Hofstee transforms of the data, both from the perspectives of 4-MU (A1 and B1) and of UDPGA (A2 and B2), appear in the panels at right.

The bisubstrate enzyme kinetics in the presence of BSA and at higher concentrations of 4-MU resulted in pronounced substrate inhibition (Figure 39, Table 13). This data set was accurately modeled by the compulsory-order ternary-complex mechanism with substrate inhibition (see Eq. 11 in Section 2.4.2). It is important to note that the K_m value for UDPGA depends on both the concentration of 4-MU and the strength of the aglycone substrate inhibition (the strength of

substrate inhibition may be defined by the K_{si}/K_m ratio; see **IV** for a more detailed discussion). Taking into account that many UGT-catalyzed reactions exhibit pronounced aglycone substrate inhibition, the accurate determination of the K_m value for UDPGA is no trivial task, and bisubstrate enzyme kinetics may present a more reliable approach than the common single-substrate assays. Moreover, the nature of substrate inhibition may provide additional information about the order of substrate binding. In the steady-state compulsory-order ternary-complex mechanism, the second substrate may bind to a binary complex between the enzyme and the second product, forming an unproductive reaction pathway. In UGT-catalyzed reactions, the aglycone substrate may bind to the “wrong” enzyme • UDP complex, instead of the “correct” enzyme • UDPGA complex, and thus forming an unproductive ternary complex enzyme • UDP • aglycone (see Figure 41). Substrate inhibition can also occur in the random-order ternary-complex mechanism, where 4-MU may bind to the enzyme • UDP complex. If, however, the rapid-equilibrium assumption remains valid, the enzyme • UDP complex concentration is zero in the absence of accumulated or added products. Since 4-MU cannot bind to enzyme species that are absent, one can exclude the rapid-equilibrium random-order ternary-complex mechanism based on this observation. The non-rapid-equilibrium (steady-state) random-order ternary-complex mechanism cannot be ruled out based on bisubstrate kinetics alone, however.

UGT1A9, 4-MU bisubstrate kinetics, No BSA

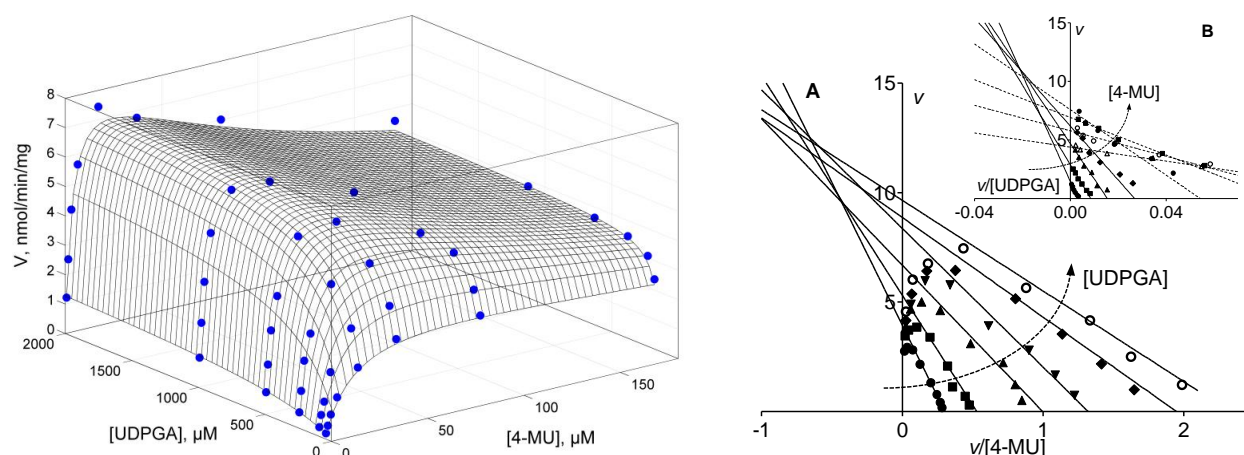


Figure 39. The effects of BSA on the bisubstrate enzyme kinetics of 4-MU glucuronidation by UGT1A9 at higher concentrations of 4-MU. The points represent the average of two samples (variation between two replicates was less than 15%). The Eadie-Hofstee transforms of the data, both from the perspectives of 4-MU (A) and of UDPGA (B), appear in the panels at right. The lines in the Eadie-Hofstee plot B at high concentrations of 4-MU, the region where aglycone substrate inhibition becomes pronounced, are indicated by dashed lines.

To understand the overall enzyme kinetic mechanism, we also investigated the reverse reaction in the presence of BSA, an experiment which previous UGT studies rarely performed (Vessey and Zakim, 1972, Rao *et al.*, 1976, Matern *et al.*, 1991), and never with recombinant UGTs. We paid close attention to preventing possible non-enzymatic 4-MUG hydrolysis and excluding the possibility that other enzymes in the insect cell membrane would catalyze UDPGA formation

from 4-MUG and UDP. We examined the latter using the insect cell control membranes that lack recombinant UGT; the assays revealed no significant 4-MU or UDPGA formation upon addition of 4-MUG and UDP. The reverse reaction in the presence of BSA occurred rather rapidly under optimal conditions, namely in the presence of high concentrations of 4-MUG (Figure 40, Table 13). The preliminary assays showed that reverse reaction also occurs in the absence of BSA, albeit at the lower rate. The results of the bisubstrate reverse reaction indicated that it also follows a ternary-complex mechanism, as is evident from the common intersection point in the second quadrant of the Eadie-Hofstee plots, just left of the y-axis (Figure 40, Eadie-Hofstee insets). The K_m value for 4-MUG was approximately 500-fold higher than the K_m value for 4-MU, whereas, perhaps surprisingly, the K_m value for UDP was approximately one order of magnitude lower than the corresponding value for UDPGA (Table 13). The relatively high affinity for UDP, compared to UDPGA, may explain why aglycone substrate inhibition occurs so frequently in UGT-catalyzed reactions.

Based on the Haldane relationship for the compulsory-order ternary-complex mechanism (see publication **IV** for details), the thermodynamic equilibrium constant of the reaction in the presence of BSA is $K_{eq} = 574$. Moreover, in the compulsory-order ternary-complex mechanism, a unique relationship exists between the enzyme kinetic parameters and the individual rate constants (Cornish-Bowden, 2012). Unfortunately, due to a lack of purified and fully active UGT1A9, we could determine only the relative ratio of the rate constants, not their absolute values. For comparison, the results were normalized by arbitrarily setting the value of V_{max}^f , the limiting reaction velocity in the forward direction, to numerical value of one and then using the expression $V_{max}^f = k_{cat}^f [E]$, where $[E]$ is the molar concentration of the enzyme (Table 14, Figure 41). It is worth noting here that, although the first-order and second-order rate constants cannot be directly compared to each other, a pseudo-first-order rate constant such as $k_1[AX]$ can be compared to other first-order constants. These results suggest that the catalytic rate constant in the forward direction, k_{cat}^f , is about 11-fold higher than the corresponding catalytic rate constant in the reverse reaction, k_{cat}^r .

UGT1A9, 4-MU bisubstrate kinetics, No BSA

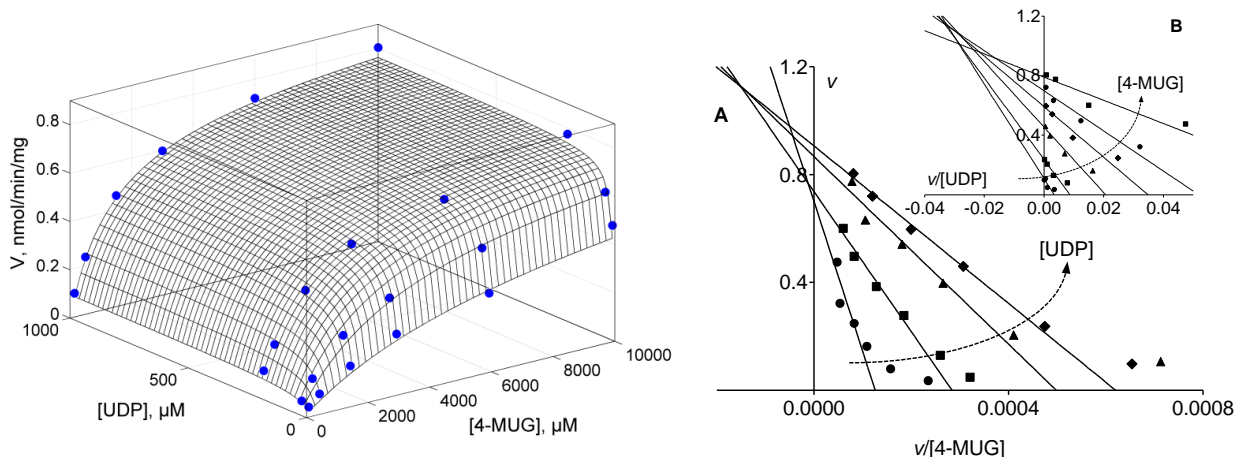


Figure 40. Bisubstrate enzyme kinetics of the UGT1A9-catalyzed reverse reaction, glucuronic acid transfer from 4-MUG to UDP. We carried out the reactions in the presence of 0.1% BSA, and the points represent the average of two samples (variation between two replicates was less than 15%). Glucuronidation rates appear as measured initial rates in $\text{nmol}\cdot\text{min}^{-1}\cdot\text{mg}^{-1}$ of protein in UGT1A9-enriched insect cells membranes. The kinetic constants derived appear in Table 13. The Eadie-Hofstee transforms of the data, both from the perspectives of 4-MUG (A) and of UDP (B), appear in the panels at right.

Table 13. The bisubstrate enzyme kinetic parameters of 4-MU glucuronidation by UGT1A9. We interpreted the data using the compulsory-order ternary-complex mechanism based on a steady-state assumption (Eqs. 6 and 11). The values represent a best-fit result \pm S.E. The 95% CI calculated appear in parenthesis. The reaction velocity is expressed per mg of total protein in UGT1A9-enriched insect cell membranes.

Bisubstrate enzyme kinetics parameters of 4-MU glucuronidation by UGT1A9						
Conditions	V_{\max}	$K_m(4\text{-MU})$	K_m (UDPGA)	K_i (UDPGA)	$K_{si}(4\text{-MU})$	Kinetic Model
	$\text{nmol}\cdot\text{min}^{-1}\cdot\text{mg}^{-1}$	μM	μM	μM	μM	(r^2)
No BSA	1.25 ± 0.04 (1.18–1.33)	12.0 ± 1.1 (9.86–14.2)	36.3 ± 8.7 (18.7–53.9)	136 ± 26 (83.2–188)	—	Eq. 6 (0.99)
0.1% BSA	9.47 ± 0.13 (9.20–9.75)	2.91 ± 0.16 (2.59–3.24)	90.2 ± 8.6 (72.8–108)	445 ± 46 (352–538)	—	Eq. 6 (0.99)
0.1% BSA with substrate inhibition	9.44 ± 0.19 (9.06–9.83)	3.08 ± 0.22 (2.65–3.52)	64.1 ± 5.4 (53.4–74.8)	574 ± 60 (454–694)	146 ± 8 (130–162)	Eq. 11 (0.99)
0.1% BSA reverse reaction	0.872 ± 0.023 (0.826–0.918)	$K_m(4\text{-MUG})$ 1339 ± 133 (1071–1607)	$K_m(\text{UDP})$ 2.48 ± 0.66 (1.23–4.86)	$K_i(\text{UDP})$ 51.0 ± 9.7 (31.3–70.6)	—	Eq. 6 (0.99)

Table 14. The relative individual rate constants for the compulsory-order ternary-complex mechanism of UGT1A9-catalyzed 4-MU glucuronidation. We normalized the different rate constants to the arbitrarily set value: $V_{max}^f = k_{cat}^f[E] = 1$. The superscripts *f* and *r* indicate the forward and the reverse reactions, respectively.

Rate constant equation	Relative value, normalized to $k_{cat}^f[E] = 1$	Order of rate constant
$k_1[E] = \frac{V_{max}^f}{K_{mAX}}$	0.011	second-order
$k_{-1}[E] = \frac{V_{max}^f K_{iAX}}{K_{mAX}}$	4.930	first-order
$k_2[E] = \frac{V_{max}^f(k_{-2} + k_3)}{k_3 + K_{mB}}$	0.359	second-order
$k_{-2}[E] = \frac{V_{max}^f V_{max}^r K_{iAX}}{V_{max}^f K_{iAX} - V_{max}^r K_{mAX}}$	0.094	first-order
$k_3[E] = \frac{V_{max}^f V_{max}^r K_{iA}}{V_{max}^r K_{iA} - V_{max}^f K_{mA}}$	2.126	first-order
$k_{-3}[E] = \frac{V_{max}^f(k_{-2} + k_3)}{k_{-2} K_{mBX}}$	0.002	second-order
$k_4[E] = \frac{V_{max}^r K_{iA}}{K_{mA}}$	1.888	first-order
$k_{-4}[E] = \frac{V_{max}^r}{K_{mA}}$	0.037	second-order
$k_{cat}^f[E] = V_{max}^f = \frac{k_3 k_4}{k_3 + k_4}$	1.000	first-order
$k_{cat}^r[E] = V_{max}^r = \frac{k_{-1} k_{-2}}{k_{-1} + k_{-2}}$	0.092	first-order

5.3.2 Product and dead-end inhibition of UGT1A9-catalyzed reactions

UDP proved to be a competitive inhibitor with respect to UDPGA, but a mixed-type inhibitor with respect to 4-MU (see publication IV for details). Although these inhibition patterns agree closely with previously published data (Luukkanen *et al.*, 2005, Fujiwara *et al.*, 2008), they are possible for both random-order and compulsory-order ternary-complex mechanisms. If, however, the reaction follows the compulsory-order ternary-complex mechanism, as the bisubstrate kinetic analyses and substrate inhibition indicate, the results of UDP inhibition support the suggestion that UDPGA is the first, and the aglycone is the second binding substrate in a compulsory-order mechanism.

In contrast to the UDP inhibition results, 1-naphthol was a predominantly competitive inhibitor of UGT1A9 with respect to 4-MU ($\alpha = 7.38 \pm 1.75$) but, importantly, proved to be uncompetitive with respect to UDPGA (see publication IV for details). This result shows that 1-naphthol, an inhibitor that probably competes with 4-MU for the aglycone substrate-binding site, does not compete for the same enzyme species as UDPGA. The uncompetitive inhibition pattern may arise from 1-naphthol binding to the pre-formed enzyme • UDPGA complex, rather than to the free enzyme. This uncompetitive inhibition provides strong positive evidence that UGT substrates bind in a compulsory-order fashion such that the initial binding of UDPGA increases

the affinity for the aglycone substrate. An affinity increase for the aglycone substrate upon UDPGA binding may be a consequence of a conformational change in the enzyme, the involvement of the bound UDPGA molecule itself in the binding of the aglycone substrate, or both.

5.3.3 Conclusions about the enzyme kinetic mechanism

The available evidence suggests that UGT1A9 follows a steady-state compulsory-order ternary-complex mechanism, regardless of the presence of BSA. Taking into account that the presence of BSA increases the apparent affinity for 4-MU (lower K_m for 4-MU) and decreases the apparent affinity for UDPGA (higher K_m for UDPGA), one may propose that BSA removes internal inhibitors that are competitive or mixed-type with respect to the aglycone substrate, but are uncompetitive with respect to UDPGA. The uncompetitiveness of the BSA-removed inhibitors with respect to UDPGA would explain why the affinity for this cosubstrate apparently decreases in the presence of BSA. Such inhibitors, tentatively marked I_1 and I_2 in the reaction scheme (Figure 41), would not bind (or would bind poorly poorly) to the free enzyme, but would bind with a higher affinity to the binary enzyme • UDPGA complex or to the ternary complex enzyme • UDPGA • 4-MU complex. While the exact nature and number of these inhibitors is currently unknown, an improved understanding of the UGT reaction mechanism and of the effects of BSA may help to rationalize and predict the effects of BSA in the future.

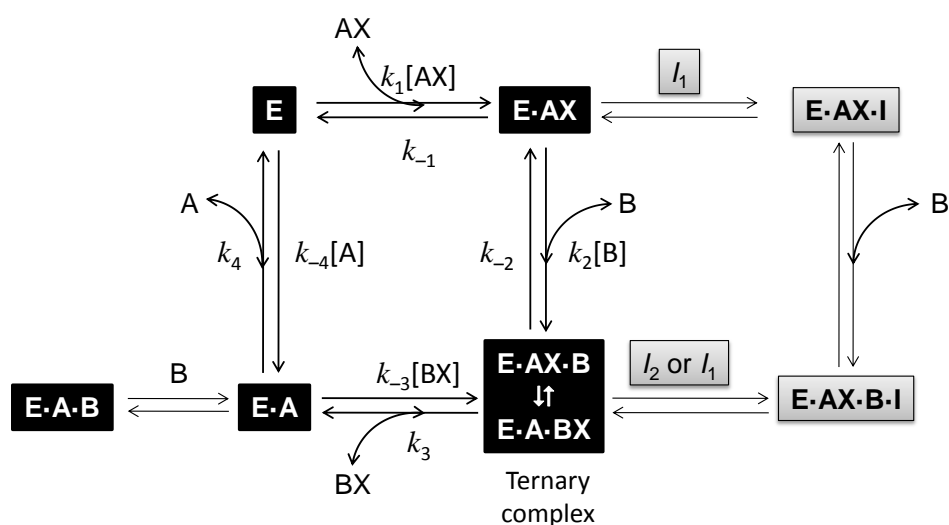


Figure 41. The proposed enzyme kinetic mechanism of the UGT1A9-catalyzed 4-MU glucuronidation reaction. The letters represent: E = enzyme (UGT1A9), AX = UDP- α -D-glucuronic acid, A = UDP, B = aglycone substrate (4-MU), I_1 and I_2 = tentative inhibitors removed by BSA.

6 Summary and Conclusions

This thesis explored the activity, assay conditions, and enzyme kinetics of human UGTs, important enzymes involved in the metabolic elimination of xenobiotics and endogenous compounds. Most importantly:

- 1) We identified the UGT enzymes involved in the glucuronidation of psilocin and 4-HI. Moreover, we performed enzyme kinetic assays and studied the expression levels of the UGTs that are active in psilocin glucuronidation. Our results suggest that psilocin is glucuronidated mainly by UGT1A9 in the liver and kidneys, but also by UGT1A10 in the intestine. In contrast to the psilocin results, 4-HI was glucuronidated mainly by UGT1A6, presumably due to the lack of a flexible side chain. However, because this study was performed in the absence of albumin, the enzyme kinetic parameters measured, especially substrate affinity and V_{\max} , are probably underestimated. Future studies will need to address this issue.
- 2) We studied the effects of albumin on 11 human UGTs, 5 of which were previously reported and 6 untested thus far. Our results show that addition of albumin enhances the activities of UGTs 1A7, 1A8, 1A10, 2A1, and 2B15. The effects of albumin are comparable to the recombinant UGTs expressed in *Sf9* insect cells and microsomes from the human liver and intestine. The addition of albumin also resulted in an increase in V_{\max} for many UGT enzymes tested, although the effects are clearly both enzyme and substrate dependent. Additional studies may be needed to identify and quantify exactly which inhibitors albumin removes.
- 3) We investigated the enzyme kinetic mechanism of UGT1A9 in both the absence and presence of albumin. The addition of albumin quantitatively changed the enzyme kinetic parameters, but did not affect the underlying compulsory-order ternary-complex mechanism. The nature of substrate inhibition, as well as the results of inhibition by 1-naphthol and UDP, suggested that UDPGA binds first and the aglycone substrate binds second to form a ternary-complex in UGT-catalyzed reactions. Activity enhancement in the presence of BSA likely arises from the BSA-mediated removal of competitive and mixed-type inhibitors with respect to the aglycone substrate, but of uncompetitive inhibitors with respect to UDPGA. We determined the equilibrium constant (K_{eq}) for the overall reaction of 4-MU glucuronidation and elucidated the relative individual rate constants.

Taken together, we trust that these results will contribute to a deeper understanding of human UGTs, serve as a starting point for new studies, and ultimately contribute to safer pharmacotherapy.

References (in alphabetical order)

- Alberty RA. (2011) *Enzyme Kinetics: Rapid-Equilibrium Applications of Mathematica*, First Edition ed. John Wiley & Sons, Inc., Hoboken, NJ, USA.
- Alonen A, Finel M, and Kostianen R. (2008) The human UDP-glucuronosyltransferase UGT1A3 is highly selective towards N2 in the tetrazole ring of losartan, candesartan, and zolarsartan. *Biochem Pharmacol* **76**:763-772.
- Anastos N, Barnett NW, Pfeffer FM, and Lewis SW. (2006) Investigation into the temporal stability of aqueous standard solutions of psilocin and psilocybin using high performance liquid chromatography. *Sci Justice* **46**:91-96.
- Argikar UA. (2012) Unusual glucuronides. *Drug Metab Dispos* **40**:1239-1251.
- Axelrod J, Inscoe JK, and Tomkins GM. (1958) Enzymatic synthesis of N-glucosyluronic acid conjugates. *J Biol Chem* **232**:835-841.
- Banhegyi G, Garzo T, Fulceri R, Benedetti A, and Mandl J. (1993) Latency is the major determinant of UDP-glucuronosyltransferase activity in isolated hepatocytes. *FEBS Lett* **328**:149-152.
- Banker MJ and Clark TH. (2008) Plasma/serum protein binding determinations. *Curr Drug Metab* **9**:854-859.
- Barbier O, Girard C, Breton R, Belanger A, and Hum D. (2000) N-glycosylation and residue 96 are involved in the functional properties of UDP-glucuronosyltransferase enzymes. *Biochemistry* **39**:11540-11552.
- Barter ZE, Bayliss MK, Beaune PH, Boobis AR, Carlile DJ, Edwards RJ, Houston JB, Lake BG, Lipscomb JC, Pelkonen OR, Tucker GT, and Rostami-Hodjegan A. (2007) Scaling factors for the extrapolation of *in vivo* metabolic drug clearance from *in vitro* data: reaching a consensus on values of human microsomal protein and hepatocellularity per gram of liver. *Curr Drug Metab* **8**:33-45.
- Battaglia E and Gollan J. (2001) A unique multifunctional transporter translocates estradiol-17 β -glucuronide in rat liver microsomal vesicles. *J Biol Chem* **276**:23492-23498.
- Benet LZ. (2009) The drug transporter-metabolism alliance: uncovering and defining the interplay. *Mol Pharm* **6**:1631-1643.
- Benoit-Biancamano MO, Connelly J, Villeneuve L, Caron P, and Guillemette C. (2009) Deferiprone glucuronidation by human tissues and recombinant UDP-glucuronosyltransferase 1A6: an *in vitro* investigation of genetic and splice variants. *Drug Metab Dispos* **37**:322-329.
- Bernard O and Guillemette C. (2004) The main role of UGT1A9 in the hepatic metabolism of mycophenolic acid and the effects of naturally occurring variants. *Drug Metab Dispos* **32**:775-778.
- Bichlmaier I, Siiskonen A, Kurkela M, Finel M, and Yli-Kauhaluoma J. (2006) Chiral distinction between the enantiomers of bicyclic alcohols by UDP-glucuronosyltransferases 2B7 and 2B17. *Biol Chem* **387**:407-416.
- Bisswanger H. (2002) *Enzyme Kinetics, Principles and Methods*, 3rd edition ed. Wiley-vch Verlag GmbH, Weinheim, Germany.
- Bjornstad K, Hulten P, Beck O, and Helander A. (2009) Bioanalytical and clinical evaluation of 103 suspected cases of intoxications with psychoactive plant materials. *Clin Toxicol* **47**:566-572.
- Boase S and Miners JO. (2002) *In vitro*-*in vivo* correlations for drugs eliminated by glucuronidation: investigations with the model substrate zidovudine. *Br J Clin Pharmacol* **54**:493-503.
- Bock KW. (2010) Functions and transcriptional regulation of adult human hepatic UDP-glucuronosyltransferases (UGTs): mechanisms responsible for interindividual variation of UGT levels. *Biochem Pharmacol* **80**:771-777.
- Bock KW and Kohle C. (2009) Topological aspects of oligomeric UDP-glucuronosyltransferases in endoplasmic reticulum membranes: advances and open questions. *Biochem Pharmacol* **77**:1458-1465.
- Bolam DN, Roberts S, Proctor MR, Turkenburg JP, Dodson EJ, Martinez-Fleites C, Yang M, Davis BG, Davies GJ, and Gilbert HJ. (2007) The crystal structure of two macrolide glycosyltransferases provides a blueprint for host cell antibiotic immunity. *Proc Natl Acad Sci U S A* **104**:5336-5341.
- Bosma PJ, Seppen J, Goldhoorn B, Bakker C, Oude Elferink RP, Chowdhury JR, Chowdhury NR, and Jansen PL. (1994) Bilirubin UDP-glucuronosyltransferase 1 is the only relevant bilirubin glucuronidating isoform in man. *J Biol Chem* **269**:17960-17964.
- Bowalgha K, Elliot DJ, Mackenzie PI, Knights KM, Swedmark S, and Miners JO. (2005) S-Naproxen and desmethylnaproxen glucuronidation by human liver microsomes and recombinant human UDP-glucuronosyltransferases (UGT): role of UGT2B7 in the elimination of naproxen. *Br J Clin Pharmacol* **60**:423-433.
- Brazier-Hicks M, Offen WA, Gershater MC, Revett TJ, Lim E, Bowles DJ, Davies GJ, and Edwards R. (2007) Characterization and engineering of the bifunctional N- and O-glucosyltransferase involved in xenobiotic metabolism in plants. *Proc Natl Acad Sci U S A* **104**:20238-20243.
- Canezin J, Cailleux A, Turcant A, Le Bouil A, Harry P, and Allain P. (2001) Determination of LSD and its metabolites in human biological fluids by high-performance liquid chromatography with electrospray tandem mass spectrometry. *J Chromatogr B Biomed Sci Appl* **765**:15-27.
- Carlile DJ, Hakooz N, Bayliss MK, and Houston JB. (1999) Microsomal prediction of *in vivo* clearance of CYP2C9 substrates in humans. *Br J Clin Pharmacol* **47**:625-635.
- Chang A, Singh S, Phillips GN, Jr., and Thorson JS. (2011) Glycosyltransferase structural biology and its role in the design of catalysts for glycosylation. *Curr Opin Biotechnol* **22**:800-8.

- Chang JH, Yoo P, Lee T, Klopff W, and Takao D. (2009) The role of pH in the glucuronidation of raloxifene, mycophenolic acid and ezetimibe. *Mol Pharmacol* **6**:1216-1227.
- Chen G, Blevins-Primeau AS, Dellinger RW, Muscat JE, and Lazarus P. (2007) Glucuronidation of nicotine and cotinine by UGT2B10: loss of function by the UGT2B10 Codon 67 (Asp>Tyr) polymorphism. *Cancer Res* **67**:9024-9029.
- Cheng Y and Prusoff WH. (1973) Relationship between the inhibition constant (K_i) and the concentration of inhibitor which causes 50 per cent inhibition (I_{50}) of an enzymatic reaction. *Biochem Pharmacol* **22**:3099-3108.
- Chimalakonda KC, Bratton SM, Le VH, Yiew KH, Dineva A, Moran CL, James LP, Moran JH, and Radominska-Pandya A. (2011) Conjugation of synthetic cannabinoids JWH-018 and JWH-073, metabolites by human UDP-glucuronosyltransferases. *Drug Metab Dispos* **39**:1967-1976.
- Ciotti M, Cho JW, George J, and Owens IS. (1998) Required buried alpha-helical structure in the bilirubin UDP-glucuronosyltransferase, UGT1A1, contains a nonreplaceable phenylalanine. *Biochemistry* **37**:11018-11025.
- Copeland RA. (2000) *Enzymes: A Practical Introduction to Structure, Mechanism, and Data Analysis*, Second edition ed. John Wiley & Sons, Inc., New York, NY, USA.
- Copeland RA. (2005) *Evaluation of Enzyme Inhibitors in Drug Discovery*, First Edition ed. John Wiley & Sons, Inc., Hoboken, NJ, USA.
- Cornish-Bowden A. (2012) *Fundamentals of Enzyme Kinetics*, 4th ed. Wiley-Blackwell, Weinheim, Germany.
- Court MH. (2010) Interindividual variability in hepatic drug glucuronidation: studies into the role of age, sex, enzyme inducers, and genetic polymorphism using the human liver bank as a model system. *Drug Metab Rev* **42**:202-217.
- Court MH. (2005) Isoform-selective probe substrates for *in vitro* studies of human UDP-glucuronosyltransferases. *Methods Enzymol* **400**:104-116.
- Court MH, Hazarika S, Krishnaswamy S, Finel M, and Williams JA. (2008) Novel polymorphic human UDP-glucuronosyltransferase 2A3: cloning, functional characterization of enzyme variants, comparative tissue expression, and gene induction. *Mol Pharmacol* **74**:744-754.
- Court MH, Zhang X, Ding X, Yee KK, Hesse LM, and Finel M. (2012) Quantitative distribution of mRNAs encoding the 19 human UDP-glucuronosyltransferase enzymes in 26 adult and 3 fetal tissues. *Xenobiotica* **42**:266-277.
- Court MH, Krishnaswamy S, Hao Q, Duan SX, Patten CJ, Von Moltke LL, and Greenblatt DJ. (2003) Evaluation of 3'-azido-3'-deoxythymidine, morphine, and codeine as probe substrates for UDP-glucuronosyltransferase 2B7 (UGT2B7) in human liver microsomes: specificity and influence of the UGT2B7*2 polymorphism. *Drug Metab Dispos* **31**:1125-1133.
- Court MH, Duan SX, Guillemette C, Journault K, Krishnaswamy S, Von Moltke LL, and Greenblatt DJ. (2002) Stereoselective conjugation of oxazepam by human UDP-glucuronosyltransferases (UGTs): *S*-oxazepam is glucuronidated by UGT2B15, while *R*-oxazepam is glucuronidated by UGT2B7 and UGT1A9. *Drug Metab Dispos* **30**:1257-1265.
- Csala M, Staines AG, Banhegyi G, Mandl J, Coughtrie MW, and Burchell B. (2004) Evidence for multiple glucuronide transporters in rat liver microsomes. *Biochem Pharmacol* **68**:1353-1362.
- Csala M, Marcolongo P, Lizak B, Senesi S, Margittai E, Fulceri R, Magyar JE, Benedetti A, and Banhegyi G. (2007) Transport and transporters in the endoplasmic reticulum. *Biochim Biophys Acta* **1768**:1325-1341.
- Dain JG, Fu E, Gorski J, Nicoletti J, and Scallen TJ. (1993) Biotransformation of fluvastatin sodium in humans. *Drug Metab Dispos* **21**:567-572.
- De Sa Alves FR, Barreiro EJ, and Fraga CA. (2009) From nature to drug discovery: the indole scaffold as a 'privileged structure'. *Mini Rev Med Chem* **9**:782-793.
- Dellinger RW, Fang JL, Chen G, Weinberg R, and Lazarus P. (2006) Importance of UDP-glucuronosyltransferase 1A10 (UGT1A10) in the detoxification of polycyclic aromatic hydrocarbons: decreased glucuronidative activity of the UGT1A10139Lys isoform. *Drug Metab Dispos* **34**:943-949.
- Dickerson JA, Laha TJ, Pagano MB, O'Donnell BR, and Hoofnagle AN. (2012) Improved detection of opioid use in chronic pain patients through monitoring of opioid glucuronides in urine. *J Anal Toxicol* **36**:541-547.
- Dixon CM, Saynor DA, Andrew PD, Oxford J, Bradbury A, and Tarbit MH. (1993) Disposition of sumatriptan in laboratory animals and humans. *Drug Metab Dispos* **21**:761-769.
- Dong D, Ako R, Hu M, and Wu B. (2012) Understanding substrate selectivity of human UDP-glucuronosyltransferases through QSAR modeling and analysis of homologous enzymes. *Xenobiotica* **42**:808-20.
- Eckford PD and Sharom FJ. (2009) ABC efflux pump-based resistance to chemotherapy drugs. *Chem Rev* **109**:2989-3011.
- El-Bacha RS, Leclerc S, Netter P, Magdalou J, and Minn A. (2000) Glucuronidation of apomorphine. *Life Sci* **67**:1735-1745.
- Engtrakul JJ, Foti RS, Strelevitz TJ, and Fisher MB. (2005) Altered AZT (3'-azido-3'-deoxythymidine) glucuronidation kinetics in liver microsomes as an explanation for underprediction of *in vivo* clearance: comparison to hepatocytes and effect of incubation environment. *Drug Metab Dispos* **33**:1621-1627.
- Falany CN, Green MD, and Tephly TR. (1987) The enzymatic mechanism of glucuronidation catalyzed by two purified rat liver steroid UDP-glucuronosyltransferases. *J Biol Chem* **262**:1218-1222.

- Fallon JK, Harbourt DE, Maleki SH, Kessler FK, Ritter JK, and Smith PC. (2008) Absolute quantification of human uridine-diphosphate glucuronosyl transferase (UGT) enzyme isoforms 1A1 and 1A6 by tandem LC-MS. *Drug Metab Lett* **2**:210-222.
- Finel M and Kurkela M. (2008) The UDP-glucuronosyltransferases as oligomeric enzymes. *Curr Drug Metab* **9**:70-76.
- Fischer V, Baldeck JP, and Tse FL. (1992) Pharmacokinetics and metabolism of the 5-hydroxytryptamine antagonist tropisetron after single oral doses in humans. *Drug Metab Dispos* **20**:603-607.
- Fisher MB, Campanale K, Ackermann BL, VandenBranden M, and Wrighton SA. (2000) *In vitro* glucuronidation using human liver microsomes and the pore-forming peptide alamethicin. *Drug Metab Dispos* **28**:560-566.
- Forgue ST, Phillips DL, Bedding AW, Payne CD, Jewell H, Patterson BE, Wrishko RE, and Mitchell MI. (2007) Effects of gender, age, diabetes mellitus and renal and hepatic impairment on tadalafil pharmacokinetics. *Br J Clin Pharmacol* **63**:24-35.
- Foti RS and Fisher MB. (2005) Assessment of UDP-glucuronosyltransferase catalyzed formation of ethyl glucuronide in human liver microsomes and recombinant UGTs. *Forensic Sci Int* **153**:109-116.
- French D, Wu A, and Lynch K. (2011) Hydrophilic interaction LC-MS/MS analysis of opioids in urine: significance of glucuronide metabolites. *Bioanalysis* **3**:2603-2612.
- Fujiwara R, Nakajima M, Yamanaka H, and Yokoi T. (2009a) Key amino acid residues responsible for the differences in substrate specificity of human UDP-glucuronosyltransferase (UGT)1A9 and UGT1A8. *Drug Metab Dispos* **37**:41-46.
- Fujiwara R, Nakajima M, Yamamoto T, Nagao H, and Yokoi T. (2009b) *In silico* and *in vitro* approaches to elucidate the thermal stability of human UDP-glucuronosyltransferase (UGT) 1A9. *Drug Metab Pharmacokinet* **24**:235-244.
- Fujiwara R, Nakajima M, Yamanaka H, Katoh M, and Yokoi T. (2008) Product inhibition of UDP-glucuronosyltransferase (UGT) enzymes by UDP obfuscates the inhibitory effects of UGT substrates. *Drug Metab Dispos* **36**:361-367.
- Gaganis P, Miners JO, and Knights KM. (2007) Glucuronidation of fenamates: kinetic studies using human kidney cortical microsomes and recombinant UDP-glucuronosyltransferase (UGT) 1A9 and 2B7. *Biochem Pharmacol* **73**:1683-1691.
- Ghosh SS, Lu Y, Lee SW, Wang X, Guha C, Roy-Chowdhury J, and Roy-Chowdhury N. (2005) Role of cysteine residues in the function of human UDP glucuronosyltransferase isoform 1A1 (UGT1A1). *Biochem J* **392**:685-692.
- Gill KL, Houston JB, and Galetin A. (2012) Characterization of *in vitro* glucuronidation clearance of a range of drugs in human kidney microsomes: comparison with liver and intestinal glucuronidation and impact of albumin. *Drug Metab Dispos* **40**:825-835.
- Girard H, Court MH, Bernard O, Fortier LC, Villeneuve L, Hao Q, Greenblatt DJ, von Moltke LL, Perused L, and Guillemette C. (2004) Identification of common polymorphisms in the promoter of the UGT1A9 gene: evidence that UGT1A9 protein and activity levels are strongly genetically controlled in the liver. *Pharmacogenetics* **14**:501-515.
- Gonzalez-Maeso J, Weisstaub NV, Zhou M, Chan P, Ivic L, Ang R, Lira A, Bradley-Moore M, Ge Y, Zhou Q, Sealfon SC, and Gingrich JA. (2007) Hallucinogens recruit specific cortical 5-HT_{2A} receptor-mediated signaling pathways to affect behavior. *Neuron* **53**:439-452.
- Grieshaber AF, Moore KA, and Levine B. (2001) The detection of psilocin in human urine. *J Forensic Sci* **46**:627-630.
- Guengerich FP. (2008) Cytochrome P450 and chemical toxicology. *Chem Res Toxicol* **21**:70-83.
- Guillemette C, Levesque E, Harvey M, Bellemare J, and Menard V. (2010) UGT genomic diversity: beyond gene duplication. *Drug Metab Rev* **42**:24-44.
- Halpern JH. (2004) Hallucinogens and dissociative agents naturally growing in the United States. *Pharmacol Ther* **102**:131-138.
- Harbourt DE, Fallon JK, Ito S, Baba T, Ritter JK, Glish GL, and Smith PC. (2012) Quantification of human uridine-diphosphate glucuronosyl transferase 1A isoforms in liver, intestine, and kidney using nanobore liquid chromatography-tandem mass spectrometry. *Anal Chem* **84**:98-105.
- Hasler F, Bourquin D, Brenneisen R, and Vollenweider FX. (2002) Renal excretion profiles of psilocin following oral administration of psilocybin: a controlled study in man. *J Pharm Biomed Anal* **30**:331-339.
- Hasler F, Bourquin D, Brenneisen R, Bar T, and Vollenweider FX. (1997) Determination of psilocin and 4-hydroxyindole-3-acetic acid in plasma by HPLC-ECD and pharmacokinetic profiles of oral and intravenous psilocybin in man. *Pharm Acta Helv* **72**:175-184.
- Hauser SC, Ziurys JC, and Gollan JL. (1984) Subcellular distribution and regulation of hepatic bilirubin UDP-glucuronosyltransferase. *J Biol Chem* **259**:4527-4533.
- Hewitt NJ, Lechon MJ, Houston JB, Hallifax D, Brown HS, Maurel P, Kenna JG, Gustavsson L, Lohmann C, Skonberg C, Guillouzo A, Tuschl G, Li AP, LeCluyse E, Groothuis GM, and Hengstler JG. (2007) Primary hepatocytes: current understanding of the regulation of metabolic enzymes and transporter proteins, and pharmaceutical practice for the use of hepatocytes in metabolism, enzyme induction, transporter, clearance, and hepatotoxicity studies. *Drug Metab Rev* **39**:159-234.

- Higgins LG and Hayes JD. (2011) Mechanisms of induction of cytosolic and microsomal glutathione transferase (GST) genes by xenobiotics and pro-inflammatory agents. *Drug Metab Rev* **43**:92-137.
- Hintikka L, Kuuranne T, Aitio O, Thevis M, Schanzer W, and Kostianen R. (2008) Enzyme-assisted synthesis and structure characterization of glucuronide conjugates of eleven anabolic steroid metabolites. *Steroids* **73**:257-265.
- Hofmann A, Heim R, Brack A, and Kobel H. (1958) Psilocybin, a psychotropic substance from the Mexican mushroom *Psilocybe mexicana* Heim. *Experientia* **14**:107-109.
- Holzmann PP. (1995) Bestimmung von Psilocybin-Metaboliten im Humanplasma and -urin. *PhD Dissertation, University of Tübingen, Germany*.
- Hoog JO, Hedberg JJ, Stromberg P, and Svensson S. (2001) Mammalian alcohol dehydrogenase - functional and structural implications. *J Biomed Sci* **8**:71-76.
- Hosokawa M. (2008) Structure and catalytic properties of carboxylesterase isozymes involved in metabolic activation of prodrugs. *Molecules* **13**:412-431.
- Houston JB and Galetin A. (2008) Methods for predicting *in vivo* pharmacokinetics using data from *in vitro* assays. *Curr Drug Metab* **9**:940-951.
- Houston JB and Kenworthy KE. (2000) *In vitro*-*in vivo* scaling of CYP kinetic data not consistent with the classical Michaelis-Menten model. *Drug Metab Dispos* **28**:246-254.
- Hyland R, Osborne T, Payne A, Kempshall S, Logan YR, Ezzeddine K, and Jones B. (2009) *In vitro* and *in vivo* glucuronidation of midazolam in humans. *Br J Clin Pharmacol* **67**:445-454.
- Ikushiro S, Emi Y, and Iyanagi T. (2002) Activation of glucuronidation through reduction of a disulfide bond in rat UDP-glucuronosyltransferase 1A6. *Biochemistry* **41**:12813-12820.
- Ikushiro S, Emi Y, Kato Y, Yamada S, and Sakaki T. (2006) Monospecific antipeptide antibodies against human hepatic UDP-glucuronosyltransferase 1A subfamily (UGT1A) isoforms. *Drug Metab Pharmacokinet* **21**:70-74.
- International Transporter Consortium, Giacomini KM, Huang SM, Tweedie DJ, Benet LZ, Brouwer KL, Chu X, Dahlin A, Evers R, Fischer V, Hillgren KM, Hoffmaster KA, Ishikawa T, Keppler D, Kim RB, Lee CA, Niemi M, Polli JW, Sugiyama Y, Swaan PW, Ware JA, Wright SH, Yee SW, Zamek-Gliszczynski MJ, and Zhang L. (2010) Membrane transporters in drug development. *Nat Rev Drug Discov* **9**:215-236.
- Itäaho K, Laakkonen L, and Finel M. (2010) How many and which amino acids are responsible for the large activity differences between the highly homologous UDP-glucuronosyltransferases (UGT) 1A9 and UGT1A10? *Drug Metab Dispos* **38**:687-696.
- Itäaho K, Mackenzie PI, Ikushiro S, Miners JO, and Finel M. (2008) The configuration of the 17-hydroxy group variably influences the glucuronidation of β -estradiol and epiestradiol by human UDP-glucuronosyltransferases. *Drug Metab Dispos* **36**:2307-2315.
- Itäaho K, Court MH, Uutela P, Kostianen R, Radomska-Pandya A, and Finel M. (2009) Dopamine is a low-affinity and high-specificity substrate for the human UDP-glucuronosyltransferase 1A10. *Drug Metab Dispos* **37**:768-775.
- Izukawa T, Nakajima M, Fujiwara R, Yamanaka H, Fukami T, Takamiya M, Aoki Y, Ikushiro S, Sakaki T, and Yokoi T. (2009) Quantitative analysis of UDP-glucuronosyltransferase (UGT) 1A and UGT2B expression levels in human livers. *Drug Metab Dispos* **37**:1759-1768.
- Jedlitschky G, Cassidy AJ, Sales M, Pratt N, and Burchell B. (1999) Cloning and characterization of a novel human olfactory UDP-glucuronosyltransferase. *Biochem J* **340** (Pt 3):837-843.
- Johnson LP and Fenselau C. (1978) Enzymatic conjugation and hydrolysis of [¹⁸O] isoborneol glucuronide. *Drug Metab Dispos* **6**:677-679.
- Johnston MM and Rapoport AM. (2010) Triptans for the management of migraine. *Drugs* **70**:1505-1518.
- Jones HM and Houston JB. (2004) Substrate depletion approach for determining *in vitro* metabolic clearance: time dependencies in hepatocyte and microsomal incubations. *Drug Metab Dispos* **32**:973-982.
- Kaivosari S, Finel M, and Koskinen M. (2011) *N*-glucuronidation of drugs and other xenobiotics by human and animal UDP-glucuronosyltransferases. *Xenobiotica* **41**:652-669.
- Kaivosari S, Toivonen P, Hesse LM, Koskinen M, Court MH, and Finel M. (2007) Nicotine glucuronidation and the human UDP-glucuronosyltransferase UGT2B10. *Mol Pharmacol* **72**:761-768.
- Kaivosari S, Toivonen P, Aitio O, Sipilä J, Koskinen M, Salonen JS, and Finel M. (2008) Regio- and stereospecific *N*-glucuronidation of medetomidine: the differences between UDP glucuronosyltransferase (UGT) 1A4 and UGT2B10 account for the complex kinetics of human liver microsomes. *Drug Metab Dispos* **36**:1529-1537.
- Kaji H and Kume T. (2005) Regioselective glucuronidation of denopamine: marked species differences and identification of human UDP-glucuronosyltransferase isoform. *Drug Metab Dispos* **33**:403-412.
- Kamata T, Nishikawa M, Katagi M, and Tsuchihashi H. (2006) Direct detection of serum psilocin glucuronide by LC/MS and LC/MS/MS: time-courses of total and free (unconjugated) psilocin concentrations in serum specimens of a "magic mushroom" user. *Forensic Toxicol* **24**:36-40
- Kamata T, Nishikawa M, Katagi M, and Tsuchihashi H. (2003) Optimized glucuronide hydrolysis for the detection of psilocin in human urine samples. *J Chromatogr B* **796**:421-427.
- Kamata T, Katagi M, Kamata HT, Miki A, Shima N, Zaito K, Nishikawa M, Tanaka E, Honda K, and Tsuchihashi H. (2006) Metabolism of the psychotomimetic tryptamine derivative 5-methoxy-*N,N*-diisopropyltryptamine in humans: identification and quantification of its urinary metabolites. *Drug Metab Dispos* **34**:281-287.

- Kato Y, Ikushiro S, Emi Y, Tamaki S, Suzuki H, Sakaki T, Yamada S, and Degawa M. (2008) Hepatic UDP-glucuronosyltransferases responsible for glucuronidation of thyroxine in humans. *Drug Metab Dispos* **36**:51-55.
- Kerdpin O, Mackenzie PI, Bowalgaha K, Finel M, and Miners JO. (2009) Influence of N-terminal domain histidine and proline residues on the substrate selectivities of human UDP-glucuronosyltransferase 1A1, 1A6, 1A9, 2B7, and 2B10. *Drug Metab Dispos* **37**:1948-1955.
- Kiang TK, Ensom MH, and Chang TK. (2005) UDP-glucuronosyltransferases and clinical drug-drug interactions. *Pharmacol Ther* **106**:97-132.
- Kilford PJ, Stringer R, Sohal B, Houston JB, and Galetin A. (2009) Prediction of drug clearance by glucuronidation from *in vitro* data: use of combined cytochrome P450 and UDP-glucuronosyltransferase cofactors in alamethicin-activated human liver microsomes. *Drug Metab Dispos* **37**:82-89.
- King C, Tang W, Ngui J, Tephly T, and Braun M. (2001) Characterization of rat and human UDP-glucuronosyltransferases responsible for the *in vitro* glucuronidation of diclofenac. *Toxicol Sci* **61**:49-53.
- King CD, Rios GR, Green MD, and Tephly TR. (2000) UDP-glucuronosyltransferases. *Curr Drug Metab* **1**:143-161.
- King CD, Rios GR, Assouline JA, and Tephly TR. (1999) Expression of UDP-glucuronosyltransferases (UGTs) 2B7 and 1A6 in the human brain and identification of 5-hydroxytryptamine as a substrate. *Arch Biochem Biophys* **365**:156-162.
- Klecker RW and Collins JM. (1997) Stereoselective metabolism of fenoldopam and its metabolites in human liver microsomes, cytosol, and slices. *J Cardiovasc Pharmacol* **30**:69-74.
- Korzekwa KR, Krishnamachary N, Shou M, Ogai A, Parise RA, Rettie AE, Gonzalez FJ, and Tracy TS. (1998) Evaluation of atypical cytochrome P450 kinetics with two-substrate models: evidence that multiple substrates can simultaneously bind to cytochrome P450 active sites. *Biochemistry* **37**:4137-4147.
- Koster AS and Noordhoek J. (1983) Kinetic properties of the rat intestinal microsomal 1-naphthol: UDP-glucuronosyl transferase. Inhibition by UDP and UDP-N-acetylglucosamine. *Biochim Biophys Acta* **761**:76-85.
- Krishnaswamy S, Hao Q, Von Moltke LL, Greenblatt DJ, and Court MH. (2004) Evaluation of 5-hydroxytryptophol and other endogenous serotonin (5-hydroxytryptamine) analogs as substrates for UDP-glucuronosyltransferase 1A6. *Drug Metab Dispos* **32**:862-869.
- Krishnaswamy S, Duan SX, Von Moltke LL, Greenblatt DJ, and Court MH. (2003a) Validation of serotonin (5-hydroxytryptamine) as an *in vitro* substrate probe for human UDP-glucuronosyltransferase (UGT) 1A6. *Drug Metab Dispos* **31**:133-139.
- Krishnaswamy S, Duan SX, Von Moltke LL, Greenblatt DJ, Sudmeier JL, Bachovchin WW, and Court MH. (2003b) Serotonin (5-hydroxytryptamine) glucuronidation *in vitro*: assay development, human liver microsome activities and species differences. *Xenobiotica* **33**:169-180.
- Kubota T, Lewis BC, Elliot DJ, Mackenzie PI, and Miners JO. (2007) Critical roles of residues 36 and 40 in the phenol and tertiary amine aglycone substrate selectivities of UDP-glucuronosyltransferases 1A3 and 1A4. *Mol Pharmacol* **72**:1054-62.
- Kuehl GE, Lampe JW, Potter JD, and Bigler J. (2005) Glucuronidation of nonsteroidal anti-inflammatory drugs: identifying the enzymes responsible in human liver microsomes. *Drug Metab Dispos* **33**:1027-1035.
- Kurkela M, Patana AS, Mackenzie PI, Court MH, Tate CG, Hirvonen J, Goldman A, and Finel M. (2007) Interactions with other human UDP-glucuronosyltransferases attenuate the consequences of the Y485D mutation on the activity and substrate affinity of UGT1A6. *Pharmacogenet Genomics* **17**:115-126.
- Kurkela M, Garcia-Horsman JA, Luukkanen L, Mörsky S, Taskinen J, Baumann M, Kostiaainen R, Hirvonen J, and Finel M. (2003) Expression and characterization of recombinant human UDP-glucuronosyltransferases (UGTs). UGT1A9 is more resistant to detergent inhibition than other UGTs and was purified as an active dimeric enzyme. *J Biol Chem* **278**:3536-3544.
- Kuuranne T, Kurkela M, Thevis M, Schänzer W, Finel M, and Kostiaainen R. (2003) Glucuronidation of anabolic androgenic steroids by recombinant human UDP-glucuronosyltransferases. *Drug Metab Dispos* **31**:1117-1124.
- Laakkonen L and Finel M. (2010) A molecular model of the human UDP-glucuronosyltransferase 1A1, its membrane orientation, and the interactions between different parts of the enzyme. *Mol Pharmacol* **77**:931-939.
- Lairson LL, Henrissat B, Davies GJ, and Withers SG. (2008) Glycosyltransferases: Structures, functions, and mechanisms. *Annu Rev Biochem* **77**:521-555.
- Lautala P, Ethell BT, Taskinen J, and Burchell B. (2000) The specificity of glucuronidation of entacapone and tolcapone by recombinant human UDP-glucuronosyltransferases. *Drug Metab Dispos* **28**:1385-1389.
- Lee KJ, Mower R, Hollenbeck T, Castelo J, Johnson N, Gordon P, Sinko PJ, Holme K, and Lee YH. (2003) Modulation of nonspecific binding in ultrafiltration protein binding studies. *Pharm Res* **20**:1015-1021.
- Lehtonen P, Sten T, Aitio O, Kurkela M, Vuorensola K, Finel M, and Kostiaainen R. (2010) Glucuronidation of racemic *O*-desmethyiltramadol, the active metabolite of tramadol. *Eur J Pharm Sci* **41**:523-530.
- Levesque E, Turgeon D, Carrier JS, Montminy V, Beaulieu M, and Belanger A. (2001) Isolation and characterization of the UGT2B28 cDNA encoding a novel human steroid conjugating UDP-glucuronosyltransferase. *Biochemistry* **40**:3869-3881.
- Levy G. (1952) The preparation and properties of β -glucuronidase. 4. Inhibition by sugar acids and their lactones. *Biochem J* **52**:464-472.

- Lewis BC, Mackenzie PI, and Miners JO. (2011) Homodimerization of UDP-glucuronosyltransferase 2B7 (UGT2B7) and identification of a putative dimerization domain by protein homology modeling. *Biochem Pharmacol* **82**:2016-2023.
- Lewis BC, Mackenzie PI, Elliot DJ, Burchell B, Bhasker CR, and Miners JO. (2007) Amino terminal domains of human UDP-glucuronosyltransferases (UGT) 2B7 and 2B15 associated with substrate selectivity and autoactivation. *Biochem Pharmacol* **73**:1463-1473.
- Li C and Wu Q. (2007) Adaptive evolution of multiple-variable exons and structural diversity of drug-metabolizing enzymes. *BMC Evol Biol* **7**:69.
- Li D, Fournel-Gigleux S, Barre L, Mulliert G, Netter P, Magdalou J, and Ouzzine M. (2007) Identification of aspartic acid and histidine residues mediating the reaction mechanism and the substrate specificity of the human UDP-glucuronosyltransferases 1A. *J Biol Chem* **282**:36514-24.
- Lindsay J, Wang LL, Li Y, and Zhou SF. (2008) Structure, function and polymorphism of human cytosolic sulfotransferases. *Curr Drug Metab* **9**:99-105.
- Little JM, Lehman PA, Nowell S, Samokyszyn V, and Radomska A. (1997) Glucuronidation of all-trans-retinoic acid and 5,6-epoxy-all-trans-retinoic acid. Activation of rat liver microsomal UDP-glucuronosyltransferase activity by alamethicin. *Drug Metab Dispos* **25**:5-11.
- Locuson CW and Tracy TS. (2007) Comparative modelling of the human UDP-glucuronosyltransferases: insights into structure and mechanism. *Xenobiotica* **37**:155-168.
- Loureiro AI, Fernandes-Lopes C, Bonifacio MJ, Wright LC, and Soares-da-Silva P. (2011) Hepatic UDP-glucuronosyltransferase is responsible for eslicarbazepine glucuronidation. *Drug Metab Dispos* **39**:1486-1494.
- Ludden LK, Ludden TM, Collins JM, Pentikis HS, and Strong JM. (1997) Effect of albumin on the estimation, *in vitro*, of phenytoin V_{max} and K_m values: implications for clinical correlation. *J Pharmacol Exp Ther* **282**:391-396.
- Luukkanen L, Taskinen J, Kurkela M, Kostianen R, Hirvonen J, and Finel M. (2005) Kinetic characterization of the 1A subfamily of recombinant human UDP-glucuronosyltransferases. *Drug Metab Dispos* **33**:1017-1026.
- Ma L, Sun J, Peng Y, Zhang R, Shao F, Hu X, Zhu J, Wang X, Cheng X, Zhu Y, Wan P, Feng D, Wu H, and Wang G. (2012) Glucuronidation of edaravone by human liver and kidney microsomes: biphasic kinetics and identification of UGT1A9 as the major UDP-glucuronosyltransferase isoform. *Drug Metab Dispos* **40**:734-741.
- Mackenzie P. (1990) The effect of *N*-linked glycosylation on the substrate preferences of UDP-glucuronosyltransferases. *Biochem Biophys Res Commun* **166**:1293-1299.
- Mackenzie P, Little JM, and Radomska-Pandya A. (2003) Glucosidation of hyodeoxycholic acid by UDP-glucuronosyltransferase 2B7. *Biochem Pharmacol* **65**:417-421.
- Mackenzie PI and Owens IS. (1984) Cleavage of nascent UDP-glucuronosyltransferase from rat liver by dog pancreatic microsomes. *Biochem Biophys Res Commun* **122**:1441-1449.
- Mackenzie PI, Rogers A, Treloar J, Jorgensen BR, Miners JO, and Meech R. (2008) Identification of UDP glycosyltransferase 3A1 as a UDP-*N*-acetylglucosaminyltransferase. *J Biol Chem* **283**:36205-36210.
- MacKenzie PI, Rogers A, Elliot DJ, Chau N, Hulin JA, Miners JO, and Meech R. (2011) The novel UDP glycosyltransferase 3A2: cloning, catalytic properties, and tissue distribution. *Mol Pharmacol* **79**:472-478.
- Mackenzie PI, Bock KW, Burchell B, Guillemette C, Ikushiro S, Iyanagi T, Miners JO, Owens IS, and Nebert DW. (2005) Nomenclature update for the mammalian UDP glycosyltransferase (UGT) gene superfamily. *Pharmacogenet Genomics* **15**:677-685.
- Magdalou J, Fournel-Gigleux S, and Ouzzine M. (2010) Insights on membrane topology and structure/function of UDP-glucuronosyltransferases. *Drug Metab Rev* **42**:159-166.
- Marheineke K, Grunewald S, Christie W, and Reilander H. (1998) Lipid composition of *Spodoptera frugiperda* (Sf9) and *Trichoplusia ni* (Tn) insect cells used for baculovirus infection. *FEBS Lett* **441**:49-52.
- Matern H, Lappas N, and Matern S. (1991) Isolation and characterization of hyodeoxycholic-acid: UDP-glucuronosyltransferase from human liver. *Eur J Biochem* **200**:393-400.
- Matern H, Matern S, and Gerok W. (1982) Isolation and characterization of rat liver microsomal UDP-glucuronosyltransferase activity toward chenodeoxycholic acid and testosterone as a single form of enzyme. *J Biol Chem* **257**:7422-7429.
- Mazur A, Licht CF, Prather PL, Zielinska AK, Bratton SM, Gallus-Zawada A, Finel M, Miller GP, Radomska-Pandya A, and Moran JH. (2009) Characterization of human hepatic and extrahepatic UDP-glucuronosyltransferase enzymes involved in the metabolism of classic cannabinoids. *Drug Metab Dispos* **37**:1496-1504.
- McBride MC. (2000) Bufotenine: toward an understanding of possible psychoactive mechanisms. *J Psychoactive Drugs* **32**:321-331.
- McEnroe JD and Fleishaker JC. (2005) Clinical pharmacokinetics of almotriptan, a serotonin 5-HT_(1B/1D) receptor agonist for the treatment of migraine. *Clin Pharmacokinet* **44**:237-246.
- McLure JA, Miners JO, and Birkett DJ. (2000) Nonspecific binding of drugs to human liver microsomes. *Br J Clin Pharmacol* **49**:453-461.
- Meech R and Mackenzie PI. (1998) Determinants of UDP glucuronosyltransferase membrane association and residency in the endoplasmic reticulum. *Arch Biochem Biophys* **356**:77-85.
- Meech R, Yogalingam G, and Mackenzie PI. (1996) Mutational analysis of the carboxy-terminal region of UDP-glucuronosyltransferase 2B1. *DNA Cell Biol* **15**:489-494.

- Meech R, Miners JO, Lewis BC, and Mackenzie PI. (2012) The glycosidation of xenobiotics and endogenous compounds: Versatility and redundancy in the UDP-glycosyltransferase superfamily. *Pharmacol Ther* **134**:200-218.
- Meyer MR and Maurer HH. (2012) Current status of hyphenated mass spectrometry in studies of the metabolism of drugs of abuse, including doping agents. *Anal Bioanal Chem* **402**:195-208.
- Miley MJ, Zielinska AK, Keenan JE, Bratton SM, Radomska-Pandya A, and Redinbo MR. (2007) Crystal structure of the cofactor-binding domain of the human phase II drug-metabolism enzyme UDP-glucuronosyltransferase 2B7. *J Mol Biol* **369**:498-511.
- Miners JO, Mackenzie PI, and Knights KM. (2010) The prediction of drug-glucuronidation parameters in humans: UDP-glucuronosyltransferase enzyme-selective substrate and inhibitor probes for reaction phenotyping and *in vitro*-*in vivo* extrapolation of drug clearance and drug-drug interaction potential. *Drug Metab Rev* **42**:189-201.
- Miners JO, Smith PA, Sorich MJ, McKinnon RA, and Mackenzie PI. (2004) Predicting human drug glucuronidation parameters: application of *in vitro* and *in silico* modeling approaches. *Annu Rev Pharmacol Toxicol* **44**:1-25.
- Mistry M and Houston JB. (1987) Glucuronidation *in vitro* and *in vivo*. Comparison of intestinal and hepatic conjugation of morphine, naloxone, and buprenorphine. *Drug Metab Dispos* **15**:710-717.
- Motulsky H. (1995) *Intuitive Biostatistics*, 1st ed. Oxford University Press, New York, USA.
- Motulsky H and Christopoulos A. (2004) *Fitting Models to Biological Data using Linear and Nonlinear Regression: A Practical Guide to Curve Fitting*, First ed. Oxford University Press, New York, USA.
- Mulichak AM, Losey HC, Walsh CT, and Garavito RM. (2001) Structure of the UDP-glycosyltransferase GtfB that modifies the heptapeptide aglycone in the biosynthesis of vancomycin group antibiotics. *Structure* **9**:547-557.
- Musshoff F, Madea B, Stuber F, and Stamer UM. (2010) Enantioselective determination of ondansetron and 8-hydroxyondansetron in human plasma from recovered surgery patients by liquid chromatography-tandem mass spectrometry. *J Anal Toxicol* **34**:581-586.
- Mutlib AE, Goosen TC, Bauman JN, Williams JA, Kulkarni S, and Kostrubsky S. (2006) Kinetics of acetaminophen glucuronidation by UDP-glucuronosyltransferases 1A1, 1A6, 1A9 and 2B15. Potential implications in acetaminophen-induced hepatotoxicity. *Chem Res Toxicol* **19**:701-709.
- Nakajima M, Koga T, Sakai H, Yamanaka H, Fujiwara R, and Yokoi T. (2010) N-Glycosylation plays a role in protein folding of human UGT1A9. *Biochem Pharmacol* **79**:1165-1172.
- Nakamura A, Nakajima M, Yamanaka H, Fujiwara R, and Yokoi T. (2008) Expression of UGT1A and UGT2B mRNA in human normal tissues and various cell lines. *Drug Metab Dispos* **36**:1461-1464.
- Nebert DW and Russell DW. (2002) Clinical importance of the cytochromes P450. *Lancet* **360**:1155-1162.
- Niemi M, Pasanen MK, and Neuvonen PJ. (2011) Organic anion transporting polypeptide 1B1: a genetically polymorphic transporter of major importance for hepatic drug uptake. *Pharmacol Rev* **63**:157-181.
- Nishimura M and Naito S. (2006) Tissue-specific mRNA expression profiles of human phase I metabolizing enzymes except for cytochrome P450 and phase II metabolizing enzymes. *Drug Metab Pharmacokinet* **21**:357-374.
- Nishiyama T, Kobori T, Arai K, Ogura K, Ohnuma T, Ishii K, Hayashi K, and Hiratsuka A. (2006) Identification of human UDP-glucuronosyltransferase isoform(s) responsible for the C-glucuronidation of phenylbutazone. *Arch Biochem Biophys* **454**:72-79.
- Obach RS. (1997) Nonspecific binding to microsomes: impact on scale-up of *in vitro* intrinsic clearance to hepatic clearance as assessed through examination of warfarin, imipramine, and propranolol. *Drug Metab Dispos* **25**:1359-1369.
- Oda S, Nakajima M, Hatakeyama M, Fukami T, and Yokoi T. (2012) Preparation of a specific monoclonal antibody against human UDP-glucuronosyltransferase (UGT) 1A9 and evaluation of UGT1A9 protein levels in human tissues. *Drug Metab Dispos* **40**:1620-1627.
- Ohno S and Nakajin S. (2009) Determination of mRNA expression of human UDP-glucuronosyltransferases and application for localization in various human tissues by real-time reverse transcriptase-polymerase chain reaction. *Drug Metab Dispos* **37**:32-40.
- Ohno S, Kawana K, and Nakajin S. (2008) Contribution of UDP-glucuronosyltransferase 1A1 and 1A8 to morphine-6-glucuronidation and its kinetic properties. *Drug Metab Dispos* **36**:688-694.
- Oleson L and Court MH. (2008) Effect of the β -glucuronidase inhibitor saccharolactone on glucuronidation by human tissue microsomes and recombinant UDP-glucuronosyltransferases. *J Pharm Pharmacol* **60**:1175-1182.
- Ouzzine M, Magdalou J, Burchell B, and Fournel-Gigleux S. (1999a) An internal signal sequence mediates the targeting and retention of the human UDP-glucuronosyltransferase 1A6 to the endoplasmic reticulum. *J Biol Chem* **274**:31401-31409.
- Ouzzine M, Magdalou J, Burchell B, and Fournel-Gigleux S. (1999b) Expression of a functionally active human hepatic UDP-glucuronosyltransferase (UGT1A6) lacking the N-terminal signal sequence in the endoplasmic reticulum. *FEBS Lett* **454**:187-191.
- Ouzzine M, Barre L, Netter P, Magdalou J, and Fournel-Gigleux S. (2006) Role of the carboxyl terminal stop transfer sequence of UGT1A6 membrane protein in ER targeting and translocation of upstream luminal domain. *FEBS Lett* **580**:1953-1958.
- Ouzzine M, Barre L, Netter P, Magdalou J, and Fournel-Gigleux S. (2003) The human UDP-glucuronosyltransferases: structural aspects and drug glucuronidation. *Drug Metab Rev* **35**:287-303.

- Patana AS, Kurkela M, Finel M, and Goldman A. (2008) Mutation analysis in UGT1A9 suggests a relationship between substrate and catalytic residues in UDP-glucuronosyltransferases. *Protein Eng Des Sel* **21**:537-543.
- Patana AS, Kurkela M, Goldman A, and Finel M. (2007) The human UDP-glucuronosyltransferase: identification of key residues within the nucleotide-sugar binding site. *Mol Pharmacol* **72**:604-611.
- Phillips IR and Shephard EA. (2008) Flavin-containing monooxygenases: mutations, disease and drug response. *Trends Pharmacol Sci* **29**:294-301.
- Picard N, Ratanasavanh D, Premaud A, Le Meur Y, and Marquet P. (2005) Identification of the UDP-glucuronosyltransferase isoforms involved in mycophenolic acid phase II metabolism. *Drug Metab Dispos* **33**:139-146.
- Pirnay SO, Abraham TT, Lowe RH, and Huestis MA. (2006) Selection and optimization of hydrolysis conditions for the quantification of urinary metabolites of MDMA. *J Anal Toxicol* **30**:563-569.
- Potrepka RF and Spratt JL. (1972) A study on the enzymatic mechanism of guinea-pig hepatic-microsomal bilirubin glucuronyl transferase. *Eur J Biochem* **29**:433-439.
- Pryde DC, Dalvie D, Hu Q, Jones P, Obach RS, and Tran T. (2010) Aldehyde oxidase: an enzyme of emerging importance in drug discovery. *J Med Chem* **53**:8441-8460.
- Radomska-Pandya A, Bratton S, and Little JM. (2005a) A historical overview of the heterologous expression of mammalian UDP-glucuronosyltransferase isoforms over the past twenty years. *Curr Drug Metab* **6**:141-160.
- Radomska-Pandya A, Ouzzine M, Fournel-Gigleux S, and Magdalou J. (2005b) Structure of UDP-glucuronosyltransferases in membranes. *Methods Enzymol* **400**:116-147.
- Radomska-Pandya A, Pokrovskaya ID, Xu J, Little JM, Jude AR, Kurten RC, and Czernik PJ. (2002) Nuclear UDP-glucuronosyltransferases: identification of UGT2B7 and UGT1A6 in human liver nuclear membranes. *Arch Biochem Biophys* **399**:37-48.
- Raisanen MJ. (1984) The presence of free and conjugated bufotenin in normal human urine. *Life Sci* **34**:2041-2045.
- Rao ML, Rao GS, and Breuer H. (1976) Investigations on the kinetic properties of estrone glucuronyltransferase from pig kidney. *Biochim Biophys Acta* **452**:89-100.
- Raungrut P, Uchaipichat V, Elliot DJ, Janchawee B, Somogyi AA, and Miners JO. (2010) *In vitro-in vivo* extrapolation predicts drug-drug interactions arising from inhibition of codeine glucuronidation by dextropropoxyphene, fluconazole, ketoconazole, and methadone in humans. *J Pharmacol Exp Ther* **334**:609-618.
- Regan SL, Maggs JL, Hammond TG, Lambert C, Williams DP, and Park BK. (2010) Acyl glucuronides: the good, the bad and the ugly. *Biopharm Drug Dispos* **31**:367-395.
- Reith MK, Sproles GD, and Cheng LK. (1995) Human metabolism of dolasetron mesylate, a 5-HT₃ receptor antagonist. *Drug Metab Dispos* **23**:806-812.
- Revesz K, Toth B, Staines AG, Coughtrie MW, Mandl J, and Csala M. (2012) Luminal accumulation of newly synthesized morphine-3-glucuronide in rat liver microsomal vesicles. *Biofactors*.
- Ritter JK, Chen F, Sheen YY, Tran HM, Kimura S, Yeatman MT, and Owens IS. (1992) A novel complex locus UGT1 encodes human bilirubin, phenol, and other UDP-glucuronosyltransferase isozymes with identical carboxyl termini. *J Biol Chem* **267**:3257-3261.
- Rowland A, Knights KM, Mackenzie PI, and Miners JO. (2009) Characterization of the binding of drugs to human intestinal fatty acid binding protein (IFABP): potential role of IFABP as an alternative to albumin for *in vitro-in vivo* extrapolation of drug kinetic parameters. *Drug Metab Dispos* **37**:1395-1403.
- Rowland A, Knights KM, Mackenzie PI, and Miners JO. (2008a) The "albumin effect" and drug glucuronidation: bovine serum albumin and fatty acid-free human serum albumin enhance the glucuronidation of UDP-glucuronosyltransferase (UGT) 1A9 substrates but not UGT1A1 and UGT1A6 activities. *Drug Metab Dispos* **36**:1056-1062.
- Rowland A, Elliot DJ, Knights KM, Mackenzie PI, and Miners JO. (2008b) The "albumin effect" and *in vitro-in vivo* extrapolation: sequestration of long-chain unsaturated fatty acids enhances phenytoin hydroxylation by human liver microsomal and recombinant cytochrome P450 2C9. *Drug Metab Dispos* **36**:870-877.
- Rowland A, Gaganis P, Elliot DJ, Mackenzie PI, Knights KM, and Miners JO. (2007) Binding of inhibitory fatty acids is responsible for the enhancement of UDP-glucuronosyltransferase 2B7 activity by albumin: implications for *in vitro-in vivo* extrapolation. *J Pharmacol Exp Ther* **321**:137-147.
- Rowland A, Elliot DJ, Williams JA, Mackenzie PI, Dickinson RG, and Miners JO. (2006) *In vitro* characterization of lamotrigine N2-glucuronidation and the lamotrigine-valproic acid interaction. *Drug Metab Dispos* **34**:1055-1062.
- Sanchez E and Tephly TR. (1975) Morphine metabolism. IV. Studies on the mechanism of morphine: uridine diphosphoglucuronyltransferase and its activation by bilirubin. *Mol Pharmacol* **11**:613-620.
- Sandberg AA and Slaunwhite WR, Jr. (1957) Studies on phenolic steroids in human subjects. II. The metabolic fate and hepato-biliary-enteric circulation of C¹⁴-estrone and C¹⁴-estradiol in women. *J Clin Invest* **36**:1266-1278.
- Schmid R. (1956) Direct-reacting bilirubin, bilirubin glucuronide, in serum, bile and urine. *Science* **124**:76-77.
- Schwaninger AE, Meyer MR, Zapp J, and Maurer HH. (2009) The role of human UDP-glucuronyltransferases on the formation of the methylenedioxyamphetamine (ecstasy) phase II metabolites R- and S-3-methoxymethamphetamine 4-O-glucuronides. *Drug Metab Dispos* **37**:2210-2220.

- Senafi SB, Clarke DJ, and Burchell B. (1994) Investigation of the substrate specificity of a cloned expressed human bilirubin UDP-glucuronosyltransferase: UDP-sugar specificity and involvement in steroid and xenobiotic glucuronidation. *Biochem J* **303** (Pt 1):233-240.
- Shareef A, Angove M, Wells J, and Johnson B. (2006) Aqueous solubilities of estrone, 17 β -estradiol, 17 α -ethynylestradiol, and bisphenol A. *J Chem Eng Data* **51**:879-881.
- Shen HW, Jiang XL, Winter JC, and Yu AM. (2010) Psychedelic 5-methoxy-*N,N*-dimethyltryptamine: metabolism, pharmacokinetics, drug interactions, and pharmacological actions. *Curr Drug Metab* **11**:659-666.
- Shiraga T, Yajima K, Suzuki K, Suzuki K, Hashimoto T, Iwatsubo T, Miyashita A, and Usui T. (2012) Identification of UDP-glucuronosyltransferases responsible for the glucuronidation of darexaban, an oral factor Xa inhibitor, in human liver and intestine. *Drug Metab Dispos* **40**:276-282.
- Shoda T, Fukuhara K, Goda Y, and Okuda H. (2009) 4-Hydroxy-3-methoxymethamphetamine glucuronide as a phase II metabolite of 3,4-methylenedioxyamphetamine: enzyme-assisted synthesis and involvement of human hepatic uridine 5'-diphosphate-glucuronosyltransferase 2B15 in the glucuronidation. *Chem Pharm Bull* **57**:472-475.
- Sim E, Fakis G, Laurieri N, and Boukouvala S. (2012) Arylamine *N*-acetyltransferases - from drug metabolism and pharmacogenetics to identification of novel targets for pharmacological intervention. *Adv Pharmacol* **63**:169-205.
- Smith PA, Sorich MJ, Low LS, McKinnon RA, and Miners JO. (2004) Towards integrated ADME prediction: past, present and future directions for modelling metabolism by UDP-glucuronosyltransferases. *J Mol Graph Model* **22**:507-517.
- Sneitz N, Court MH, Zhang X, Laajanen K, Yee KK, Dalton P, Ding X, and Finel M. (2009) Human UDP-glucuronosyltransferase UGT2A2: cDNA construction, expression, and functional characterization in comparison with UGT2A1 and UGT2A. *Pharmacogenet Genomics* **19**:923-934.
- Soars MG, Ring BJ, and Wrighton SA. (2003) The effect of incubation conditions on the enzyme kinetics of UDP-glucuronosyltransferases. *Drug Metab Dispos* **31**:762-767.
- Soars MG, Burchell B, and Riley RJ. (2002) *In vitro* analysis of human drug glucuronidation and prediction of *in vivo* metabolic clearance. *J Pharmacol Exp Ther* **301**:382-390.
- Soars MG, Petullo DM, Eckstein JA, Kasper SC, and Wrighton SA. (2004) An assessment of UDP-glucuronosyltransferase induction using primary human hepatocytes. *Drug Metab Dispos* **32**:140-148.
- Sorich MJ, McKinnon RA, Miners JO, and Smith PA. (2006) The importance of local chemical structure for chemical metabolism by human uridine 5'-diphosphate-glucuronosyltransferase. *J Chem Inf Model* **46**:2692-2697.
- Sprong H, Kruithof B, Leijendekker R, Slot JW, van Meer G, and van der Sluijs P. (1998) UDP-galactose: ceramide galactosyltransferase is a class I integral membrane protein of the endoplasmic reticulum. *J Biol Chem* **273**:25880-8.
- Stamets P. (2003) *Psilocybin Mushrooms of the World: An Identification Guide*, 1st edition ed. Ten Speed Press.
- Sten T, Bichlmaier I, Kuuranne T, Leinonen A, Yli-Kauhala J, and Finel M. (2009) UDP-glucuronosyltransferases (UGTs) 2B7 and UGT2B17 display converse specificity in testosterone and epitestosterone glucuronidation, whereas UGT2A1 conjugates both androgens similarly. *Drug Metab Dispos* **37**:417-423.
- Sten T, Qvisen S, Uutela P, Luukkanen L, Kostianen R, and Finel M. (2006) Prominent but reverse stereoselectivity in propranolol glucuronidation by human UDP-glucuronosyltransferases 1A9 and 1A10. *Drug Metab Dispos* **34**:1488-1494.
- Sticht G and Kaferstein H. (2000) Detection of psilocin in body fluids. *Forensic Sci Int* **113**:403-407.
- Stone AN, Mackenzie PI, Galetin A, Houston JB, and Miners JO. (2003) Isoform selectivity and kinetics of morphine 3- and 6-glucuronidation by human UDP-glucuronosyltransferases: evidence for atypical glucuronidation kinetics by UGT2B7. *Drug Metab Dispos* **31**:1086-1089.
- Strassburg CP, Oldhafer K, Manns MP, and Tukey RH. (1997) Differential expression of the UGT1A locus in human liver, biliary, and gastric tissue: identification of UGT1A7 and UGT1A10 transcripts in extrahepatic tissue. *Mol Pharmacol* **52**:212-220.
- Strassburg CP, Kneip S, Topp J, Obermayer-Straub P, Barut A, Tukey RH, and Manns MP. (2000) Polymorphic gene regulation and interindividual variation of UDP-glucuronosyltransferase activity in human small intestine. *J Biol Chem* **275**:36164-36171.
- Strolin Benedetti M, Tipton KF, and Whomsley R. (2007) Amine oxidases and monooxygenases in the *in vivo* metabolism of xenobiotic amines in humans: has the involvement of amine oxidases been neglected? *Fundam Clin Pharmacol* **21**:467-480.
- Tang C, Lin Y, Rodrigues AD, and Lin JH. (2002) Effect of albumin on phenytoin and tolbutamide metabolism in human liver microsomes: an impact more than protein binding. *Drug Metab Dispos* **30**:648-654.
- Thompson AJ and Lummis SC. (2007) The 5-HT₃ receptor as a therapeutic target. *Expert Opin Ther Targets* **11**:527-540.
- Trapnell CB, Klecker RW, Jamis-Dow C, and Collins JM. (1998) Glucuronidation of 3'-azido-3'-deoxythymidine (zidovudine) by human liver microsomes: relevance to clinical pharmacokinetic interactions with atovaquone, fluconazole, methadone, and valproic acid. *Antimicrob Agents Chemother* **42**:1592-1596.

- Trdan Lusin T, Trontelj J, and Mrhar A. (2011) Raloxifene glucuronidation in human intestine, kidney, and liver microsomes and in human liver microsomes genotyped for the UGT1A1*28 polymorphism. *Drug Metab Dispos* **39**:2347-2354.
- Tsoutsikos P, Miners JO, Stapleton A, Thomas A, Sallustio BC, and Knights KM. (2004) Evidence that unsaturated fatty acids are potent inhibitors of renal UDP-glucuronosyltransferases (UGT): kinetic studies using human kidney cortical microsomes and recombinant UGT1A9 and UGT2B7. *Biochem Pharmacol* **67**:191-199.
- Tsujikawa K, Kanamori T, Iwata Y, Ohmae Y, Sugita R, Inoue H, and Kishi T. (2003) Morphological and chemical analysis of magic mushrooms in Japan. *Forensic Sci Int* **138**:85-90.
- Tukey RH and Strassburg CP. (2000) Human UDP-glucuronosyltransferases: metabolism, expression, and disease. *Annu Rev Pharmacol Toxicol* **40**:581-616.
- Turfus SC, Braithwaite RA, Cowan DA, Parkin MC, Smith NW, and Kicman AT. (2011) Metabolites of lorazepam: Relevance of past findings to present day use of LC-MS/MS in analytical toxicology. *Drug Test Anal* **3**:695-704.
- Turgeon D, Carrier JS, Levesque E, Hum DW, and Belanger A. (2001) Relative enzymatic activity, protein stability, and tissue distribution of human steroid-metabolizing UGT2B subfamily members. *Endocrinology* **142**:778-787.
- Turgeon D, Chouinard S, Belanger P, Picard S, Labbe JF, Borgeat P, and Belanger A. (2003) Glucuronidation of arachidonic and linoleic acid metabolites by human UDP-glucuronosyltransferases. *J Lipid Res* **44**:1182-1191.
- Uchaipichat V, Mackenzie PI, Elliot DJ, and Miners JO. (2006) Selectivity of substrate (trifluoperazine) and inhibitor (amitriptyline, androsterone, canrenoic acid, hecogenin, phenylbutazone, quinidine, quinine, and sulfapyrazone) "probes" for human UDP-glucuronosyltransferases. *Drug Metab Dispos* **34**:449-456.
- Uchaipichat V, Raungrut P, Chau N, Janchawee B, Evans AM, and Miners JO. (2011) Effects of ketamine on human UDP-glucuronosyltransferases *in vitro* predict potential drug-drug interactions arising from ketamine inhibition of codeine and morphine glucuronidation. *Drug Metab Dispos* **39**:1324-1328.
- Uchaipichat V, Galetin A, Houston JB, Mackenzie PI, Williams JA, and Miners JO. (2008) Kinetic modeling of the interactions between 4-methylumbelliferone, 1-naphthol, and zidovudine glucuronidation by UDP-glucuronosyltransferase 2B7 (UGT2B7) provides evidence for multiple substrate binding and effector sites. *Mol Pharmacol* **74**:1152-1162.
- Uchaipichat V, Winner LK, Mackenzie PI, Elliot DJ, Williams JA, and Miners JO. (2006) Quantitative prediction of *in vivo* inhibitory interactions involving glucuronidated drugs from *in vitro* data: the effect of fluconazole on zidovudine glucuronidation. *Br J Clin Pharmacol* **61**:427-439.
- Uchaipichat V, Mackenzie PI, Guo XH, Gardner-Stephen D, Galetin A, Houston JB, and Miners JO. (2004) Human UDP-glucuronosyltransferases: isoform selectivity and kinetics of 4-methylumbelliferone and 1-naphthol glucuronidation, effects of organic solvents, and inhibition by diclofenac and probenecid. *Drug Metab Dispos* **32**:413-423.
- Van der Vusse GJ. (2009) Albumin as fatty acid transporter. *Drug Metab Pharmacokinet* **24**:300-307.
- Vasiliou V, Pappa A, and Estey T. (2004) Role of human aldehyde dehydrogenases in endobiotic and xenobiotic metabolism. *Drug Metab Rev* **36**:279-299.
- Vessey DA and Zakim D. (1972) Regulation of microsomal enzymes by phospholipids. V. Kinetic studies of hepatic uridine diphosphate-glucuronyltransferase. *J Biol Chem* **247**:3023-3028.
- Walsham NE and Sherwood RA. (2012) Ethyl glucuronide. *Ann Clin Biochem* **49**:110-117.
- Walsky RL, Bauman JN, Bourcier K, Giddens G, Lapham K, Negahban A, Ryder TF, Obach RS, Hyland R, and Goosen TC. (2012) Optimized assays for human UDP-glucuronosyltransferase (UGT) activities: altered alamethicin concentration and utility to screen for UGT inhibitors. *Drug Metab Dispos* **40**:1051-1065.
- Watanabe Y, Nakajima M, Ohashi N, Kume T, and Yokoi T. (2003) Glucuronidation of etoposide in human liver microsomes is specifically catalyzed by UDP-glucuronosyltransferase 1A1. *Drug Metab Dispos* **31**:589-595.
- Waters NJ, Jones R, Williams G, and Sohal B. (2008) Validation of a rapid equilibrium dialysis approach for the measurement of plasma protein binding. *J Pharm Sci* **97**:4586-4595.
- Wattanachai N, Tassaneeyakul W, Rowland A, Elliot DJ, Bowalgaha K, Knights KM, and Miners JO. (2012) Effect of albumin on human liver microsomal and recombinant CYP1A2 activities: impact on *in vitro*-*in vivo* extrapolation of drug clearance. *Drug Metab Dispos* **40**:982-989.
- Wattanachai N, Polasek TM, Heath TM, Uchaipichat V, Tassaneeyakul W, Tassaneeyakul W, and Miners JO. (2011) *In vitro*-*in vivo* extrapolation of CYP2C8-catalyzed paclitaxel 6 α -hydroxylation: effects of albumin on *in vitro* kinetic parameters and assessment of interindividual variability in predicted clearance. *Eur J Clin Pharmacol* **67**:815-824.
- Welsch ME, Snyder SA, and Stockwell BR. (2010) Privileged scaffolds for library design and drug discovery. *Curr Opin Chem Biol* **14**:347-361.
- Wen Z, Tallman MN, Ali SY, and Smith PC. (2007) UDP-glucuronosyltransferase 1A1 is the principal enzyme responsible for etoposide glucuronidation in human liver and intestinal microsomes: structural characterization of phenolic and alcoholic glucuronides of etoposide and estimation of enzyme kinetics. *Drug Metab Dispos* **35**:371-380.
- Williams JA, Hyland R, Jones BC, Smith DA, Hurst S, Goosen TC, Peterkin V, Koup JR, and Ball SE. (2004) Drug-drug interactions for UDP-glucuronosyltransferase substrates: a pharmacokinetic explanation for typically observed low exposure (AUC_i/AUC) ratios. *Drug Metab Dispos* **32**:1201-1208.
- Wu B. (2011) Substrate inhibition kinetics in drug metabolism reactions. *Drug Metab Rev* **43**:440-456.

- Wu B, Kulkarni K, Basu S, Zhang S, and Hu M. (2011) First-pass metabolism *via* UDP-glucuronosyltransferase: a barrier to oral bioavailability of phenolics. *J Pharm Sci* **100**:3655-81.
- Yin H, Bennett G, and Jones JP. (1994) Mechanistic studies of uridine diphosphate glucuronosyltransferase. *Chem Biol Interact* **90**:47-58.
- Yue QY, Hasselstrom J, Svensson JO, and Sawe J. (1991) Pharmacokinetics of codeine and its metabolites in Caucasian healthy volunteers: comparisons between extensive and poor hydroxylators of debrisoquine. *Br J Clin Pharmacol* **31**:635-642.
- Zhang H, Tolonen A, Rousu T, Hirvonen J, and Finel M. (2011) Effects of cell differentiation and assay conditions on the UDP-glucuronosyltransferase activity in Caco-2 cells. *Drug Metab Dispos* **39**:456-464.
- Zhang H, Patana AS, Mackenzie PI, Ikushiro S, Goldman A, and Finel M. (2012a) Human UDP-glucuronosyltransferase expression in insect cells: ratio of active to inactive recombinant proteins and the effects of a C-terminal His-tag on glucuronidation kinetics. *Drug Metab Dispos* **40**:1935-1944.
- Zhang H, Soikkeli A, Tolonen A, Rousu T, Hirvonen J, and Finel M. (2012b) Highly variable pH effects on the interaction of diclofenac and indomethacin with human UDP-glucuronosyltransferases. *Toxicol in vitro* **26**:1286-93.
- Zhou D, Guo J, Linnenbach AJ, Booth-Genthe CL, and Grimm SW. (2010) Role of human UGT2B10 in *N*-glucuronidation of tricyclic antidepressants, amitriptyline, imipramine, clomipramine and trimipramine. *Drug Metab Dispos* **38**:863-70.
- Zhou J, Tracy TS, and Rimmel RP. (2011) Correlation between bilirubin glucuronidation and estradiol-3-glucuronidation in the presence of model UDP-glucuronosyltransferase 1A1 substrates/inhibitors. *Drug Metab Dispos* **39**:322-329.
- Zhou J, Tracy TS, and Rimmel RP. (2010) Glucuronidation of dihydrotestosterone and trans-androsterone by recombinant UDP-glucuronosyltransferase (UGT) 1A4: evidence for multiple UGT1A4 aglycone binding sites. *Drug Metab Dispos* **38**:431-440.
- Zhou Q, Matsumoto S, Ding LR, Fischer NE, and Inaba T. (2004) The comparative interaction of human and bovine serum albumins with CYP2C9 in human liver microsomes. *Life Sci* **75**:2145-2155.
- Zhu B, Bush D, Doss GA, Vincent S, Franklin RB, and Xu S. (2008) Characterization of 1'-hydroxymidazolam glucuronidation in human liver microsomes. *Drug Metab Dispos* **36**:331-338.